STRENGTH, MODULUS OF ELASTICITY, CREEP AND SHRINKAGE OF CONCRETE USED IN FLORIDA

By

BORIS HARANKI

A THESIS PRESENTED TO THE GRADUATE SCHOOL
OF THE UNIVERSITY OF FLORIDA IN PARTIAL FULFILLMENT
OF THE REQUIREMENTS FOR THE DEGREE OF
MASTER OF ENGINEERING

UNIVERSITY OF FLORIDA

2009

To my parents, Pedro Haranki and Rosalia Haranki, for their financial and emotional support throughout these years

ACKNOWLEDGMENTS

I consider this thesis to be a collective work from friends and people whom without this would have not been possible. I thank God for listening to my prayers, guiding me, and blessing me with all the people that have supported me in one way or another throughout these years.

First of all, I want to thank Dr. Mang Tia for his help, guidance, flexibility, knowledge, and words of wisdom all through the length of this project: you are one of the persons I respect the most in my life. I also thank Dr. Yanjun Liu for giving out a helping hand whenever needed.

Second of all, I want to thank the personnel at the Florida Department of Transportation (FDOT) for their help and friendship: Richard DeLorenzo, Craig Roberts, Joseph Fitzgerald, Christopher Ferraro, Toby Dillow, and Luke Goolsby. I also want to thank Gene Ingle from Florida Rock Industries for donating materials needed to finish this project.

Third of all, I want to thank everyone that helped me over at the University of Florida including: Chuck Broward, Nard Hubert, and Scott Ellis.

Finally, I want to thank my family and close friends for sharing some insight when everything seemed so blurry. My dad for his support and inspiration: words cannot describe how much I appreciate all the hard work you have done to give me this opportunity. My mom for her love and emotional support: you made me laugh in times when I felt depressed and unhappy. Ashley Young for your love and motivation to finish strong: I love you.

TABLE OF CONTENTS

page

LIST OF TABLES

LIST OF FIGURES

Abstract of Thesis Presented to the Graduate School
of the University of Florida in Partial Fulfillment of the
Requirements for the Degree of Master of Engineering

STRENGTH, MODULUS OF ELASTICITY, CREEP AND SHRINKAGE OF CONCRETE USED IN FLORIDA

By

Boris Haranki

May 2009

Chair: Mang Tia
Cochair: Fazil Najafi
Major: Civil Engineering

Shrinkage deformation affects durability, serviceability, long-term reliability, and structural integrity of concrete. Creep of concrete is an important factor in structural design because when a concrete member is put in service, it will experience temporary and/or permanent deformations which might result in structural failure over the years. This research project is focused on the effects of different compositions of concrete mixtures on these deformations, how the individual components affect these deformations, and how these deformations can be predicted to reduce economic impacts and ensure structural integrity of concretes typically used in Florida.

CHAPTER 1
INTRODUCTION

1.1 Background and Research Needs

Concrete members that are subjected to sustained stresses will exhibit increase in strain known as creep deformation. When these concrete members are exposed to ambient humidities that are below 100% saturation, the concrete will lose this water to the environment leading to drying shrinkage. Studies of these deformations are very important because of the volatility of the creep properties and the need for better developed models that can account for concretes containing mineral additives. These phenomena are very important in concrete design and cannot be ignored. This is especially true for typical concretes since very limited creep testing has been performed and therefore empirical data is scarce.

1.2 Hypothesis

- Creep can be related to strength and non-strength properties such as compressive strength and modulus of elasticity. It is possible to predict creep strains from these relatively short tests.
- Shrinkage can be related to water content, strength and non-strength properties such as compressive strength and modulus of elasticity. It is possible to predict shrinkage strains from its water content and these relatively short tests.
- A maximum value of 2.0 for the ultimate creep coefficient is usually assumed in concrete structural design. Creep testing is needed to obtain ultimate creep coefficient.

1.3 Objectives of Study

This research has the following major objectives:

- To design and recommend an effective and reliable laboratory testing set-up and procedure for performing creep tests on concrete.
- To evaluate the effects of aggregate, mineral additives and water to cementitious materials ratio on strength, elastic modulus, shrinkage and creep behavior of concrete.
- To determine the strength, elastic modulus, shrinkage and creep behavior of the typical concretes used in Florida.

- To determine the relationship among compressive strength, splitting tensile strength and modulus of elasticity of concretes made with typical Florida aggregate.

- To develop prediction equations or models for estimation of shrinkage and creep characteristics of typical Florida concretes.

1.4 Scope of Study

The scope of this research covered the following major tasks:

- To review and analyze current and previous models that predict modulus of elasticity, shrinkage and creep of concrete.

- To obtain strength and non-strength properties of concrete made with Miami Oolite limestone and Georgia granite aggregates. To perform creep and shrinkage testing on these mixtures. A total of 18 different concrete mixes were evaluated.

- To analyze and establish relationship between creep and shrinkage behavior of concrete and strength and non-strength properties of concrete.

1.5 Research Approach

Objectives of this study are realized by the following research approaches:

- The strength and non-strength properties of concrete are obtained in accordance with ASTM standard test methods. The creep testing is done by means of a recently designed creep frame set-up.

- Statistical analysis is performed on the obtained data to establish relationships between the fundamental properties of concrete and its creep and shrinkage behavior.

- Existing creep and shrinkage prediction models are evaluated and compared to the obtained results.

CHAPTER 2
LITERATURE REVIEW

2.1 Introduction

The content that follows defines the strength, elastic modulus, shrinkage and creep of concrete. This information is a systematic review of published works on these topics from various sources listed in the bibliography.

2.2 Strength of Concrete

2.2.1 Significance of Studying Strength of Concrete

Strength is the ability of a material to resist an induced amount of stress that would make it fail, generally expressed in pounds per square inch (psi) or megapascals (MPa). It is one of the most sought-after properties of concrete, especially for designers and quality control engineers, because of the simplicity of the routine strength tests, because the value gives an indication of overall quality and uniformity, because it provides a load-carrying measure useful for design strength purposes, and because other technically important nonstrength properties, such as modulus of elasticity and flexural strength which are measured by more complicated tests, can be related to strength. Even though the strength tests are relatively easy to perform, strength is a very volatile property. Consistent fabrication and testing procedures of concrete still give significant variations in the results of concrete strength.

These variations in strength of results concrete can be attributed to:

Mixing water: As a rule, if water is potable, it can be used as mixing water. Water should not have excess undesirable organic or inorganic substances which can potentially have an adverse effect not only in the strength, but also in the setting time, surface efflorescence (deposits of white salts on the surface of concrete), and resistance to degradation. Water that is not drinkable might be used as mixing water as long as it in compliance with the acceptance

criteria listed in ASTM "Ready-Mixed Concrete" (C 94). ASTM C 94 states that the mixing water needs to be clear and apparently clean free of substances that discolor it, makes it taste or smell in unusual way. Other sources such as sea water increases the risk of corrosion in reinforced and prestressed concrete, but it does not have any effects on the strength of plain concrete, as long as the pH is between 6.0 and 8.0, possibly even 9.0. It needs to be mentioned that this also applies to water present on the surface and pores of aggregates used for concrete production.

Age of concrete: Based on typical strength-time curves, it can be appreciated that the older the concrete is, the stronger it will be because of a longer hydration process.

Characteristics and proportions of the materials: Gradation, shape, and surface texture of the aggregate are of great importance. Coarse aggregate desired characteristics include strength, high resistance to abrasion, and high modulus of elasticity. These desired characteristics are discussed in more detail in the next section.

Mixing time: Longer mixing times will result in loss of moisture which will result in drier concrete which in turn is harder to compact. This will lead to high volume of voids and thus lower strength results.

Physical condition and properties of the specimen: To ensure uniform load transfer to the test specimens, ASTM C39 states that the ends of the specimen to be tested must be within 1/8 inches for every 12 inches in the perpendicular direction from the specimen axis, and that the ends must be plane to within 0.002 inches after being ground in the grinder. According to Lamond and Pielert, specimens that do not meet the ASTM requirements will yield relatively lower strength test results. Specimens must have consistent physical conditions at the time of

testing as well. For example, specimens that are allowed to dry will give relatively higher strength results.

Degree of consolidation/ Porosity: Neville states that the volume of pores in concrete influences the strength of concrete by the following power function type: $f_c = f_{c,0} \cdot (1-p)^n$, where p is the volume of voids, f_c the strength of concrete with porosity p, $f_{c,0}$ strength at zero porosity, and n a coefficient obtained by regression analysis. If the previous formula was plotted on a log scale, a general linear relationship can be established – as porosity increases, the compressive strength decreases. Specimens that have low degrees of compaction will have, as a result, high volume of voids and, therefore, will yield lower strength results.

How and how well the testing procedure is performed: Rate of loading can have an effect on the strength of concrete. Specimens loaded at a very slow rate, fail at loads that are about 25% lower than the standard test strength, and specimens loaded at a very high rate fail at loads about 15% higher than the standard test strength. If the rate of loading is adjusted during testing, it can have a similar, but milder, effect. If the diameter of the specimen is not taken in the center, the use of a faulty measuring device, can lead to errors in strength calculations. The calibration of the loading apparatus is of great importance, as well as a smooth and continuous application of the load by the apparatus. Surface planeness of both the spherically seated and the solid bearing blocks must satisfy requirements of surface planeness. The spherically seated bearing block must have the proper dimensions to run the test on a 6" diameter specimen, and the specimen needs to be under the center of the bearing face to avoid reduction in strength results.

Because of the potential variability of the strength tests results, the appropriate test must be performed whenever a specific nonstrength property is of interest. Characteristics and proportions of coarse aggregate and how it affects the strength of concrete are discussed next.

2.2.2 Effect of Coarse Aggregate on Strength of Concrete

Usually it is the water to cementitious materials (w/c) ratio the reason behind concrete strength, but strength is influenced by properties of coarse aggregate as well. Coarse aggregate makes up about 75% of concrete by volume, so its characteristics cannot be overlooked. It is defined in the US as aggregate that does not pass the No. 4 ASTM sieve, which is 4.75 mm (3/16 in.) in size, and it contributes to both economic and technical advantages of concrete considerably. Undesired properties of coarse aggregate may affect the strength, durability, and performance of concrete negatively; therefore tests on coarse aggregate are needed to evaluate its suitability in concrete.

According to Kaplan, "no relationship between the strength of the coarse aggregate and the strength of concrete was established. This finding should not be taken to mean that aggregates of low strength will not affect the concrete strength." This seems to be the case of non high-strength concretes according to Wu, Chen, Yao, and Zhang. Wu, et. al., conducted a study on the effects of coarse aggregate type on mechanical properties of concrete using 4 different types of aggregate: crushed granite, limestone, marble, and crushed quartzite. They found that concretes containing granite where stronger than concretes containing limestone and had higher elastic moduli for different w/c ratios (0.26, 0.44, and 0.55). As the w/c ratio increased, effect of the type of aggregate used was not significant. So, the type of aggregate makes an important role in concretes with low w/c ratios because the bond between mortar and coarse aggregate in concretes has similar strength, allowing full strength potential.

2.2.3 Prediction of Strength of Concrete

As we deal with more complex, flexible, and bigger structural designs, a prediction of the strength of concrete can have a beneficial impact on the construction project budget by reducing

the amount of formwork needed knowing that the cost of formwork can be as much as 60% of the total cost of the concrete in place (ACI 347R).

Since compressive strength is the most common measure by which the adequacy of concrete is judged, different equations to predict the compressive strength of concrete at different ages has been developed over the years. These equations are simplified expressions representing average laboratory data obtained under steady environmental and loading conditions. It must also be mentioned that these equations are for concretes containing no admixtures.

In engineering practice, water-cementitious material ratio is one of the principal factors governing the strength of concrete. Duff Abrams developed a relationship between water-cementitious material ratio and strength of fully compacted concrete containing about 1% of air voids. Abrams found that the actual compressive strength is equal to:

$$f_c = \frac{K_1}{K_2^{w/c}}$$

where w/c represents the water/cement ratio of the mix, and K_1 and K_2 are empirical constants obtained through regression analysis. The following figure shows the relationship of a range of typical strength to water-cement ratio based on over 100 different concrete mixtures.

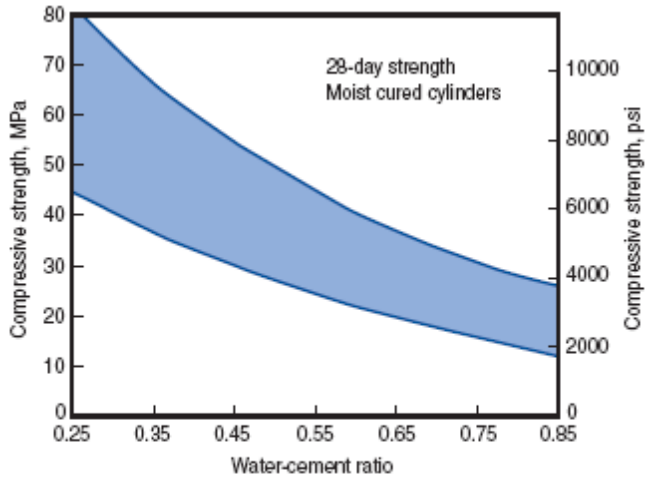

Figure 2-1. Relationship between strength and water/cement ratio of concrete

It can be appreciated from the figure above that strength is inversely proportional to the water/cement ratio.

The following equation is similar to Abram's and relates the actual compressive strength of concrete to the absolute volumetric proportions of cement, water, and air. This equation was formulated by René Féret in 1896 and has the form

$$f_c = K\left(\frac{c}{c+w+a}\right)^2$$

where c, w, and a represent the values of the volumetric proportions of cement, water, and air, respectively, and K is a constant that is obtained through regression analysis.

The following empirical equation has been provided by ACI 209R to predict the specified compressive strength,

$$(f_c^{'})t = \frac{t}{a+\beta t}(f_c^{'})_{28}$$

where a and β are constants and are dependent on type of cement used and type of curing, $(f_c^{'})_{28}$= 28-day strength, and t is the age of the concrete in days. For this study type I cement was used, specimens were moist cured, and constants a and β become 4.0 and 0.85 respectively.

It is also of importance to realize the relationship between the 28-day compressive strength and the compressive strength at other ages if one wants to predict strength development. For normal concrete, the strength at 7 days is about 75% of the 28 day strength; the strength at 56 and 91 days are about 10% to 15% greater relative to 28 day strength (Kosmatka et al.). This trend is shown in Figure 2-2.

If the strength development is known, formwork can be removed, economy can be achieved by reusing them in other areas of the project, productivity of the construction process can reach maximum efficiency, and thus time of completion can be improved drastically. While

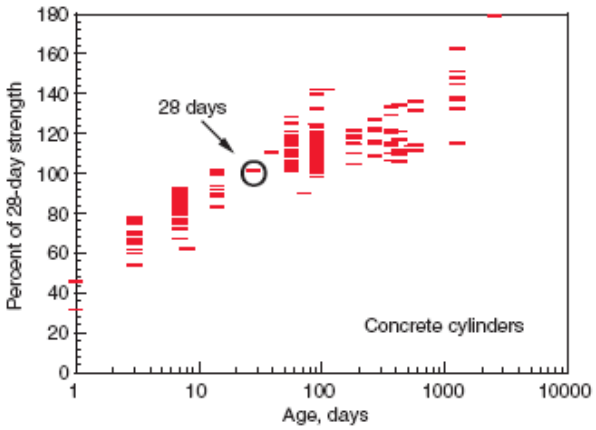

Figure 2-2. Strength development for various concrete mixes

these equations can help predict the strength of concrete at different ages, it must be noted that, without a doubt, the best prediction is made based on historical data rather than by batching trial mixes. Whenever data is not available, it is highly recommended spending time on trial batching to ensure that the desired results can be achieved on the field at the time of construction.

2.3 Elastic Modulus of Concrete

2.3.1 Definition and Determination of Elastic Modulus of Concrete

The modulus of elasticity, denoted as E, is defined as the ratio between normal stress to strain below the proportional limit of a material, according to ASTM E6-89, and it is used to measure instantaneous elastic deformation. Since no test exist to evaluate the direct elastic modulus of concrete, the proportional limit is evaluated by means of ASTM C 39 first, and this value is used to establish the limit used for the curves in the repeated applications of load. The elastic modulus is then calculated by determining the slope of the straight line in the stress-strain diagram. Figure 2-3 illustrates the stress-strain plot of a concrete as it is going through one loading cycle.

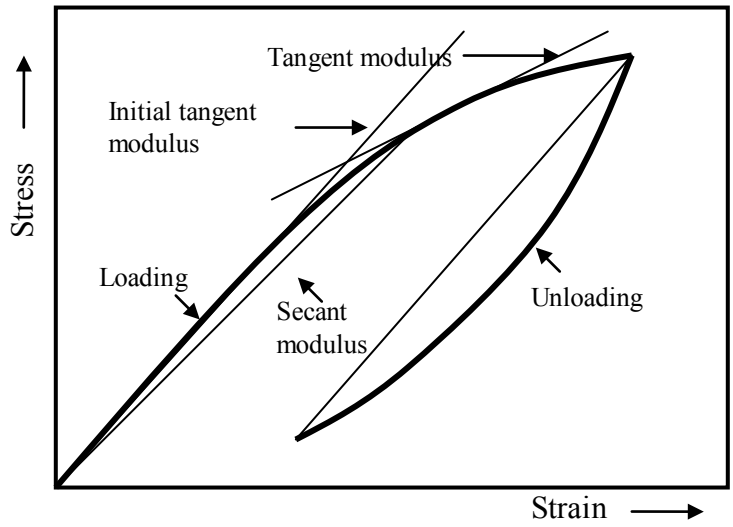

Figure 2-3. Representation of the stress-strain relation for concrete

2.3.2 Significance of Studying Elastic Modulus of Concrete

When concrete is subjected to loading, it exhibits a linear stress-strain relationship in the elastic range. The ratio, which is the slope of this linear portion of the relationship, is known as the modulus of elasticity. The elastic limit is "the greatest stress which a material is capable of sustaining without any deviation from proportionality of stress to strain (Hooke's law)."

As defined in the previous section, the modulus of elasticity is the ratio between stress and the reversible strain. When a load is applied to concrete, it will deform depending on the magnitude of the load and its rate of application. The value of strain is of immense importance because it represents the rigidity of the structural design and the stress at which the concrete will experience permanent deformation if exceeded. Most structures are subject to cyclic loading and it is, therefore, important to know the elastic portion for design purposes, especially the amount of steel required for reinforcement.

According to Klieger and Lamond, modulus of elasticity can be measured in tension, compression, or shear. For this research project, the modulus elasticity was measured by means

of a compressometer between two points on the stress-strain curve: 300 psi and 40% of the compressive strength.

2.3.3 Effect of Coarse Aggregate on Elastic Modulus of Concrete

According to the Canadian Portland Cement Association (CPCA), the elastic modulus of concretes will be influenced by the properties of different aggregate types with different elastic moduli.

The following figure was taken from a report to the Florida Department of Transportation by Tia, Liu, and Brown. It shows the Stress-Strain relation curves for aggregate, concrete, and cement paste.

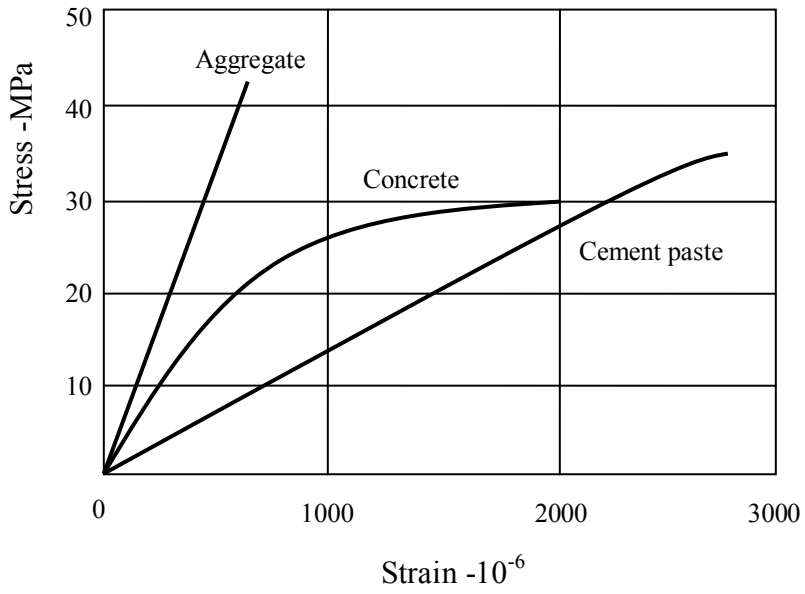

Figure 2-4. Stress-strain relations for cement paste, aggregate and concrete

From the previous figure, it can be determined that aggregate has a substantially larger elastic modulus as compared to concrete and cement paste, so it is could be guessed that aggregate and aggregate content has a significant effect on the elastic modulus of concrete. Parrot (1979) developed an equation that can estimate the elastic modulus of concrete; it must be

noticed that his model is the only model that relates modulus of elasticity to strength and type of aggregate.

$$E_c = K_0 + 0.2f_c^{'}$$

where E_c is the modulus of elasticity, K_0 is a factor depending on the type of aggregate, and $f_c^{'}$ is the compressive strength of the concrete ranging from 20MPa to 70 MPa.

On his technical paper titled "Mechanical Properties of High-Performance Concrete," Iravani determined that concrete containing granite aggregate yield lower elastic modulus relative to concrete containing limestone aggregate as shown in the following figure. He concluded that the amount of coarse aggregate in concrete has a "major effect on the static modulus of elasticity" of concrete.

Table 2-1. Recommended coarse aggregate coefficients

Kind of coarse aggregate	Recommended $\boldsymbol{K_0}$ factor	Coefficient of Variation
Sandstone gravel	0.71	0.066
Siliceous gravel	0.76	---
Limestone	0.92	0.093
Dolomite	0.92	0.087
Quartzite	0.97	0.055
Granite	0.82	0.072
Trap rock	0.97	0.018
Sandstone	0.61	0.143

On their discussion paper published by ACI Materials Journal (Sep/Oct 2006) Yilmaz et al, state that aggregate influences the elastic modulus of concrete significantly when the w/c ratio of the mix is less than 0.40.

The following table was taken from ACI Materials Journal article by Aïtcin and Mehta titled "Effect of Coarse-Aggregate Characteristics on Mechanical Properties of High-Strength Concrete." It shows that the elastic modulus of concretes made with limestone aggregate is higher at 28 and 56 days as compared to concretes made with granite aggregate.

Table 2-2. Compressive strengths and elastic moduli of very high strength concrete mixtures containing different aggregate types

Age, days	f', MPa (psi)			
	Diabase	Limestone	Gravel	Granite
1	41.1 (5960)	42.5 (6160)	40.6 (5880)	37.2 (5390)
28	100.7 (14,600)	97.3 (14,200)	92.1 (13,350)	84.8 (12,300)
56	104.8 (15,200)	101.3 (14,700)	95.9 (13,900)	88.6 (12,850)
Age, days	E', GPa (10^6 psi)			
	Diabase	Limestone	Gravel	Granite
28	36.6 (5.3)	37.9 (5.5)	33.8 (4.9)	31.7 (4.6)
56	37.9 (5.5)	40.7 (5.9)	35.9 (5.2)	33.8 (4.9)

They concluded that even as granite is "as hard and strong" as the other types of aggregates investigated in the study, concretes with granite yielded lower elastic modulus at all test ages. From the table it can be seen that concretes containing granite have a compressive strength of about 87% to that of limestone concretes at 28 days, and about 84% elastic modulus. They attribute the results to the failure surface of the concretes which showed a fracture path through the granite aggregate particles which was not the case in the limestone concrete. It must be noted that all concretes had identical w/c ratios. The following figure shows the stress-strain curves for concretes containing different types of aggregate. It can be seen from the figure that concretes containing limestone have a steeper stress-strain slope as compared to concretes containing granite which translates into higher elastic moduli.

2.3.4 Models for Predicting Elastic Modulus of Concrete

It is safe to assume that if concrete is very strong, its elastic modulus would be very high because it would resist deformations at high stress applications. This also means that the initial slopes of the stress-strain diagrams are steeper in stronger concretes. The models used in this research to predict the elastic modulus of concrete are the following:

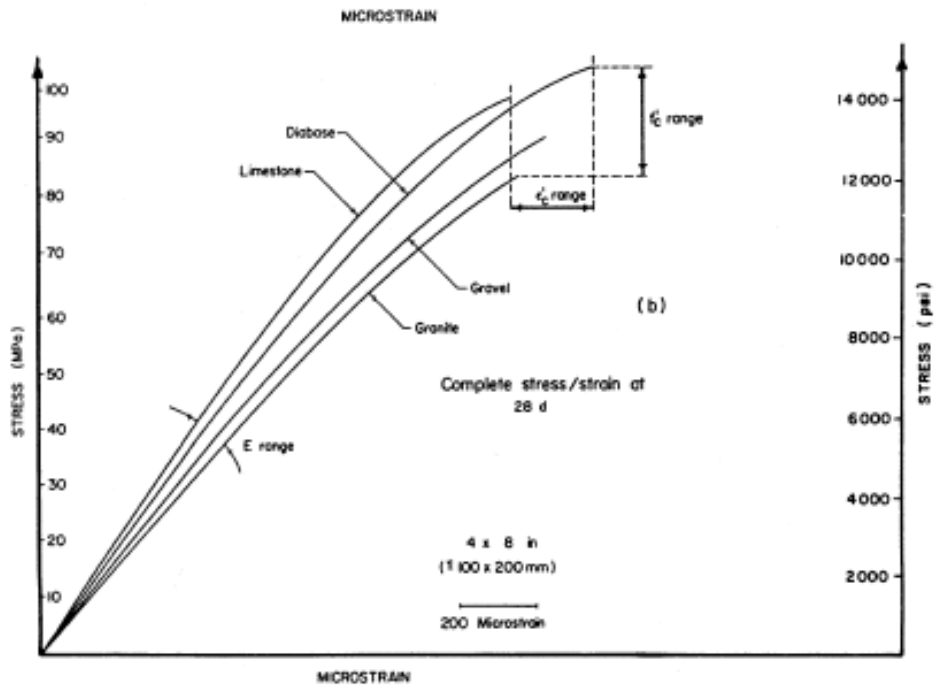

Figure 2-5. Stress-Strain curves at 28 days

- Model recommended by ACI Section 8.5.1:

$$E_c = 33(w^{1.5})\sqrt{f_c'}$$

where w is the unit weight of the concrete in lb/ft^3, f_c' the design compressive strength in psi and is valid for unit weights ranging from 90 to 155 lb/ft^3.

- Model recommended by ACI Section 8.5.1 for normal-weight concrete with a density of 145 lb/ft^3:

$$E_c = 57{,}000\sqrt{f_c'}$$

- Model recommended by ACI Committee 363 for high-strength concretes:

$$E_c = 40{,}000\sqrt{f_c'} + 1.0 \times 10^6$$

- Model by CEB-FIP Code (1990):

$$E_{ci}(t) = \left(exp\left(s\left(1 - \left(\frac{28}{t/t_1} \right)^{0.5} \right) \right) \right)^{0.5} \cdot E_{ci}$$

where s is a coefficient depending on the type of cement, t is the age of concrete (days), t_1 is 1 day, and E_{ci} is the elastic modulus of concrete at 28 days.

It is important to realize that the results of tests with different types of aggregate will result in wide scattered data for all the models. Regression analysis needs to be performed to account for different types of aggregate.

2.4 Shrinkage Behavior of Concrete

2.4.1 Origin of Shrinkage of Concrete

Concrete is subject to volume changes from the time it's in its plastic state throughout its service life due to movement towards moisture equilibrium with the environment where it is located. These volumetric changes are termed as strain and their magnitude is referred to as shrinkage. Shrinkage is the change in length per unit length and is, therefore, a dimensional number expressed as percent. Shrinkage is time-dependent and its value includes plastic shrinkage, autogenous shrinkage, drying shrinkage, and carbonation shrinkage usually quantified in terms of microstrain which is equal to $1 \times 10^{-6} \frac{in}{in}$ or $1 \times 10^{-6} \frac{m}{m}$.

Autogeneous shrinkage, also known as "basic shrinkage," is the shrinkage due to chemical reactions between cement with water, known as hydration, and do not include environmental effects such as temperature and moisture changes. Its magnitude is usually ignored in concretes with w/c more than 0.40 (ACI 209.1 R-05), but "may be a significant component" in concretes with w/c less than 0.4 (Tazawa 1999). According to Lamond and Pielert, the magnitude of autogeneous shrinkage is dependent on expansion due to disjoining pressure inside the cement matrix as a result from water adsorption from C-S-H, and shrinkage due to disjoining pressure inside the cement matrix as a result from self-desiccation.

Plastic shrinkage is contraction in volume due to water movement from the concrete while still in the plastic state, or before it sets. This movement of water can be during the hydration process or from the environmental conditions leading to evaporation of water that resides on the surface on the wet concrete. So, the more the concrete bleeds, the greater the plastic shrinkage should be. According to Neville, plastic shrinkage is proportional to cement content and, therefore, inversely proportional to the w/c ratio.

Carbonation shrinkage is caused by chemical reactions between carbon dioxide and the hydration products of cement (C-S-H, CH, ettringite, and monosulfate hydrate); this process increases the mass of the concrete sample according to Lamond and Pielert, and it's dependent on physical condition and characteristics of the sample, the environmental conditions where the sample is during its curing phase, and the lime content of the cement used. The carbonation reaction that follows shows the production of water when carbon dioxide reacts with calcium hydroxide in cement and could explain the increase in mass:

$$Ca(OH)_2 + CO_2 \rightarrow CaCO_3 + H_2O$$

An increase of 44 units in atomic mass due to the reaction with carbon dioxide can be appreciated from the previous reaction.

2.4.2 Significance of Studying Shrinkage of Concrete

With the rapid development of massive concrete structures, the effects and magnitude of shrinkage in the performance of concrete cannot be overlooked. Shrinkage affects durability, serviceability, long-term reliability, and even structural integrity of concrete. It is important to take also into account when the concrete was casted and the environmental conditions where it is loaded. According to Jianyong and Yan, the stress distribution in concrete gets affected significantly by deflections caused by shrinkage.

Shrinkage is a major concern because most concrete members are restrained from movement and since shrinkage in concrete cannot be prevented, it means that these members will experience tensile stresses and will thus develop cracks that will affect its aesthetic appearance as well as its serviceability. The structural designer must take shrinkage into account when designing for reinforcement because cracks produced by tensile stresses, especially at early ages, make the concrete permeable and the reinforcement in concrete is then vulnerable to corrosion.

According to Liu, shrinkage is heavily influenced by the materials that make up concrete. The study states that an increase in coarse aggregate leads to a decrease in cement content and thus a decrease in shrinkage.

2.4.3 Effect of Raw Materials on Shrinkage of Concrete

2.4.3.1 Effect of aggregate content on shrinkage behavior of concrete

According to ACI 209.1R-5, an increase in aggregate content leads to a decrease in the shrinkage of the cement paste. Aggregate content has been found to be the most important factor in affecting shrinkage behavior in concrete according to ACI 209.1R-05. Shrinkage of concrete can be related to aggregate content by the following equation developed by Pickett in his synopsis "Effect of Aggregate on Shrinkage of Concrete and a Hypothesis Concerning Shrinkage:"

$$S_C = S_P(1 - g)^n$$

where S_P is the shrinkage of the concrete if no aggregate were present, or simply the shrinkage of the paste; S_C is the shrinkage of concrete; g is the aggregate volumetric fraction, usually between 60% and 80%; and n is a variable between 1.2 and 1.7. It can be appreciated from the previous formula that as the aggregate volumetric content g increases, S_P approaches S_C. The following figure illustrates the results which show the shrinkage of concrete for different aggregate volumetric content, ranging from 0% to 36%:

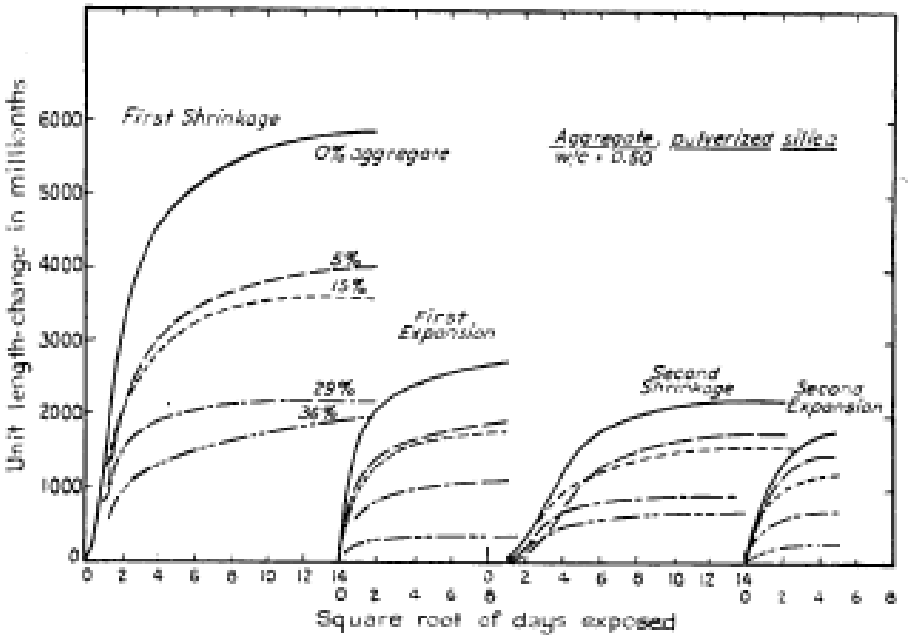

Figure 2-6. Shrinkage during drying and expansion using high-early strength cement and w/c = 0.50

The previous formula can be rearranged to establish a linear relationship between aggregate content and shrinkage into the form:

$$\log \frac{S_p}{S_c} = n \log \frac{1}{1-g}$$

The graph of $\log \frac{S_p}{S_c}$ against $\log \frac{1}{1-g}$ is plotted in Figure:2-7.

According to Liu a possible reason for this reduced effect in shrinkage is because concrete with high aggregate volumetric content will have a higher resistance to stresses due to a stiff aggregate skeleton. An illustration of this theory is shown on top of the next page.

Another way to look at the aggregate content effect is that since shrinkage of concrete is generally attributed to the shrinking of the cement paste, so it can be assumed that the higher the aggregate content, the less the cement paste content and therefore, the less the shrinkage.

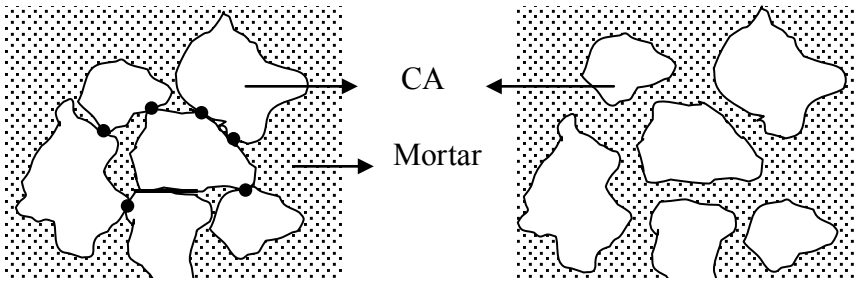

a. Lean concrete b. Rich concrete

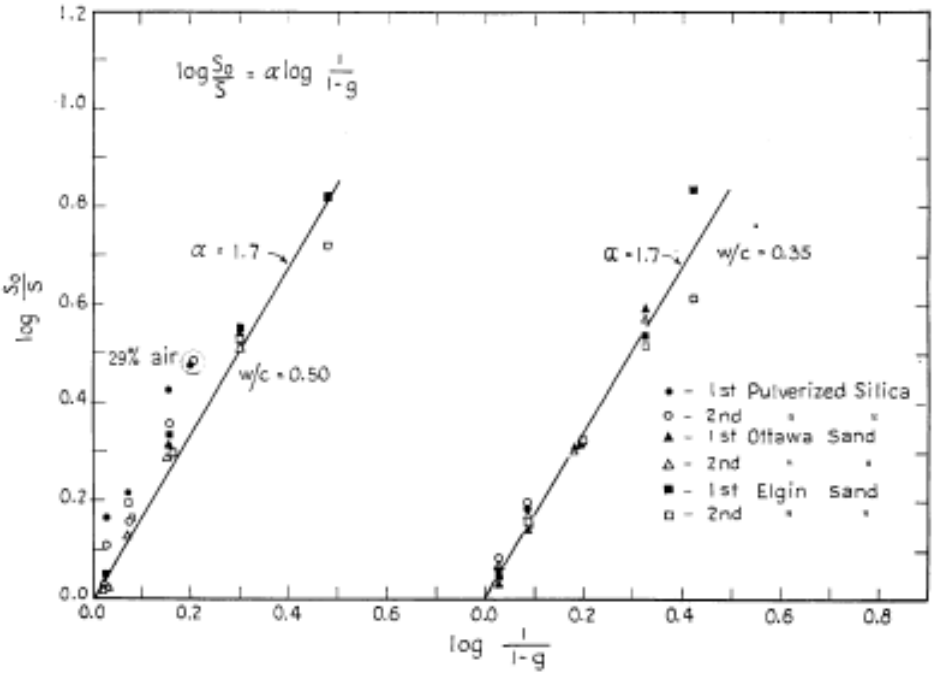

Figure 2-7. Effect of aggregate on shrinkage

Table 2-3. Typical Value of Shrinkage of Mortar and Concrete Specimens, 5 in. (127 mm) Square in Cross-section, Stored at a Relative Humidity of 50 % and 21°C (70°F)

Aggregate/ cement ratio	Shrinkage after six months (10-6) for water/ cement ratio of:			
	0.4	0.5	0.5	0.7
3	800	1200	-	-
4	550	850	1050	-
5	400	600	750	850
6	300	400	550	650
7	200	300	400	500

Table 2-3 illustrates similar findings on this phenomenon in a study by Lea (1970), it shows that for any w/c ratio, increasing the aggregate to cement ratio will lead to a decrease in shrinkage.

The table also indicates proportionality between shrinkage and water to cement ratio: for the same aggregate to cement ratio, shrinkage increases as water to cement ratio increases.

2.4.3.2 Effects of coarse aggregate type on concrete shrinkage

Different aggregate type will have different properties and will therefore have different effects on concrete shrinkage. In general, concretes made with high moduli of elasticity non-shrinking aggregates will have low shrinkage.

Studies made by Han and Walraven state that concretes containing limestone exhibit less of a shrinkage rate as compared to any other aggregate type. The figure below shows a graph on the effects of different types of aggregate on relative shrinkage of concrete.

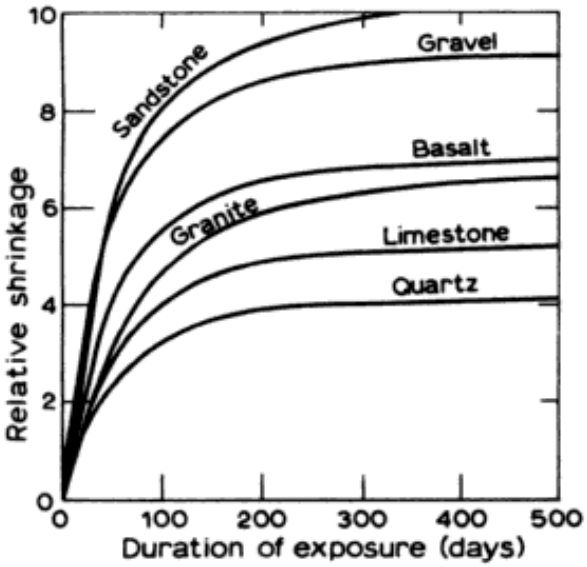

Figure 2-8. Effect of aggregate type on shrinkage

On the contrary, according to findings in a research program for the Kansas Department of Transportation by Richard McReynolds, P.E., it is reported that concretes made with limestone experience higher shrinkage relative to concretes made with quartzite and granite.

2.4.3.3 Effects of size and shape of coarse aggregate on concrete shrinkage

According to Kong and Evans, size and shape of coarse aggregate influence the loss of moisture and it has therefore an indirect effect on the shrinkage of concrete. In general, the smaller the aggregate size, the more surface area, more water is absorbed as a result and, therefore, more shrinkage. This means that whenever low shrinkage is desired, largest aggregate size should be used. This is consistent with a report made by Videla et al, in their technical paper published by ACI where they concluded that large aggregate size affects voids and aggregate content leading to lower shrinkage. Their research consisted on the testing of 72 specimens and shrinkage strains were measured for 15 months.

Concretes made with aggregates that are angular in shape tend to have higher shrinkage as well as these shapes need more cement paste to coat their surface. According to recommendations from the National Cooperative Highway Research Program (NCHRP Project 4-20C), aggregates angular in shape tend to require more mixing water leading to higher shrinkage.

2.4.3.4 Effect of other factors on shrinkage behaviors of concrete

According to Gribniak et al, other factors that have an effect on the magnitude of shrinkage include mix proportions, material properties, curing methods, environmental conditions, and geometry of the specimen.

Water content has been found to affect the magnitude and rate of drying shrinkage in concrete. Han et al, found that for every additional 10 kg/m^3 of water, there's an increase of -

$0.8x10^{-4}$ in shrinkage strain. According to ACI 209.1R-05, this higher magnitude in shrinkage is due to a decrease in aggregate volumetric content of the mix as water content increases.

Other factors include elastic properties of the aggregate used in the concrete mix; in general, aggregate with a high elastic modulus will produce low shrinkage concrete. Aggregates which contain clay minerals will affect shrinkage behavior as well. According to Rhoades and Mielenz,

According to Roper, the type of cement plays a significant role in shrinkage of concrete as well. Using type III cement will result in greater shrinkage of concrete due to its fineness. This is also the case for cements containing low sulfate content.

Total air contents of 8% or more, will have an effect on the drying shrinkage of concrete according to Davis and Teoxell.

Brooks reported that the use of admixtures, both chemical and cementitious materials, will affect the magnitude of drying shrinkage in concrete as well. The following table lists the effects these admixtures have on shrinkage of concrete:

Table 2-4. Ingredients affecting the magnitude of drying shrinkage in concrete

Ingredient	Shrinkage
Water-reducing and high-range water-reducing admixtures	May increase by 20% at the same water content depending on composition
Ground slag	May increase shrinkage with increase in replacement
Fly ash	No change
Silica fume (less than 7.5% replacement)	Decrease

Other factors include size and shape of the specimen, method of curing, and relative humidity of the environment where the concrete is mixed, placed, and cured. In general, the rate

of shrinkage is inversely proportional to the ratio of the volume to surface area of the specimen, shown in the following equation from ACI 209.1R-05:

$$shrinkage \propto \frac{1}{\left(\frac{V}{S}\right)^2}$$

where V is volume, and S is surface area. Shrinkage results from Hansen and Mattock supporint this statement are illustrated in the following figure.

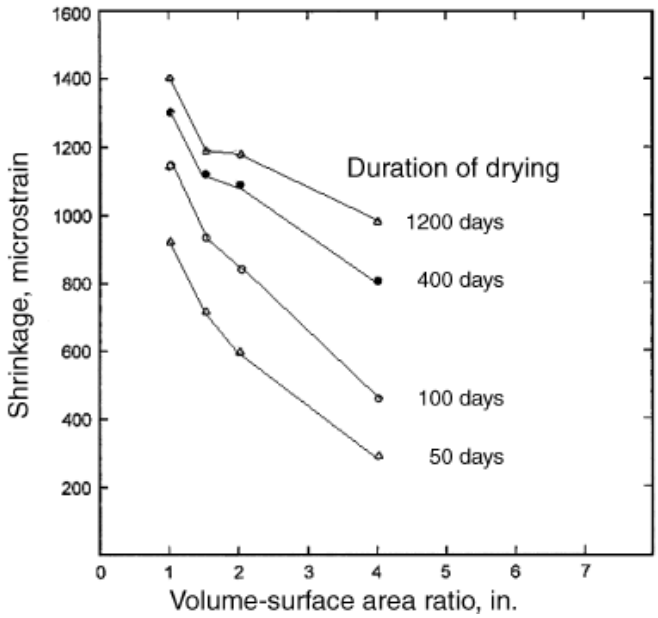

Figure 2-9. Shrinkage strain at different ages versus volume-surface area ratio

2.4.4 Models to Predict Concrete Shrinkage

2.4.4.1 CEB-FIP Model for shrinkage strain prediction

The model to predict creep strain developed by CEB-FIP is shown below:

$$\varepsilon_{cr}(t, t_0) = \frac{\sigma_c(t_0)}{E_{ci}} \cdot \phi_{28}(t, t_0)$$

where $\varepsilon_{cr}(t, t_0)$ is the creep strain at time t, $\sigma_c(t_0)$ is the applied stress, E_{ci} is the modulus of elasticity at the age of 28 days, and $\phi_{28}(t, t_0)$ is the creep coefficient.

The modulus of elasticity, E_{ci}, can be determined by the following equation:

$$E_{ci} = \alpha_E \times 10^4 \cdot \left(\frac{f_{ck} + \Delta_f}{f_{cmo}}\right)^{\frac{1}{3}}$$

where f_{ck} is the characteristic strength of concrete in MPa, Δ_f is equal to 8 MPa, f_{cmo} is equal to 10 MPa, and α_E is equal to 2.15x10^4 MPa

The creep coefficient, $\phi_{28}(t, t_0)$, can be determined by the following equation:

$$\phi_{28}(t, t_0) = \phi_0 \cdot \beta_c(t - t_0)$$

where ϕ_0 is the notational creep coefficient, β_c is the coefficient to describe the development of creep with time after loading, t is the age of concrete in days, t_0 is the age of concrete at time of loading in days.

The notational creep coefficient, ϕ_0, can be determined by the following equations:

$$\phi_0 = \phi_{RH} \cdot \beta(f_{cm}) \cdot \beta(t_0)$$

$$\phi_{RH} = 1 + \frac{1 - \frac{RH}{RH_0}}{0.46 \cdot \left(\frac{h}{h_0}\right)^{\frac{1}{3}}}$$

$$\beta(f_{cm}) = \frac{5.3}{\sqrt{\frac{f_{cm}}{f_{cmo}}}}$$

$$\beta(t_0) = \frac{1}{0.1 + \left(\frac{t_0}{t_1}\right)^{0.2}}$$

$$\beta(t - t_0) = \left[\frac{\left(\frac{t - t_0}{t_1}\right)}{\beta_H + \frac{t - t_0}{t_1}}\right]^{0.3}$$

$$\beta_H = 150 \cdot \left[1 + \left(1.2 \cdot \frac{RH}{RH_0}\right)^{18}\right] \cdot \frac{h}{h_0} + 250 \leq 1500$$

where $f_{cm} = f_{ck} + \Delta_f$, $h = \frac{2A_c}{u}$ is the notational size of the member in mm, A_c is the cross-sectional area in mm^2, u is the perimeter of the member exposed to the atmosphere in mm, h_0 is equal to 100 mm, RH is the relative humidity of the ambient environment expressed in %, RH_0 is equal to 100%, and t_1 is 1 day.

2.4.4.2 Prediction model recommended by ACI-209 Report [1992]

The general equation for predicting shrinkage of concrete is presented next:

$$(\varepsilon_{sh})_t = \frac{t^\alpha}{f + t^\alpha} \cdot (\varepsilon_{sh})_u$$

where $(\varepsilon_{sh})_t$ is the time dependent shrinkage strain, $(\varepsilon_{sh})_u$ is the ultimate shrinkage strain, t is the time after loading, f is in days, and α depends on size and shape of the specimen. For shrinkage after age 7 days for moist cured concrete, ACI recommends a value of 35 for f. The previous equation then becomes:

$$(\varepsilon_{sh})_t = \frac{t^\alpha}{35 + t^\alpha} \cdot (\varepsilon_{sh})_u$$

In the case of absent specific shrinkage data for local aggregates and conditions, ACI recommends the following average value:

$$(\varepsilon_{sh})_u = 780\gamma_{sh} \times 10^{-6} \text{ in./in. (m/m)}$$

where γ_{sh} is the product of the ultimate shrinkage strain under standard conditions by applicable factors. These factors include initial moist curing, ambient relative humidity, average thickness of member or volume –surface ratio, temperature, and concrete composition.

2.5 Creep of Concrete

2.5.1 Rheology of Materials and Definition of Creep of Concrete

There is always strain associated with applied stresses to any material. ASTM E 6-03 defines creep as "the time-dependent increase in strain in a solid resulting from force."

MacGregor and Wight explain that when a load is applied to concrete, it experiences an instantaneous elastic strain which develops into creep strain if the load is sustained. The magnitude of this creep strain is one to three times the value of the instantaneous elastic strain, it is proportional to cement-paste content and, thus, inversely proportional to aggregate volumetric content. The magnitude of creep is dependent upon the magnitude of the applied stress, the age and strength of the concrete, properties of aggregates and cementitious materials, amount of cement paste, size and shape of concrete specimen, volume to surface ratio, amount of steel reinforcement, curing conditions, and environmental conditions. The following figure shows the elastic and creep strains curves as a specimen is being loaded and then unloaded. A recovery can be observed as soon as the stress is removed.

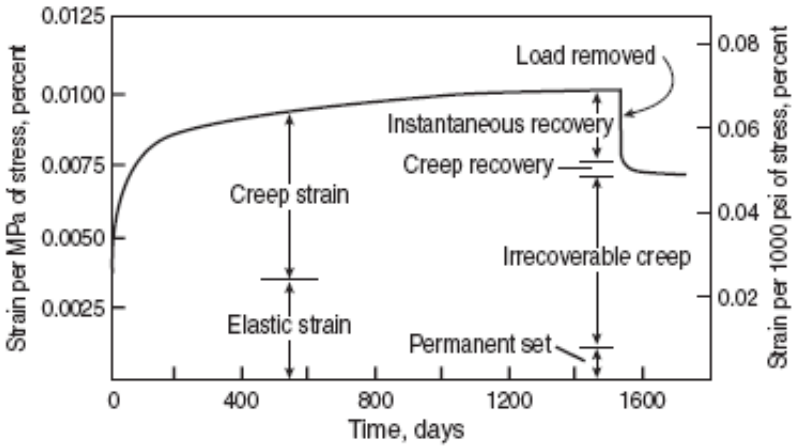

Figure 2-10. Combined curve of elastic and creep strains showing amount of recovery

From the previous figure, several things can be appreciated about how concrete responds to sustain stresses. Concrete exhibits initial elastic strain which depends on the magnitude and rate of applied stress. This strain increases over time due to creep where the concrete will experience inelastic deformation. If the stress is removed, the specimen shows an instantaneous recovery strain lower than the elastic strain on loading, followed by gradual decrease in strain (creep recovery) over time. This recovery curve resembles the creep strain curve, only that the recovery

curve reaches its maximum at a faster rate than the creep strain curve. It must be noted that there is always a residual deformation because the recovery of creep is incomplete, known as irrecoverable creep.

According to Lamond and Pielert, it's the cement paste that exhibits creep upon application of load on a concrete specimen, and this creep is in part due to water movement inside the porous structure of the paste. This could mean that as long as the cement paste hydrates, concrete will experience creep under constant stress.

2.5.2 Significance of Studying Creep Behavior of Concrete

As mentioned before, when concrete is loaded it experiences a large strain upon loading known as the instantaneous elastic strain. Concrete will experience a gradual increase in strain because of this sustained load, and its consideration is therefore of vital importance in structural design.

Creep behavior of concrete is also of great importance especially in today's construction techniques. Because of rapid construction techniques, concrete members will experience loads that can be as large as the design loads at very early age; these can cause deflections due to cracking and early age low elastic modulus. So, creep has a significant effect on both the structural integrity and the economic impact that it will produce if predicted wrong. Engineers must be able to, not only calculate stresses from observed strains, but also calculate the amount of steel reinforcement required to avoid excessive deflections.

According to Liu, misprediction of the actual creep affects the economic factors such as durability, serviceability, and long-term reliability instead of structural failure. Therefore, he claims that it is of great importance to have an accurate prediction model for creep strain of concrete can avoid potentially huge economic losses. Bažant and Panula collected shrinkage and creep data from all over the world to set up a databank known as RILEM databank in 1978, and

this data has been used to evaluate different shrinkage and creep prediction models, namely the ACI 209 model, the CEB 90 model, the B3 model, and the GL 2000 model. ACI recommends short-term testing of creep of concrete to predict the ultimate creep of concrete because shrinkage and creep "may vary with local conditions" (ACI 209.2R-5).

2.5.3 Effect of Aggregate on Creep of Hardened Concrete

Same as with shrinkage, aggregate content affects the amount of creep in concrete. In a study by Neville called "Creep of concrete as a function of its cement paste content," it was found that an increase from 65 to 75 % of volumetric content of the aggregate will decrease the creep by 10 %. According to Neville, the most important factor affecting creep of concrete is the modulus of elasticity and not the strength. Aggregate with high modulus of elasticity means that the aggregate offers great resistance to the strains produced by the stresses applied to the concrete. Neville also has stated that the aggregate restrains the potential creep of the cement paste, expressed by the following formula:

$$log\frac{c_p}{c} = \alpha \cdot log\frac{1}{1-g-u}$$

and

$$\alpha = \frac{3(1-\mu)}{1+\mu+2(1-2\mu_a)\frac{E}{E_a}}$$

where the first equation relates creep to volumetric content of the aggregate and unhydrated cement paste as a function of physical properties of the aggregate and the cement paste expressed in the second equation. Porosity is one physical property that has an indirect effect on the creep of concrete because aggregates with high porosity will usually have a low elastic modulus which will lead to higher relative creep. The table on the next page shows the typical elastic moduli for various types of aggregate as found by Alexander and Mindess.

Aggregate has therefore a direct effect on the long-term deformations of concrete because a high elastic modulus aggregate will produce a stiffer concrete that will have relatively higher resistance to deformation. A linear equation shown in the next page, developed by Teychenné, relates modulus of elasticity of concrete to aggregate properties:

Table 2-3. Strength and elastic modulus of some common aggregates

Aggregate	*Compressive strength* (MPa)	*Elastic modulus* (GPa)
Granite	35–450	15–60
Limestone	90–270	10–80
Sandstone	35–240	5–50
Quartzite	110–470	~80
Marble	50–240	20–65
Gneiss	95–235	25–70
Schist	90–290	~50

$$E_c = K_0 + \beta f_{cu}$$

where E_c is the elastic modulus of concrete, f_{cu} is characteristic of concrete strength, β is a coefficient determined through regression analysis, and K_0 is an aggregate stiffness factor related to the aggregate elastic modulus and its density in the concrete mix. The following figure shows the linear relationship between strength and elastic modulus of concrete, for different types of aggregates.

2.5.4 Prediction Models and Their Limitations of Concrete Creep

For this research, only two creep prediction models are reviewed, namely the CEB-FIP model and the ACI 209 model.

The model recommended by CEB was developed by Muller and Hilsdorf. According to the ACI Committee 209, some engineers prefer this model over the ACI 209 model. The model is indifferent to curing duration or curing conditions of the concrete, but it requires information on

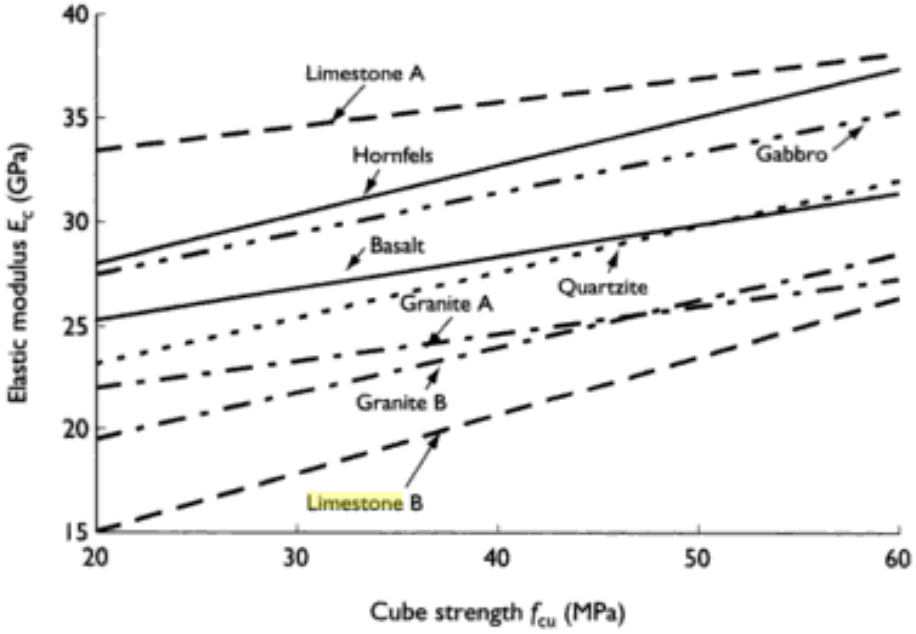

Figure 2-11. Elastic modulus-cube strength relation at 28 days

age of concrete when curing ends, loading age, compressive strength at 28 days, relative humidity, volume to surface ratio of the specimens, and cement type.

The model recommended by ACI 209 was developed by Branson and Christiason and it has been used in the structural design for many years. Some disadvantages include the accuracy if size of specimen tested is not accommodated, and that it does not model shrinkage or creep phenomena and it is therefore empirically based. Another disadvantage is that it does not calculate the compliance, the total load induced strain caused by applied uniaxial sustained load, but it calculates the creep coefficient instead.

2.5.4.1 C.E.B-F.I.P Model Code

The model to predict creep strain developed by CEB-FIP is shown below:

$$\varepsilon_{cr}(t, t_0) = \frac{\sigma_c(t_0)}{E_{ci}} \cdot \phi_{28}(t, t_0)$$

where $\varepsilon_{cr}(t, t_0)$ is the creep strain at time t, $\sigma_c(t_0)$ is the applied stress, E_{ci} is the modulus of elasticity at the age of 28 days, and $\phi_{28}(t, t_0)$ is the creep coefficient..

The modulus of elasticity, E_{ci}, can be determined by the following equation:

$$E_{ci} = \alpha_E \times 10^4 \cdot \left(\frac{f_{ck} + \Delta_f}{f_{cmo}}\right)^{\frac{1}{3}}$$

where f_{ck} is the characteristic strength of concrete in MPa, Δ_f is equal to 8 MPa, f_{cmo} is equal to 10 MPa, and α_E is equal to 2.15x10^4 MPa

The creep coefficient, $\phi_{28}(t, t_0)$, can be determined by the following equation:

$$\phi_{28}(t, t_0) = \phi_0 \cdot \beta_c(t - t_0)$$

where ϕ_0 is the notational creep coefficient, β_c is the coefficient to describe the development of creep with time after loading, t is the age of concrete in days, t_0 is the age of concrete at time of loading in days.

The notational creep coefficient, ϕ_0, can be determined by the following equations:

$$\phi_0 = \phi_{RH} \cdot \beta(f_{cm}) \cdot \beta(t_0)$$

$$\phi_{RH} = 1 + \frac{1 - \frac{RH}{RH_0}}{0.46 \cdot \left(\frac{h}{h_0}\right)^{\frac{1}{3}}}$$

$$\beta(f_{cm}) = \frac{5.3}{\sqrt{\frac{f_{cm}}{f_{cmo}}}}$$

$$\beta(t_0) = \frac{1}{0.1 + \left(\frac{t_0}{t_1}\right)^{0.2}}$$

$$\beta(t-t_0)=\left[\frac{\left(\frac{t-t_0}{t_1}\right)}{\beta_H+\frac{t-t_0}{t_1}}\right]^{0.3}$$

$$\beta_H=150\cdot\left[1+\left(1.2\times\frac{RH}{RH_0}\right)^{18}\right]\cdot\frac{h}{h_0}+250\leq 1500$$

where $f_{cm}=f_{ck}+\Delta_f$, $h=\frac{2A_c}{u}$ is the notational size of the member in mm, A_c is the cross-sectional area in mm^2, u is the perimeter of the member exposed to the atmosphere in mm, h_0 is equal to 100 mm, RH is the relative humidity of the ambient environment expressed in %, RH_0 is equal to 100%, and t_1 is 1 day.

2.5.4.2 Model of ACI 209

The model presented by ACI 209R-5 to predict creep of concrete at any time is shown below:

$$v_t=\frac{t^{\psi}}{d+t^{\psi}}\cdot v_u$$

where $v_t$is the creep coefficient at any time, d is in days (normal range is 6 to 30 days), ψ is a constant dependent on shape and size (normal range is 0.40 to 0.80), and v_u is the ultimate creep coefficient (normal range is 1.30 to 4.15).

For creep coefficient, v_t, for a loading age of 7 days, for moist cured concrete, the previous formula can be rewritten as followed:

$$v_t=\frac{t^{0.60}}{10+t^{0.60}}\cdot v_u$$

ACI recommends an average value of $2.35\gamma_c$ for v_u whenever specific creep data for aggregates and conditions, where γ_c is the product of applicable factors that account for loading age, ambient relative humidity, thickness of member, slump, percent fine aggregate, and air content shown next:

$$\gamma_c = \gamma_{la} \cdot \gamma_\lambda \cdot \gamma_h \cdot \gamma_s \cdot \gamma_\psi \cdot \gamma_\alpha$$

The calculations for each applicable factor are shown next:

$$\gamma_{la} = 1.25(t_{la})^{-0.118}$$

where t_{la} is the loading age in days. This formula is valid for loading ages later than 7 days for moist cured concrete.

$$\gamma_\lambda = 1.27 - 0.0067\lambda$$

where λ is the relative humidity in percent. This formula is valid for ambient relative humidity greater than 40%.

$$\gamma_h = 1.14 - 0.023h$$

where h is the average thickness in inches. This formula is from the average-thickness method, and is valid during the first year after loading. For ultimate values, the formula becomes:

$$\gamma_h = 1.10 - 0.017h$$

where h is the average thickness in inches.

The second method is called volume-surface method and is listed next:

$$\gamma_h = \frac{2}{3}\left[1 + 1.13\ exp\left(-0.54\frac{v}{s}\right)\right]$$

where $\frac{v}{s}$ is the ratio of the member in inches.

$$\gamma_s = 0.82 + 0.067s$$

where s is the slump in inches.

$$\gamma_\psi = 0.88 + 0.0024\psi$$

where ψ is the ratio of fine aggregate to total aggregate by weight expressed as percentage.

$$\gamma_\alpha = 0.46 + 0.09\alpha$$

where α is the air content in percent, not less than 1.0.

CHAPTER 3
MATERIALS AND EXPERIMENTAL PROGRAMS

3.1 Introduction

The following chapter presents the mixes that were studied in this research. It also includes information on preparation, fabrication, and testing procedure. Designation of ASTM standards is added for the testing methods and procedures throughout each phase.

3.2 Concrete Mixtures Evaluated

3.2.1 Mix Proportions of Concrete

A total of 30 batches were prepared for the 18 mix proportions involved in this study. In the first 8 mixes, Miami Oolite aggregate was used and the coarse aggregate was replaced with Georgia Granite by equal volume. For the other 2 remaining mixes Stalite lightweight aggregate was used. The mixes contain different types of admixtures as well. The mixes where fly ash was used are designated with the letter F, while the mixes where slag was used are designated with the letter S. The testing period for each mix is either 1 year, designated as (1y), or 3 months, designated as (3m). Other admixtures including air entrainment, and water reducing agents were used as well, the last being adjusted to achieve the target slump specified by the Florida Department of Transportation (FDOT). All the mixes are presented in Table 3-1.

3.2.2 Mix Ingredients

Information on the ingredients used in each of the mix proportions are presented next:

- Water

  As a general rule, if water is suitable for consumption, it is suitable to use in a concrete mix. Potable water was used as ingredient for each batch.

- Cement

  CEMEX Type I/II Portland cement was provided by the FDOT and used in the batching of the concrete mixes. The properties of this type of cement are shown in Table 3-2.

- Fly ash

  The fly ash was donated by Florida Rock Industries located in Gainesville, Florida. The properties of this admixture are presented in Table 3-3.

- Slag

  The slag was also donated by Florida Rock Industries. Its properties are presented in Table 3-4.

- Fine aggregate

  The fine aggregate used was silica concrete sand from Goldhead of Florida. Table 3-5 shows its properties based on an analysis performed by the FDOT. This document is presented also in the appendix of this research paper.

- Air-entraining admixture

  The air-entraining admixture used is the Darex AEA. This admixture has a density of 63.58 lb/ft^3 and whenever used, the workability and durability of concrete is improved. Workability is improved because bleeding and segregation are minimized due to a reduction in mixing water, and the durability is increased, particularly during freezing and thawing cycles, due to the entrainment of millions of tiny air bubbles.

- Coarse aggregates

  The aggregates used in this part of the study are Florida Limestone and Georgia Granite. The physical properties and gradation of these aggregates are listed in Figure 3-4. The aggregates were in saturated surface dry condition (SSD) at the time the batch was made. To reach this condition, the aggregates were bagged and placed under water for at least 48 hours and then the water was allowed to drain so the surface of the aggregate is "dried up."

- Water-reducing admixture

  The admixtures used include the high-range water-reducing admixture ADVA 140M and ADVA 60. ASTM defines a water reducing admixture as "an admixture that reduces the quantity of mixing water required to produce concrete of a given consistency," and a high range water-reducing admixture as "an admixture that reduces the quantity of mixing water required to produce concrete of a given consistency by 12% or greater." ADVA 60 has a density of 71.74 lb/ft^3 and it's used to produce concrete with lower water concrete with improved workability and higher strength. According to the product description, ADVA 140M has a density of 65.83 lb/ft^3 and does not contain intentionally added chloride. Because low w/c concretes are very dry and thus hard to work with, ADVA 140M provides the necessary workability for easy placement and consolidation without affecting the strength.

Table 3-1. Mix proportions of the 14 concrete mixtures used in this study

Coarse Agg.	No. of Mix	W/C	Cement (lbs/yd^3)	Fly ash (lbs/yd^3)	Slag (lbs/yd^3)	Water (lbs/yd^3)	FA (lbs/yd^3)	CA (lbs/yd^3)	Admixture	
									AE	WRDA/ADVA
Miami Oolite	Mix-1F	0.24	800	200	---	236.0	931	1679	7.5 OZ	(WRDA60)-30OZ (ADVA120)-60OZ
	Mix-2F	0.33	656	144	---	265.6	905	1740	12.0 OZ	(WRDA60) -30OZ
	Mix-3F	0.41	494	123	---	254.0	1175	1747	0.5 OZ	(WRDA60)-33.4OZ
	Mix-4F	0.37	600	152	---	278.0	1000	1774	2.0 OZ	(WRDA60) -56OZ
	Mix-5S	0.33	400	---	400	262.0	1062	1750	6.0 OZ	(WRDA60)-24OZ (ADVA120)-48OZ
	Mix-6S	0.36	380	---	380	270.0	1049	1736	1.9 OZ	(ADVA120) -38OZ
	Mix-7S	0.41	197	---	461	267.0	1121	1750	4.6 OZ	(WRDA60)-32.9OZ
	Mix-8S	0.44	306	---	306	269.0	1206	1710	3.1 OZ	(WRDA60)-30.6OZ
Stalite lightweight	Mix-9LF	0.31	602	150	---	235.3	952	1239	9.6 OZ	(WRDA64) -30OZ
	Mix-10LS	0.39	282	---	423	275.0	853	1300	8.8 OZ	(WRDA64)-31.7OZ
Georgia Granite	Mix-1GF	0.24	800	200	---	236.0	960	1948	7.5 OZ	(WRDA60)-30OZ (ADVA120)-160OZ
	Mix-2GF	0.33	656	144	---	265.6	909	1981	12.0 OZ	(WRDA60) -30OZ
	Mix-3GF	0.41	494	123	---	254.0	1176	2027	0.5 OZ	(WRDA60)-33.4OZ
	Mix-4GF	0.37	600	152	---	278.0	1000	2056	2.0 OZ	(WRDA60)-56OZ
	Mix-5GS	0.33	400	---	400	262.0	1066	2045	6.0 OZ	(WRDA60)-24OZ (ADVA120)-48OZ
	Mix-6GS	0.36	380	---	380	270.0	1049	2075	1.9 OZ	(ADVA120) -38OZ
	Mix-7GS	0.41	197	---	461	267.0	1125	2045	4.6 OZ	(WRDA60)-32.9OZ
	Mix-8GS	0.44	306	---	306	269.0	1125	2044	3.1 OZ	(WRDA60)-30.6OZ

Table 3-2. Physical properties of Type I cement

Loss on Ignition (%)	Insoluble Residue (%)	Setting Time (min)	Fineness (m^2/kg)	Compressive Strength at 3 days (psi)	Compressive Strength at 7days (psi)
1.5%	0.48%	125/205	402.00	2400 psi	2930 psi

Table 3-3. Chemical ingredients of Type I cement

Ingredients	SiO_2	Al_2O_3	CaO	SO_3	Na_2O-K_2O	MgO	Fe_2O_3	C_3A	C_3S	C_2S	C_4AF+C_2F
(%)	20.3%	4.8%	63.9%	3.1%	0.51%	2.0%	3.3%	7%	59%	13.8%	15.8%

Table 3-4. Physical and chemical properties of fly ash

SO_3 (%)	Oxide of Si, Fe, Al (%)	Fineness (%) (ASTM C430)	Strength (7d) (%) (ASTM C109)	Strength (28d) (%) (ASTM C109)	Loss on Ignition (%) (ASTM C311)	Moisture Content (%) (ASTM C-618)
0.35	87.82	N/A	77.1	82.8	3.52	0.1

Table 3-5. Physical and chemical properties of slag

SO_3 (%)	Oxide of Si, Fe, Al	Fineness (%) (ASTM C430)	Strength (7d) (%) (ASTM C109)	Strength (28d) (ASTM C109) (%)	Loss on Ignition (%) (ASTM C311)	% of water (ASTM C-618)
1.7%	N/A	4	92%	129	N/A	N/A

Table 3-6. Physical properties of fine aggregate

Fineness Modulus	SSD Specific Gravity	Apparent Specific Gravity	Bulk Specific Gravity	Absorption
2.20	2.640	2.651	2.634	0.20%

Table 3-7. Physical properties of coarse aggregates

Aggregate	SSD Specific Gravity	Apparent Specific Gravity	Bulk Specific Gravity	Absorption
Miami Oolite	2.371	2.504	2.283	3.88%
Stalite	1.55	-	-	6.60%
Georgia Granite	2.815	2.845	2.798	0.58%

Figures 3-1 through 3-3 show the gradation charts based on standard sieves on all the aggregates used. These are the gradation of Goldenhead fine aggregate, the gradation of Miami Oolite limestone coarse aggregate, and the Georgia granite coarse aggregate. The graphs show that these aggregates meet ASTM standards by falling within the standard limits.

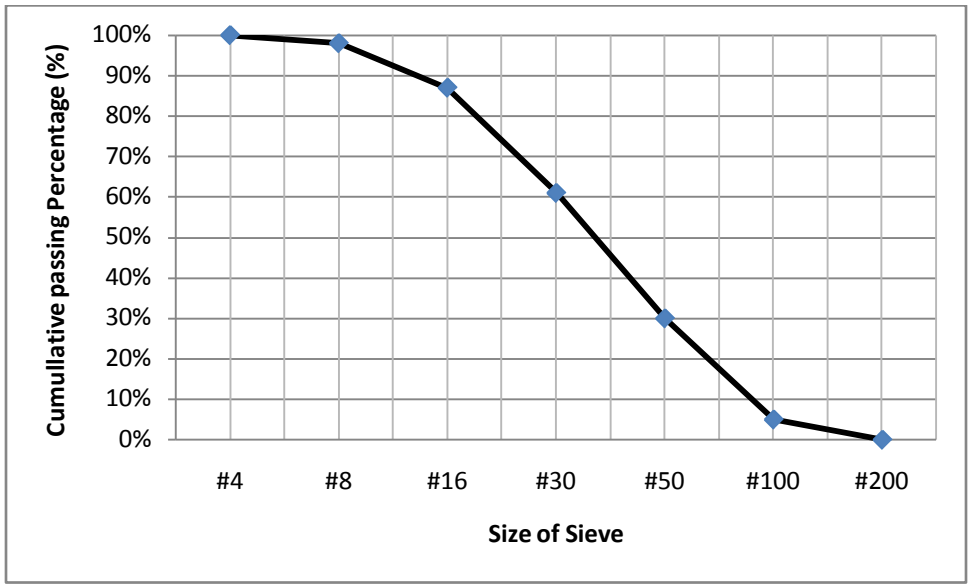

Figure 3-1. Gradation of fine aggregate (Goldenhead sand)

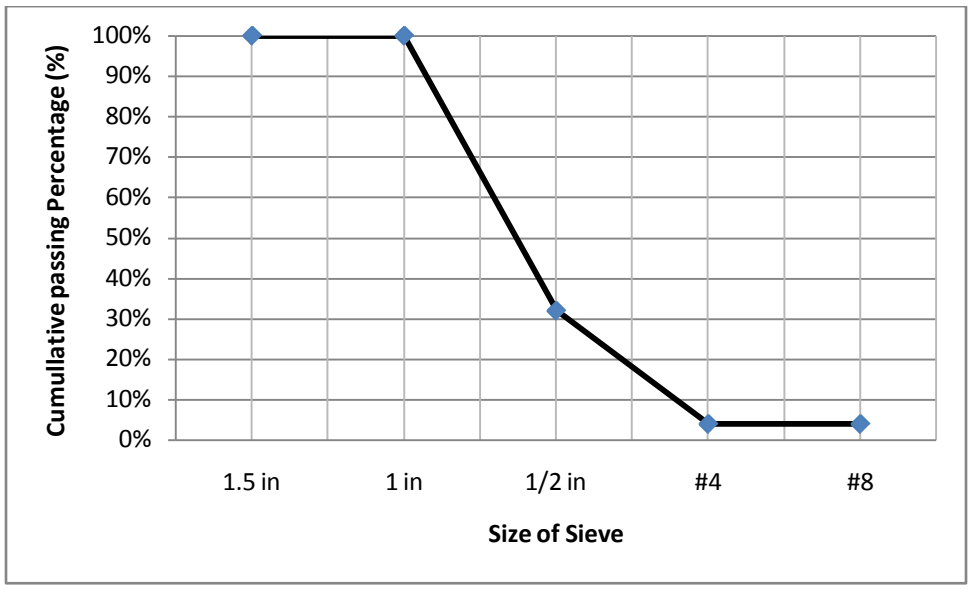

Figure 3-2. Gradation of coarse aggregate (Miami Oolite limestone)

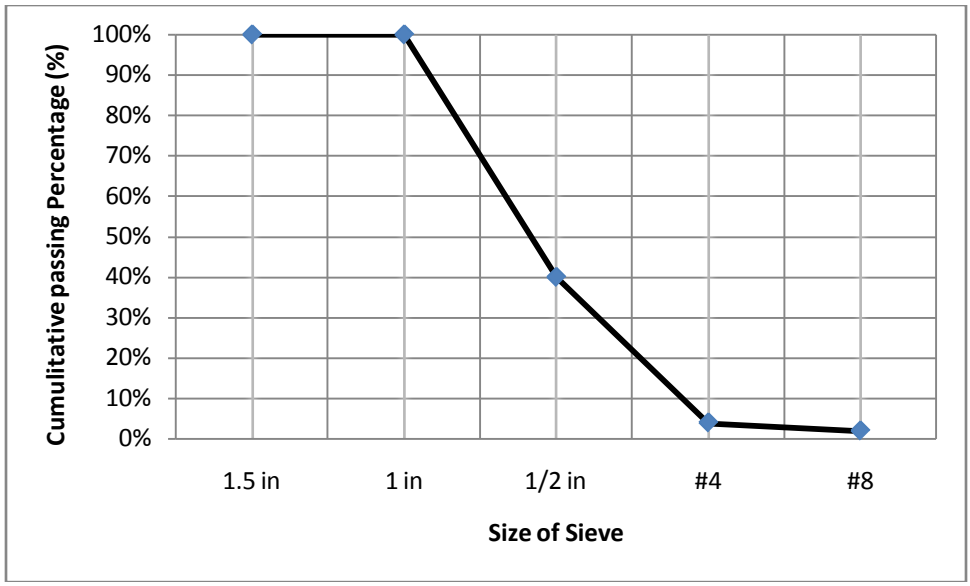

Figure 3-3. Gradation of coarse aggregate (Georgia granite)

3.3 Fabrication of Concrete Specimens

The standard procedures involved in the preparation of specimens are listed in Table 3-8

Table 3-8. Testing procedures involved in the preparation of specimens

Test	Making and Curing Concrete Test Specimens in the Field	Making and Curing Concrete Test Specimens in the Laboratory	Molds for Forming Concrete Test Cylinders Vertically	Capping Cylindrical Concrete Specimens
Designation	ASTM C31	ASTM C192	ASTM C470	ASTM C617

3.3.1 The Procedure to Mix Concrete

A compulsive pan mixer with capacity of 17 cubic feet was implemented to fabricate the specimens from the mixes investigated in this study. The mixes from Table 3-1 were scaled down to 10 to 13 cubic feet depending on number of plastic molds available to fabricate the specimens. Care was taken as to batch the mixes with about 10% excess to account for the tests on fresh concrete and waste. Before mixing each batch, the mixer was “buttered” as well, which

consists of about 10% of all mixing ingredients excluding coarse aggregate and admixtures. This is done to compensate for mortar loss when fresh concrete is discharged from the mixer.

Figure 3-4. Compulsive Pan Mixer

The steps that were used to mix each batch are listed below:

- All the mixing ingredients, including the admixtures, were scaled down and weighed out. 10% of all ingredients excluding coarse aggregate and admixtures were additionally weighed as well.
- The aggregate (both coarse and fine) were added to the mixer. The mixer was started and while it was running, the cementitious materials and about 2/3 of the water together with the air entraining admixture were added. The remaining 1/3 of the water was added while the mixer was running.
- The water reducing admixture(s) was/were added gradually over about 1 minute while the mixer was still running. The total mixing time at this phase is about 3 minutes. The mixer was then shut off for about 3 minutes to let the aggregate absorb some of the paste, and then it was turned on again for a final mixing time of 2 minutes.
- During the 3 minute rest, the slump was measured to ensure that the target slump was reached. The slump was tested in accordance with ASTM C143. If the target slump was not reached, then additional water reducing admixture was added, mixed again, and the slump was again measured.

3.3.2 The Procedure to Fabricate Specimens

After the mix is batched, the cylinder molds need to be filled. These molds are approximately 6 inches in diameter and 12 inches in height and are made by a non absorbent plastic. These molds were placed on the vibrating table before being filled with concrete. The

molds were filled depending on the slump of the concrete. For example, if the slump is less than 7 inches, the molds were filled in three equal layers, and each layer was consolidated by means of the vibrating table. The length of the vibrating time is mix and effectiveness of the vibrator dependent, and is usually determined by looking at how frequent air bubbles come to the surface. If the slump is 7 inches or more, then the consolidation process is done by hand by rodding each layer 25 times. Regardless of the consolidation method used, the last layer was overfilled to compensate for concrete loss when it is being vibrated.

After consolidation, strike off any excess concrete and finish with a trowel. Carefully place the finished molds on a flat surface and cover to prevent evaporation. The specimens are cured for about 24 hours before being demolded and placed in the 100% moisture room, where they will remain until hardened properties are needed.

3.3.3 The Procedure to Test Specimens

Before the compressive strength, modulus of elasticity, and creep tests are run, the surfaces of each concrete specimen need to be grinded to ensure a plane surface when applying the load. The specimens that are used for determining the tensile strength can be tested directly after removing them from the moisture room.

3.4 Curing Conditions for Concrete Specimens

The curing condition varies depending on the testing as well as testing age. Samples for splitting tensile test, compressive strength, and modulus of elasticity, were cured in the 100% moisture room up to the time they were about to be tested. Samples for shrinkage and creep tests are cured up to 7 and 14 days from the day they are casted in 100% moisture room, and then cured in 50% moisture room until they are ready to be tested.

3.5 Tests on Fresh Concrete

Table 3-9 presents the tests that were done on concrete when it was still in plastic state.

These tests were performed by FDOT trained technicians.

Table 3-9. The testing programs on fresh concrete

Test	Slump	Air Content	Unit Weight	Temperature
Test Standard	ASTM C143	ASTM C 173	ASTM C138/ C231	ASTM C 1064

- Slump test

  The slump test was determined in accordance with ASTM C143. The slump test is a measure of relative fluidity and was performed to determine the consistency of the fresh concrete. The test was run during the 3 minute-resting period of the mixing process.

- Air content test

  The air concrete test was determined in accordance with both ASTM C173 and ASTM C231. The test determines the entrained air as well as the entrapped air in the concrete.

- Unit weight test

  The unit weight test was determined in accordance with ASTM C138. This test is an indicator of the quality of fresh concrete. Lower strengths are expected if the test yields a lower unit weight relative to the theoretical unit weight. The test was run at the time the sample was obtained.

- Temperature test

  The temperature was determined in accordance with ASTM C1064. Determining the temperature of fresh concrete is important because its value can predict quality, time of set, and strength. Temperature affects the performance of admixtures and initial high temperatures will lead to high early strengths but lower quality at later ages. The sensing part of the thermometer was submerged at least 3inches into the fresh concrete right after the sample was obtained. When the reading was stable, the thermometer was then removed and the reading was recorded.

The results for the tests run on fresh concrete for all mixes involved in this study are presented in Table 3-10. An additional column is added with the theoretical unit weight for comparison purposes that may explain some of the result of the strength tests.

Table 3-10. Properties of fresh concrete

Mix	Slump (in)	Air Content (%)	Unit Weight (pcf)	Theoretical Unit Weight (pcf)	Temperature (^{o}F)
1F(1y)	7.75 (9.75)*	1.50 (1.25)*	143.1 (145.5)*	142.4	80 (81)*
2F(1y)	7.50 (4.25)*	7.30 (4.50)*	133.4 (137.7)*	137.4	79 (73)*
3F(1y)	1.50 (2.00)*	1.60 (2.50)*	145.7 (143.9)*	140.5	79 (76)*
4F(1y)	3.00 (3.00)*	1.30 (2.00)*	142.6 (143.8)*	140.9	74 (74)*
5S(1y)	8.25	7.30	133.3	143.5	75
5S(3m)	7.25 (9.00)*	6.80 (3.75)*	136.9 (141.6)*	143.5	81 (78)*
6S (1y)	1.50	3.80	139.3	141.3	76
6S(3m)	3.50 (5.50)*	3.40 (2.25)*	143.4 (140.4)*	141.3	79 (81)*
7S(1y)	4.50	8.60	129.8	140.6	76
7S(3m)	4.00 (5.75)*	5.50 (5.50)*	138.8 (138.1)*	140.6	77 (79)*
8S(1y)	6.50	6.80	135.1	140.6	78
8S(3m)	2.75 (3.00)*	5.30 (3.75)*	138.9 (140.4)*	140.6	80 (76)*
9LF(1y)	3.75 (2.50)*	5.20 (3.00)*	116.9 (117.7)*	117.7	79 (80)*
10LS(1y)	3.50 (2.75)*	5.50 (5.25)*	111.6 (109.2)*	116.0	77 (78)*
1GF(1y)	2.00	2.70	150.8	152.4	81
1GF(3m)	1.00	2.90	147.0	153.5	85
2GF(1y)	7.50	3.40	144.9	146.5	78
2GF(3m)	3.50	6.00	144.1	146.5	79
3GF(1y)	7.50	1.50	150.1	150.9	79
3GF(3m)	3.25	3.00	150.5	150.9	83
4GF(1y)	8.50	3.00	147.0	151.3	81
4GF(3m)	2.50	1.90	150.7	151.3	85
5GS(1y)	6.50	5.50	145.8	154.6	76
5GS(3m)	7.25	8.50	138.8	154.6	80
6GS(1y)	4.25	1.70	150.5	153.9	77
6GS(3m)	2.50	2.60	151.0	153.9	77
7GS(1y)	2.25	3.80	147.3	151.7	74
7GS(3m)	5.75	3.50	146.6	151.7	80
8GS(1y)	6.50	2.90	147.6	150.0	78
8GS(3m)	6.00	6.90	144.1	150.0	75

*Note: * the values in ( ) were those obtained from the replicate mixes from the previous phase of this study.*

3.6 Tests on Hardened Concrete

Table 3-11 presents the tests that were done on hardened concrete. These tests were performed at the FDOT and UF.

Table 3-11. The testing program on hardened concrete

Test	Compressive Strength	Splitting Tensile Strength	Elastic Modulus	Shrinkage	Creep
Test Standard	ASTM C 39	ASTM C 496	ASTM C 469	Described in this chapter	Described in this chapter

3.6.1 Compressive Strength Test

Compressive strength can be defined as the maximum stress a concrete specimen can withstand when loaded axially; it is one of the most important properties since concrete is subjected to compressive stresses in most structural applications. The actual compressive strength is computed from the formula

$$f_c = \frac{P}{\pi D^2}$$

where f_c = actual compressive strength

P = failure load

D = diameter of the specimen

The concrete specimens in this study where casted and tested in accordance with ASTM Standards "Making and Curing Concrete Specimens in the Field" (C 31), and "Compressive Strength of Cylindrical Concrete Specimens" (C 39). The purpose of this test is to analyze the compressive strength development of the various mixes as well as determine the load to be applied for the creep testing portion of this study. Since all the mixes involved in this study contain admixtures, this data can also be used to develop equations necessary to predict the compressive strength of concrete mixes containing admixtures at different ages.

For each mix, a total of 18 cylindrical specimens were casted and tested after 3, 7, 14, 28, 56, and 91 days of mixing; 3 specimens per testing age. Each specimen was 6" ± 0.02" in diameter, and a length of about 11.75" after grinding top and bottom ends. The diameter was measured at the mid section of the specimen, 90° apart, to the nearest 0.01 inch. The specimens are grinded in the grinding machine prior to the testing procedure. Grinding the specimens ensures an even distribution of the load applied by the compression machine. The load on each specimen was applied at a rate of 35±5 psi/s until failure. During the testing procedure, no

adjustments were made to the loading rate. The actual compressive strength at a certain age was calculated by means of equation (3-1) and the average result of the three samples tested. Sketches of types of fractures are shown in the figure below. The figure was taken from ASTM C39.

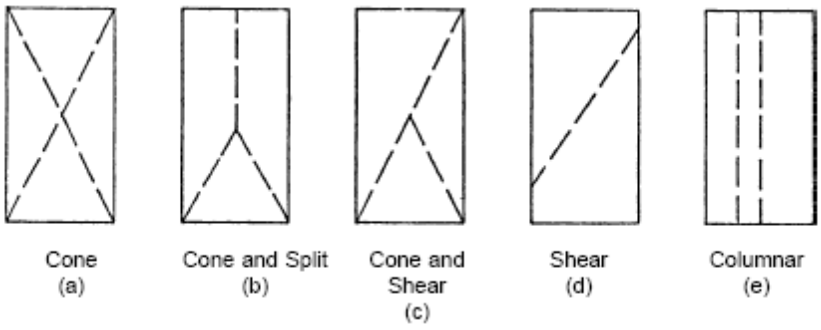

Figure 3-5. Sketches of types of fracture

3.6.2 Splitting Tensile Strength Test (or Brazilian Test)

For each mix, a total of 18 cylindrical specimens were casted and tested after 3, 7, 14, 28, 56, and 91 days of mixing; 3 specimens per testing age. The diameter was taken near the ends and at the mid section of the specimen to the nearest 0.01 inch. Two length measurements are taken along the plane where the specimen is going to be loaded. The specimen is then placed in a special frame with bearing strips made out of plywood placed at both the upper and lower bearing blocks. These bearing strips are used to ensure an even distribution of the load and are their lengths are longer than the specimens. The aligning jig containing the specimen and the bearing strips is then centered in a way that the platens of the testing machine are aligned with the bearing strips when the load is applied. The next figure is a picture showing a specimen being tested.

The specimen was then loaded within 100 to 200 psi/min until failure without adjusting the loading rate.

Splitting tensile strength can be defined as the maximum stress a concrete specimen can withstand under axial tensile loading along two axial lines which are diametrically opposite

Figure 3-6. Specimen being tested for splitting tensile strength

(Mehta and Monteiro). While most structures and structural members are subjected to compressive loads, the value of the tensile strength is of practical significance in slab design, shear strength, and resistance to cracking, because cracking is due to tensile failure regardless of loading or environmental conditions (Popovics, 1998). The splitting tension strength is computed with the formula

$$T = \frac{2P}{\pi l d}$$

where T = Tensile strength

P = failure load

l = length

d = diameter of the specimen

The value of splitting tension strength is closely related to compressive strength and has a low magnitude and its value lies between 8% and 14% to that of the compressive strength.

Despite this close relationship, one cannot assume direct proportionality. In fact, the tensile strength development rate decreases as the compressive strength development increases beyond 28 days of age (Neville, 1996).

3.6.3 Elastic Modulus Test

The pre-testing procedure to determine the elastic modulus is complicated. A companion specimen from the same mix, with the same conditions, and same age, is tested for compressive strength by means of ASTM C39 and this value is recorded. Then, the next specimen needs to be aligned in the compressometer (shown in fig 3-8) before it can be loaded. When the specimen is properly centered under the bearing block of the compressive strength machine (shown in fig 3-8), the specimen is loaded a total of three times. The first time is a 'trial' run to check the seating of the gauges, the rate of loading, and any other unusual or erroneous set up. Therefore, no data is recorded for this run. For the second and third runs, the modulus of elasticity is determined by loading the each specimen to 40% of the compressive strength of the companion specimen. The program at the FDOT allows you to choose the straight part of the stress-strain diagram to calculate the slope and thus the elastic modulus based on ultimate load and gauge length. The specimens are loaded at a rate of 35 ± 5 psi, without adjusting the rate of loading during the runs. More detailed procedure is listed in ASTM C469.

3.6.4 Shrinkage Test

Each mix has three 6" x 12" samples for each curing condition. The first curing condition involves curing the specimens for 7 days in the 100% moisture room, followed by 50% moisture curing until the day of testing. The other condition involves curing the specimens for 14 days in the 100% moisture room, followed by 50% moisture curing until the day of testing.

To measure the unrestrained shrinkage of each specimen, 3 sets of gages are installed on each sample. To install these sets of gages is an intricate process. First, a gage positioning guide

Figure 3-7. Extensometer attached to specimen

is used to put marks on the cylinder molds. The gage positioning guide is shown in Figure 3.9. A drill is then used to drill holes in the cylinder molds; these holes must be as big as the diameter of the gauges to be installed. Once the holes are drilled, their inside of the molds must be cleaned by executing a "sanding" motion with a razor blade where the hole was drilled. This is to make sure that all the holes are free of any obstruction when installing gages inserts and that there are no plastic leftovers when samples are made.

Figure 3-8. Gauge Positioning Guide

Once the molds are cleaned, the gage inserts are installed with temporary screws that will hold the inserts in place. When the samples are casted and cured for about 24 hours, these screws are then removed so the samples can be demolded. The samples are then cured accordingly (curing conditions is explained at the beginning of this section) and the gages are then installed and fixed with epoxy compound. Figure 3.10 shows three samples with the gage already installed.

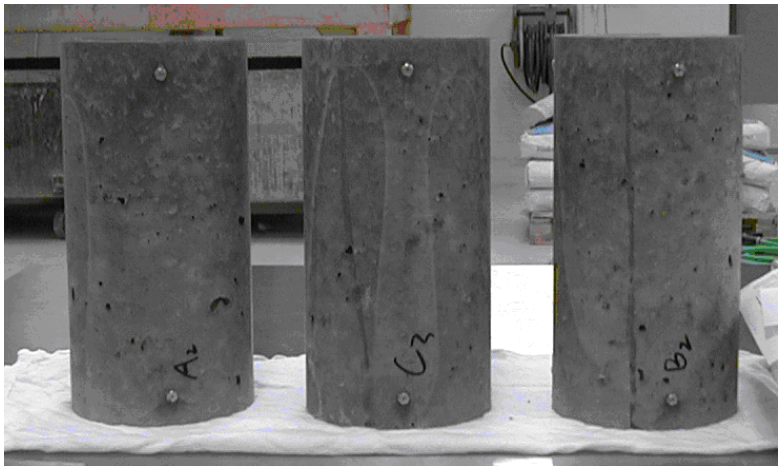

Figure 3-9. Cylindrical specimen with gage points installed

A digital extensometer is used to measure the distance between gages in each set to the nearest 0.0001 inch. For each specimen 3 readings are taken, and for each curing condition 9 readings are taken in total.

The occurrence of each reading is explained next. Readings must be taken 2 to 6 hours after the initial reading was taken (which should correspond with the first reading on the samples of the same mix tested for creep), then each day for 2 weeks, once a week for one month, and once a month until the end of the testing period.

The formula to calculate the shrinkage strain is presented next.

$$\varepsilon_{sh} = \frac{1}{9}\sum_{i=1}^{9}\frac{(l_i - l_0)}{l_0}$$

where ε_{sh} is the average shrinkage strain of the sample, l_i is the measured distance between the ith pair of gage points, and l_0 is the initial distance between the ith pair of gage points and taken as initial reading. As can be seen from the formula, the shrinkage strain is an average of 9 readings with respect to the initial reading, l_0. So, extra care must be taken when l_0 is taken because the calculated strain depends on its value.

3.6.5 Creep Test

The preparation for the samples to be tested under creep is the same as the ones for shrinkage testing. The loading procedure is explained next. Before the specimens are loaded in the creep frames, the compressive strength of companion samples from the same mix need to be determined by means of ASTM C39 so that they can be loaded at 40% of this ultimate strength. The taking of the readings is exactly as for the shrinkage samples, only that readings need to be taken right before and right after loading them. Figure 3-10 shows a set of specimens loaded in the creep frame.

Figure 3-10. Specimens in the creep frame

The creep strain is calculated by the following formula:

$$\varepsilon_c = \frac{1}{9}\sum_{i=1}^{9}\frac{(l_i - l_0)}{l_0}$$

where ε_c is the average creep strain of the sample, l_i is the measured distance between the ith pair of gage points, and l_0 is the initial distance between the ith pair of gage points and taken as initial reading. As can be seen from the formula, the creep strain is an average of 9 readings with respect to the initial reading, l_0. So, extra care must be taken when l_0 is taken because the calculated strain depends on its value.

CHAPTER 4
CREEP FRAME AND CREEP TESTING PROCEDURE

4.1 Introduction

This chapter describes the creep frames and the creep testing procedure step by step, as well as the instrumentation used to carry out the experiments.

4.2 Creep Test Apparatus

Figure 4-1 shows a picture of the creep frame and the different components it includes:

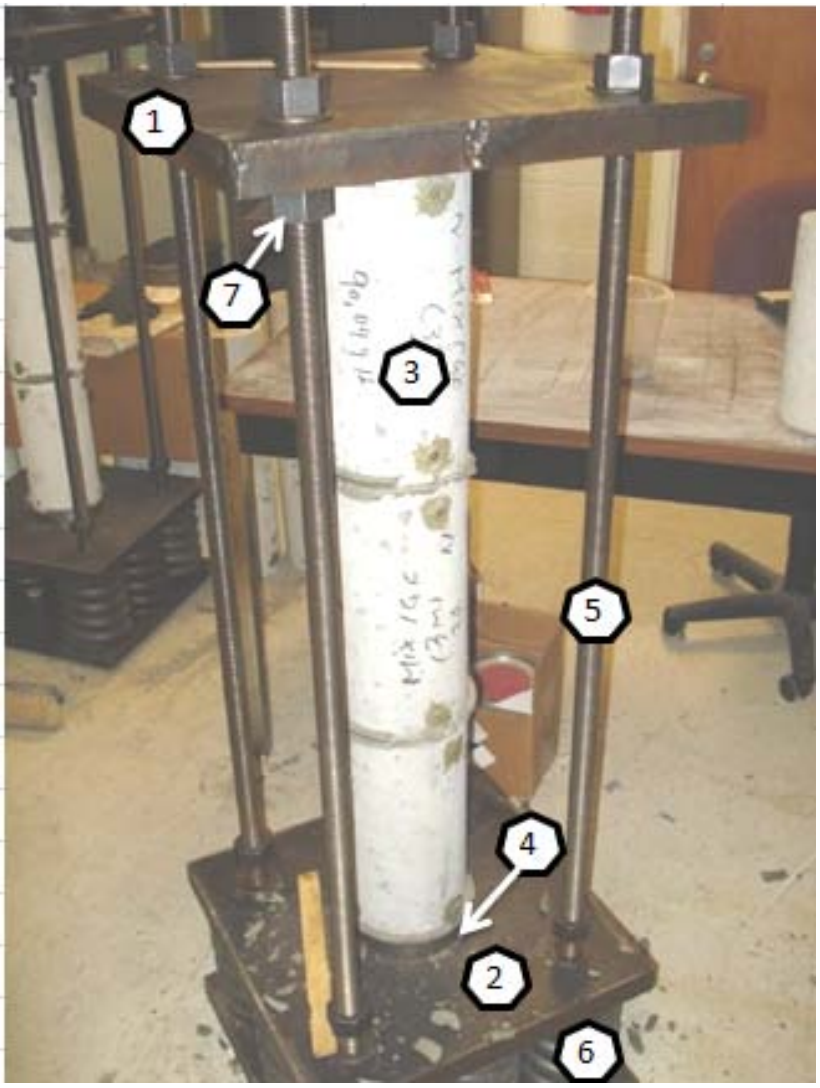

Figure 4-1. Creep test apparatus

The creep apparatus is designed to carry 10 ksi of compressive strength of concrete

mixtures commonly used in Florida. Since the creep tests are run based on 40% or 50% of the ultimate load, the ultimate load that the creep frame can carry is of:

$$P_{max} = 50\% \cdot 10{,}000 \cdot \pi \cdot 3^2 = 141{,}300\ lb$$

1. Header plate
2. Bottom plate
3. Concrete column made up by stacking 3 concrete specimens vertically
4. Metal plate placed at bottom and top of the concrete column
5. Steel rod
6. 9 steel springs
7. Nuts

4.3 Gage-Point Positioning Guide

Figure 4-2 shows the picture of the gage-positioning guide used to position the gage-points on the 6" x 12" cylinder molds.

Figure 4-2. Gauge position guide

The cylinder mold is placed in this frame and the guides are used to mark tiny holes on the mold itself. The guides are unscrewed and holes having the same diameter as the strain gage are made by using a drill machine. Temporary screws with gage seats are then installed. When the

hardened concrete is ready to be demolded, the temporary screws are removed and the strain gages are then placed.

4.4 Preparation of Specimens

Before aligning the specimens for the creep test there are several steps that take precedence. First, the specimens are ground in the grinder and capped with a special sulfur mortar compound. Figure 4-3 shows a specimen capped with this compound. The capping procedure is in accordance with ASTM C 617 Standard Practice for Capping Cylindrical Concrete Specimens.

Figure 4-3. Capping procedure for specimen to be tested in creep frame

When all specimens are capped, the strain gages are screwed into the embedded seats and the specimens are stacked up and placed in the creep frame as Figure 4-1 depicts. Each set consists of 3 cylinders stacked vertically in a columnar shape. Two circular plates are placed between the top specimen and the bottom one.

4.5 Mechanical Strain Gauge

Figure 4-4 on the next page shows the mechanical strain gage used to measure the distances between the strain gage pairs on each specimen. The mechanical strain gage is accompanied by a instrument frame made of aluminum alloy that does not change length with changes in temperature. The mechanical strain gage can make measurements to the nearest 0.0001 in.

Figure 4-4. Mechanical Strain Gage

4.6 Creep Testing Procedure

After the strain gages are installed, the specimens are capped, they are stacked in the creep frame in a columnar shape, and the gage points have been identified properly, this is the procedure that follows:

1. Specimens need to be centered so that they make contact with the middle of the plate. To achieve this, points can be marked on the top and bottom plate surfaces. These mark points are the perimeter of a 6in circle.

2. When the specimens are centered, the header plate needs to be brought down by unscrewing the four nuts that hold it in place until it's in contact with the steel plate on top of the concrete column. At this point, it must be make sure that the concrete column is centered on both the top and bottom, and that there is enough clearing distance between the four nuts that hold the header plate and the header plate itself. When the creep frame is loaded, the header plate will come down so the travel path is needs to be free of obstructions. The four nuts that are on the top of the header plate can be screwed slightly to provide stability.

3. Next, the jack cylinder is centered on the top of the header plate. The load cell is placed on top of the jack cylinder. It needs to make sure that the concrete column is on the same axis as the jack cylinder and the load cell prior to the loading procedure to avoid eccentricity.
4. Next, a water level is used to check that the top plate is level. There are four nuts on top of this plate and 2 underneath. These six nuts can be adjusted until the plate is level.

5. The creep frame is preloaded to 500 lb to properly seat the cylinders in the creep frame. At this point, the initial measurements are taken for all pair of gages for all concrete specimens.

6. Jackets are placed around each cylinder making up the concrete column prior to the application of the load. This is a safety measure in case the cylinders explode because of eccentricity during the loading process. Then, the load is applied manually until the desired load level is reached, the four nuts on the top of the header plate are tightened up and the instantaneous measures are taken.

7. Measurements are taken at 1 hour, 3 hours, 6 hours, every day for the first two weeks, and once a week for the first 3 month. If the specimens are tested for longer periods, then measurements need to be taken once a month until the end of the testing period.

The following formula is used to calculate the creep strain for all specimens in each creep frame:

$$\varepsilon_C = \varepsilon_T - \varepsilon_S = \frac{1}{9}\left(\sum_{i=1}^{9} \frac{l_i^T - l_{0(i)}^T}{l_{0(i)}^T} - \sum_{i=1}^{9} \frac{l_i^S - l_{0(i)}^S}{l_{0(i)}^S}\right)$$

where ε_C is the creep strain of concrete, ε_T is the sum of creep strain and shrinkage strain, ε_S is the shrinkage strain of concrete, l_i^T is the measurement taken from the ith pair of gage points for creep test, $l_{0(i)}^T$ is the initial length of the ith pair of gage points for creep test, l_i^S is the measurement taken from the ith pair of gage points for shrinkage test, $l_{0(i)}^S$ is the initial length of the ith pair of gage points for shrinkage test, and i is the number of pair gage points from 1 to 9.

The formula to calculate the creep coefficient is presented next:

$$C_{cr} = \frac{\varepsilon_C}{\varepsilon_E}$$

where C_{cr} is the creep coefficient, ε_C is the creep strain of concrete, and ε_E is the elastic strain of concrete.

The formula to calculate the creep modulus is presented next:

$$E_c = \frac{\sigma}{\varepsilon_E - \varepsilon_C}$$

where E_c is the creep modulus, σ is the applied stress to the creep frame, $\varepsilon_E - \varepsilon_C$ is the total strain excluding the shrinkage strain.

4.7 Summary on the Creep Testing Procedure

As with any testing procedure, errors should be minimized whenever possible by carefully executing the pre-test and the testing procedure with consistence. When making the holes in the plastic molds, extra care must be taken that the drill is used properly so that the pair of holes made is exactly 10 inches apart. The stacking up of the cylinders in the creep frame can be time consuming as well. Sometimes, the gage points are not fixed on the specimens. To solve this problem, before the initial measurements are taken, epoxy can be used to fix the gages to the specimens. Other things to consider include avoiding pushing the concrete when finishing to avoid movement of the gage seats when the concrete starts to set. Manual hydraulic pump should be avoided because it seems to have an effect on the instantaneous strain.

CHAPTER 5
ANALYSIS OF STRENGTH TEST RESULTS

5.1 Introduction

The results and analysis for the different strength tests as well as modulus of elasticity tests are presented in this chapter. The relationship between compressive strength and splitting tensile strength is discussed, as well as the relationship between compressive strength and modulus of elasticity.

5.2 Results and Analysis of Compressive Strength Tests

The following table lists the compressive strength for each mix at the different testing ages. The compressive strength was calculated by calculating the compressive strength of 3 specimens by means of equation 3-1, and averaging the results. The concrete mixes which are tested up to one year are designated as (1y), and the concrete mixes which are tested up to 3 months are designated as (3m). The individual compressive strength values for the 18 mixes evaluated in this study are shown in Table A-1 in Appendix A.

Table 5-1. Compressive strength of the concrete mixtures evaluated (psi)

Mix		Fly		Age of Testing (days)					
Number	W/C	ash	Slag	3	7	14	28	56	91
1F(1y)	0.24	20%		8077	8572	8993	9536	10771	11267
2F(1y)	0.33	20%		4077	4658	6028	6506	6838	7607
3F(1y)	0.41	20%		5289	6470	7567	8241	8449	9426
4F(1y)	0.37	20%		5712	6919	7114	7236	8996	9271
5S(1y)	0.33		50%	4382	5270	5899	5574	6131	6459
5S(3m)	0.33		50%	5554	7235	8248	8832	9139	9456
6S(1y)	0.36		50%	5253(6)*	5816	5915	6039(30)*	---	7019(94)*
6S(3m)	0.36		50%	6375	7699	8587	9111	9529	9661
7S(1y)	0.41		70%	3642(6)*	3868	4260	5299(30)*	4622	4097
7S(3m)	0.41		70%	4324	5374	5927	6392	6794	6917
8S(1y)	0.44		50%	3101	3955	4517	4793	4880	4548
8S(3m)	0.44		50%	4795	6114	6939	7525	8119	8208
9LF(1y)	0.31	20%		3039	3941	5136	5929	6690	6961
10LS(1y)	0.39		60%	1467	2191	2937	3744	4312	4727
1GF(1y)	0.24	20%		6941	7334	7246	8379	8466(89)*	---
1GF(3m)	0.24	20%		6552	7519	6686	7954	8609	8697
2GF(1y)	0.33	20%		3885	4952	5807	6469	6952	7201
2GF(3m)	0.33	20%		3855	4422	4918	5654	6289	6595
3GF(1y)	0.41	20%		3818	5151	6137	7262	7782	8041

Table 5-1. Continued

3GF(3m)	0.41	20%		3922	4523	5175	5748	6395	6805
4GF(1y)	0.37	20%		4889	4987	5640	6446	7528(89)*	---
4GF(3m)	0.37	20%		4244	4810	5605	6219	6991	7405
5GS(1y)	0.33		50%	2961	4692	5692	7008	7854	8105
5GS(3m)	0.33		50%	2713	4262(10)*	4502	5163	5898	5130
6GS(1y)	0.36		50%	2654	3571	5113(16)*	5628	6984	6543(92)*
6GS(3m)	0.36		50%	---	5045	6047	6951	6769	7253
7GS(1y)	0.41		70%	2267	4303	5222	6612	6741	7233
7GS(3m)	0.41		70%	2277	3568(10)*	4036	5088	5207(54)*	5806(100)*
8GS(1y)	0.44		50%	2123	---	3949(16)*	4994	6258	6157(92)*
8GS(3m)	0.44		50%	---	3545	3899	4789	5304	5181

Note: number in parenthesis ( ) indicates actual age in days of samples when tested.*

5.2.1 Effects of Water to Cement Ratio and Water Content on Compressive Strength

As a rule, the strength of comparable concretes is inversely proportional to the water to cement ratio. Higher water cement ratios will produce relatively weaker concretes and lower water cement ratios will produce stronger concretes. Figures 5-1 to 5-3 show the effects of water to cementitious materials ratio for two types of coarse aggregates, Miami Oolite and Georgia Granite, on compressive strength at 28 days and 91 days. The graph resembles a hyperbola and it seems that as the strength of concrete does not get affected at high water to cementitious materials ratios. Figures 5-4 and 5-5 show the effects of water content on compressive strength at 28 days of mixes using both types of aggregates. It can be appreciated from the figures that the relationship is linear and inversely proportional between water content and strength of concrete at 28 days. Higher water content means lower cement content which leads to large air-filled voids in the concrete making it porous. This results in a decrease in materials, reduced number of bonds between paste and aggregates, and they act as stress concentrations leading to a reduction in strength.

5.2.2 Effects of Aggregate Types on Compressive Strength

Figures 5-6 to 5-13 show the effects of aggregate on strength of the comparable mixes investigated in this study. Each graph shows mixes with identical mix proportions except that the aggregate has been replaced by volume. The mixes containing the letter “G” are the mixes

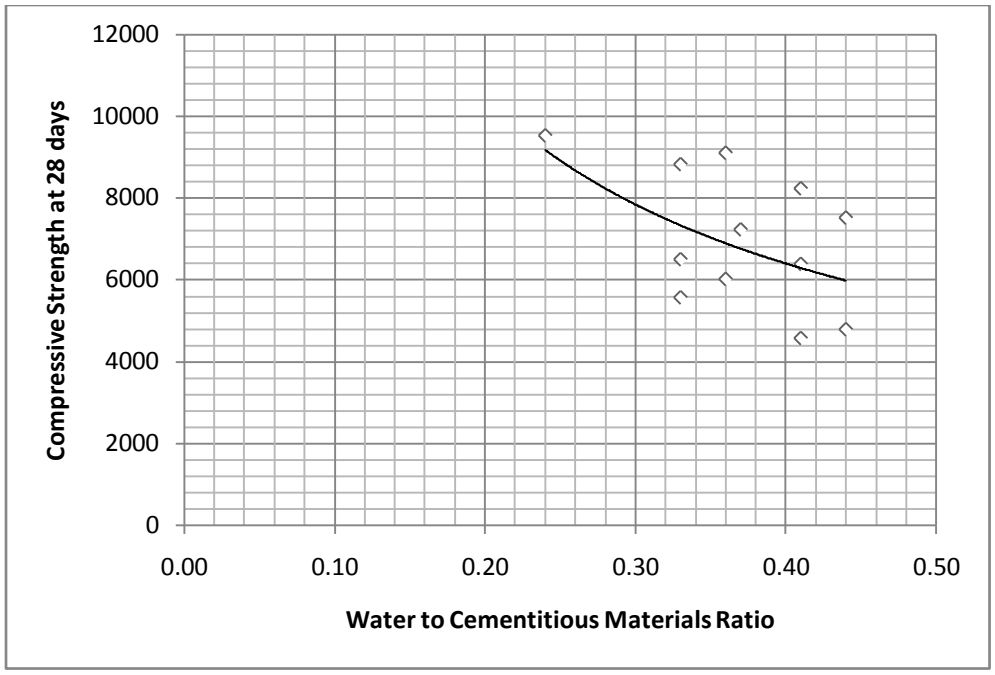

Figure 5-1. Effects of water to cementitious materials ratio on compressive strength at 28 days of mixes using Miami Oolite limestone aggregate

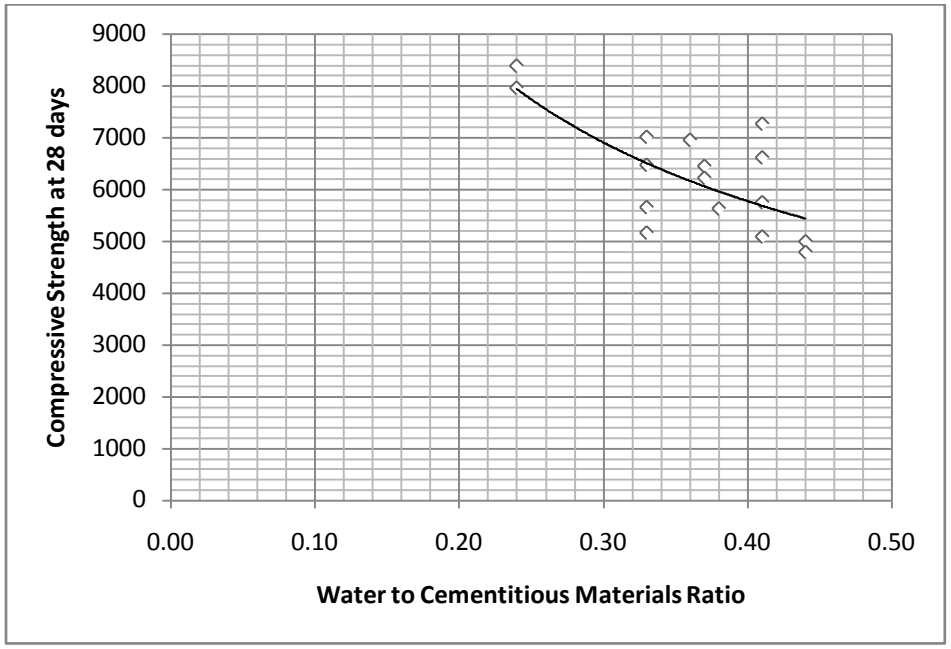

Figure 5-2. Effects of water to cementitious materials ratio on compressive strength at 28 days of mixes using Georgia granite aggregate

containing Georgia Granite as coarse aggregate. For example, Figure 5-6 shows the compressive strength development of mixes 1F made with Miami Oolite, and 1GF made with

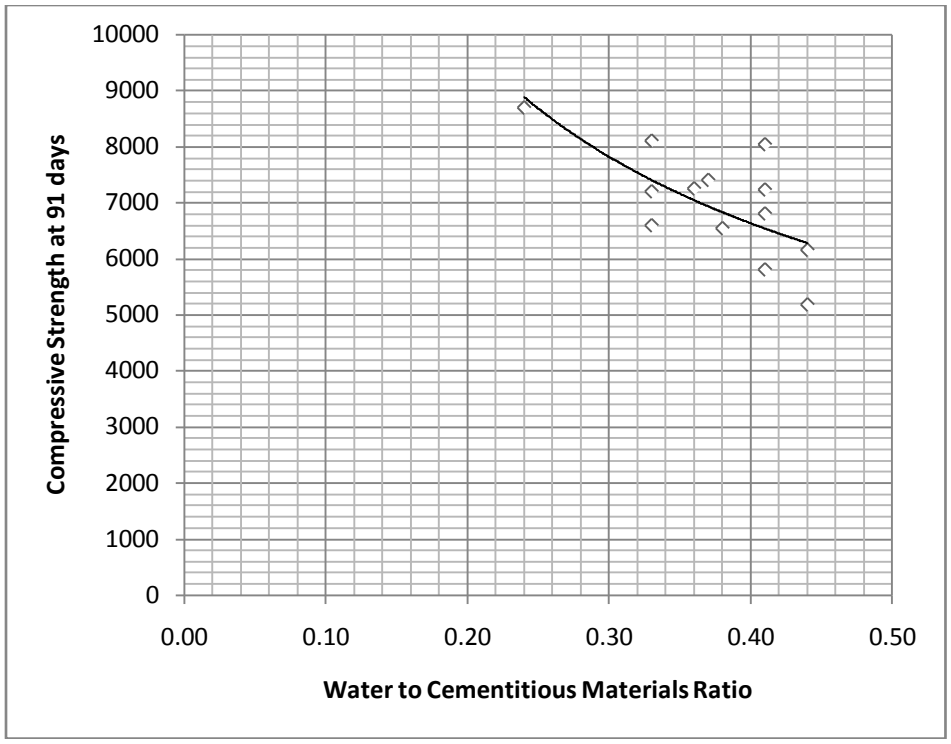

Figure 5-3. Effects of water to cementitious materials ratio on compressive strength at 91 days of mixes using Miami Oolite limestone aggregate

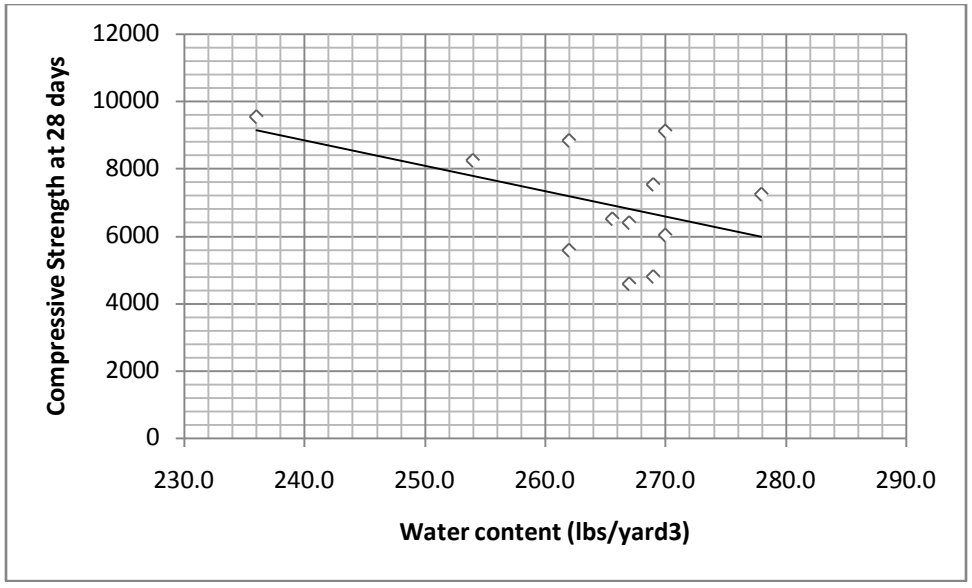

Figure 5-4. Effects of water content on compressive strength at 28 days of mixes using Miami Oolite limestone aggregate

Georgia Granite. From Figure 5-6 it can be seen that the mixes Mix-1F and Mix-1GF have really high early strengths, but Mix-1F develop strength does not seem to level off while the

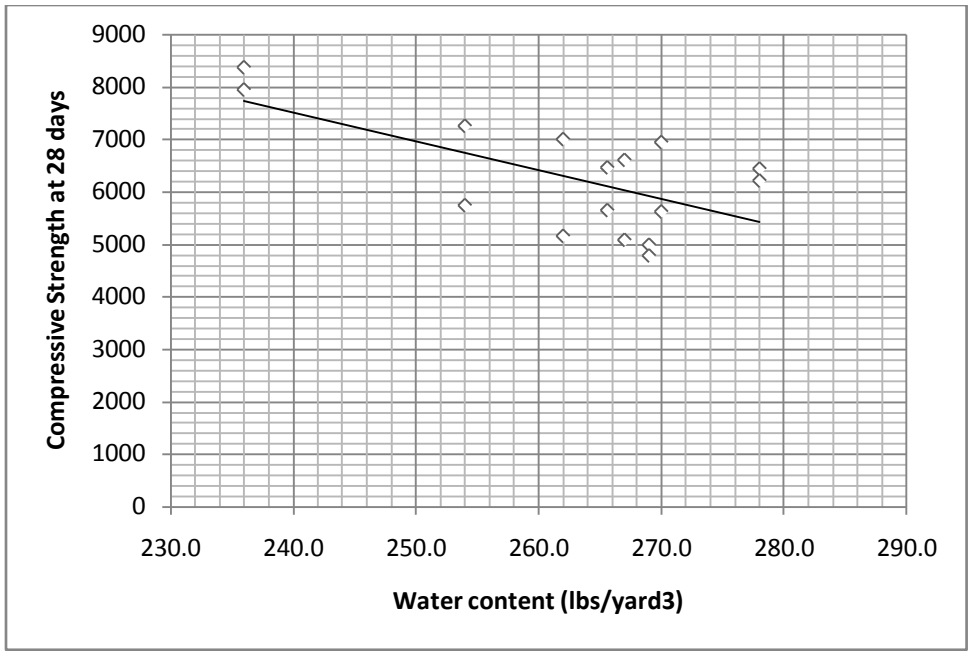

Figure 5-5. Effects of water content on compressive strength at 28 days of mixes using Georgia granite aggregate

strength development seems to stabilize after 28 days for Mix-1GF. Mix 1GF has overall lower compressive strength relative to Mix-1F. Figure 5-7 shows the mixes Mix-2F and Mix-2GF. The strength development for these mixes is very similar with Mix-2GF being slightly weaker than Mix-2F. In this case also, Mix-2F does not seem to level off, while Mix 2GF does. In Figure 5-8 it can be seen that Mix-3F is considerably stronger than Mix-3GF, especially at early ages. Mix-3F seems to level off before Mix-3GF does. From Figure 5-9 it can be appreciated that Mix-4F is significantly stronger than Mix-4GF as well. Mix-4F seems to have a volatile compressive strength development while Mix-4GF is more stable. Figure 5-10 shows the strength development for mixes Mix-5S and Mix-5GS. Mix-5GS is overall weaker than Mix-5S, especially at early ages, but it seems to catch up at later ages with Mix-5S. Figure 5-11 trends between mixes Mix-6S and Mix-6GS are similar, but Mix-6GS is different in terms of comparable strength; it is drastically weaker as compared to Mix-6S. Figure 5-12 shows mixes Mix-7S and Mix-7GS. Mix-7S has a relatively higher early strength as compared to Mix-7GS

but it levels off, while Mix-7GS is stronger at later ages. Last, Figure 5-13 shows the strength development of mixes Mix-8S and Mix-8GS. The results are consistent with most of the other mixes, that is, Mix-8GS is weaker than Mix-8S and seem to level off at around the same age.

Overall, comparable mixes containing Miami Oolite limestone aggregate are stronger than mixes containing Georgia Granite aggregate. This can be attributed not only to difference in physical characteristics of the aggregates, but also difference in fabrication of specimens as mentioned in Chapter 2. According to Neville, the properties of coarse aggregate, such as shape and surface texture, affect the vertical cracking of a specimen when subjected to uniaxial load, which starts at about 50 to 75 % of the ultimate load. Perry and Gillot found that, in general, smooth surface aggregates lead to lower compressive strengths, about 10 %, relative to concretes made with relatively roughened coarse aggregates.

In general, Georgia granite has elongated and flaky aggregates, while Miami Oolite limestone has aggregates that are spherical in shape. Therefore, comparable mixes that contain Miami Oolite limestone will be stronger because of the lower surface to volume ratio and the ability to create a tighter interlock between the aggregate and the mortar matrix. The influence of different types of aggregates on compressive strength of concrete seems to affect concretes with low water to cement ratios only.

According to findings by Kuczynski, as the water to cement ratio increases, the influence of different types of coarse aggregate is insignificant. The aggregate to cement ratio, however, influences the strength of concrete for constant water to cement ratios according to Erntroy and Shacklock. They found that mixes that are leaner, that is, mixes that contain more coarse aggregate per volume, have higher strengths. According to Neville, the reason of this behavior is due to the fact that there is less water per volume of concrete in leaner mixes. This is only true

for concretes containing 40 to 80 % of aggregate per volume of concrete. According to findings by Stock and Hannant, concretes containing 0 to 40 % of aggregate by volume exhibit a decrease in strength, and an increase in strength from 40 to 80 %.

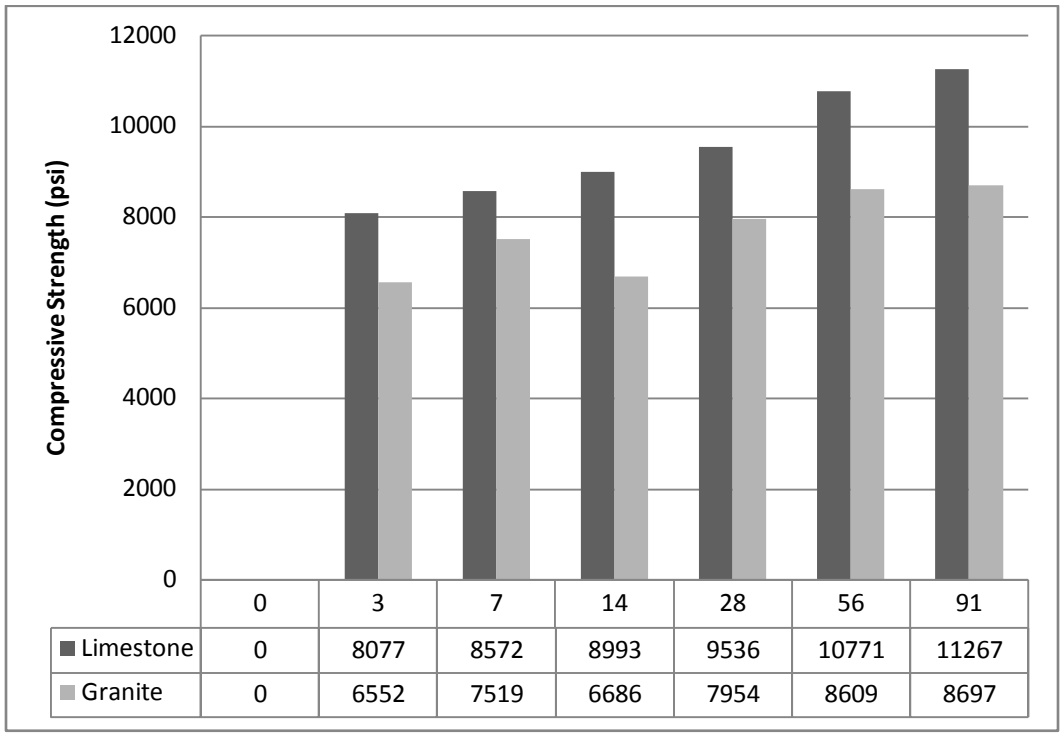

	0	3	7	14	28	56	91
Limestone	0	8077	8572	8993	9536	10771	11267
Granite	0	6552	7519	6686	7954	8609	8697

Figure 5-6. Effects of coarse aggregate type on compressive strengths of Mix-1Fand Mix-1GF

5.2.3 Effects of Fly Ash and Slag on Compressive Strength of Concrete

Both fly ash and slag were donated by Florida Rock Industries located in Gainesville, FL. Figure 5-14 shows the percentage of 91 day compressive strengths for all mixes investigated in this study. From the figure it can be appreciated that mixes containing slag develop compressive strengths at a much faster rate than mixes containing fly ash. As can be seen from the same figure, the mixes containing fly ash reach 90 % of their 91-day compressive strength in less than 28 days. The information in Table 5-1 shows the percentage of fly ash and slag used as substitutes for cement as cementitious materials. All mixes containing fly ash substitute 20 % of cement content by mass, while mixes containing slag substitute 50 to 70 % of cement by mass.

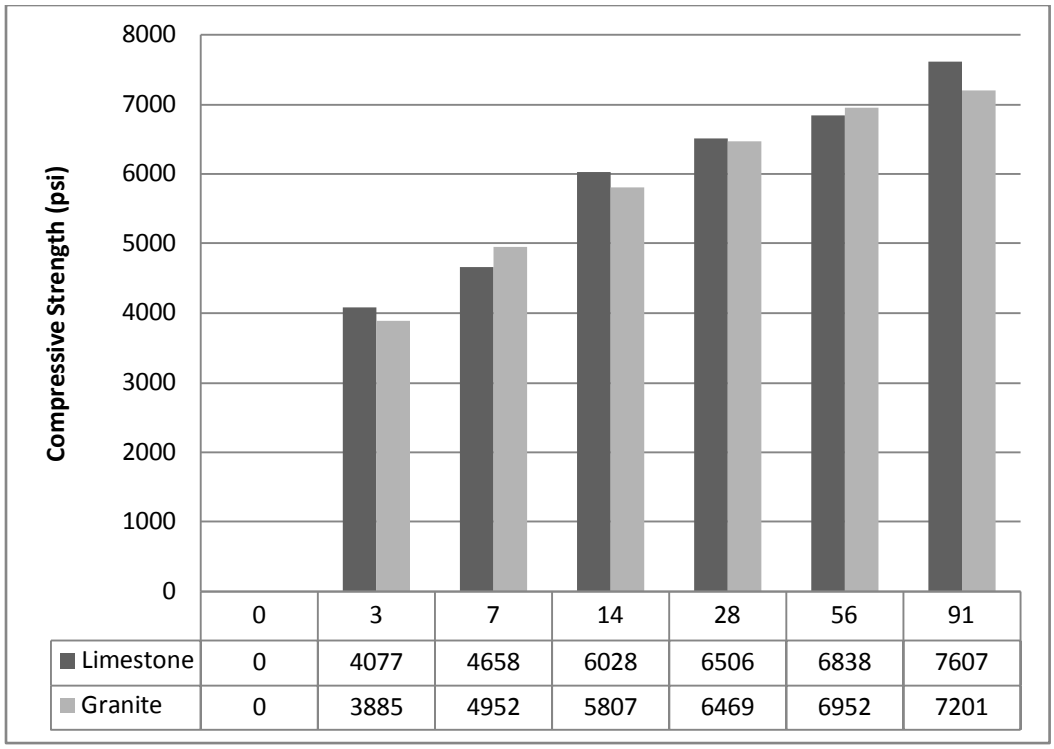

	0	3	7	14	28	56	91
Limestone	0	4077	4658	6028	6506	6838	7607
Granite	0	3885	4952	5807	6469	6952	7201

Figure 5-7. Effects of coarse aggregate type on compressive strengths of Mix-2Fand Mix-2GF

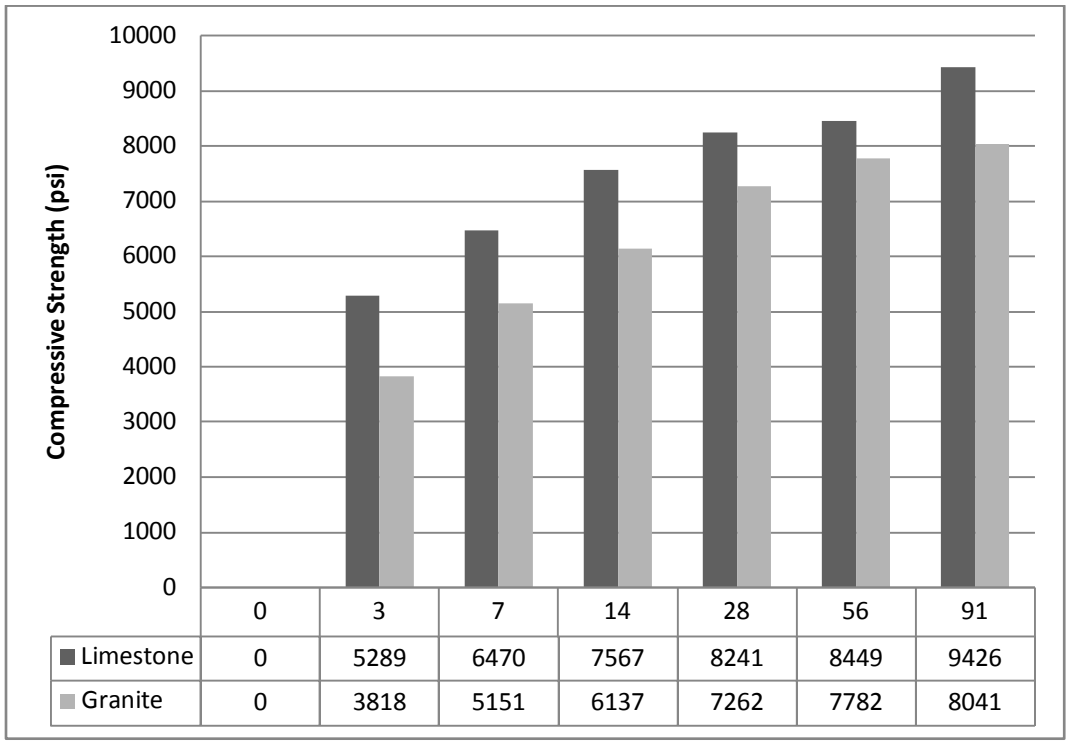

	0	3	7	14	28	56	91
Limestone	0	5289	6470	7567	8241	8449	9426
Granite	0	3818	5151	6137	7262	7782	8041

Figure 5-8. Effects of coarse aggregate type on compressive strength of Mix-3Fand Mix-3GF

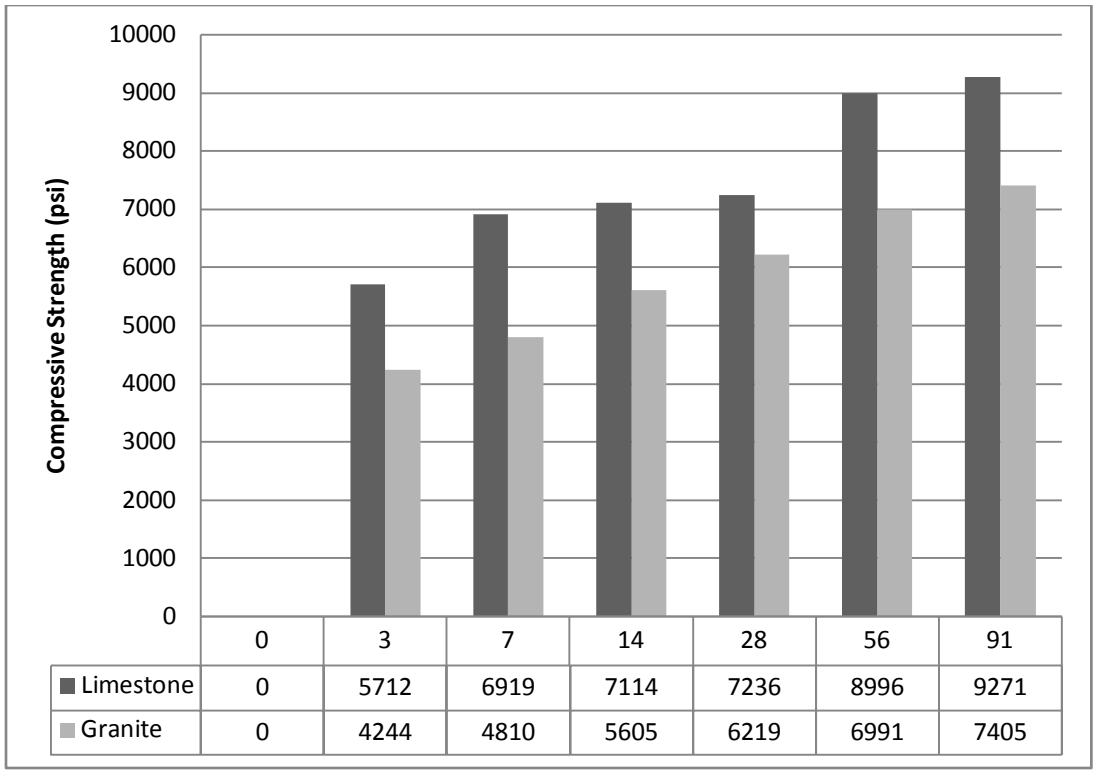

	0	3	7	14	28	56	91
Limestone	0	5712	6919	7114	7236	8996	9271
Granite	0	4244	4810	5605	6219	6991	7405

Figure 5-9. Effects of coarse aggregate type on compressive strength of Mix-4Fand Mix-4GF

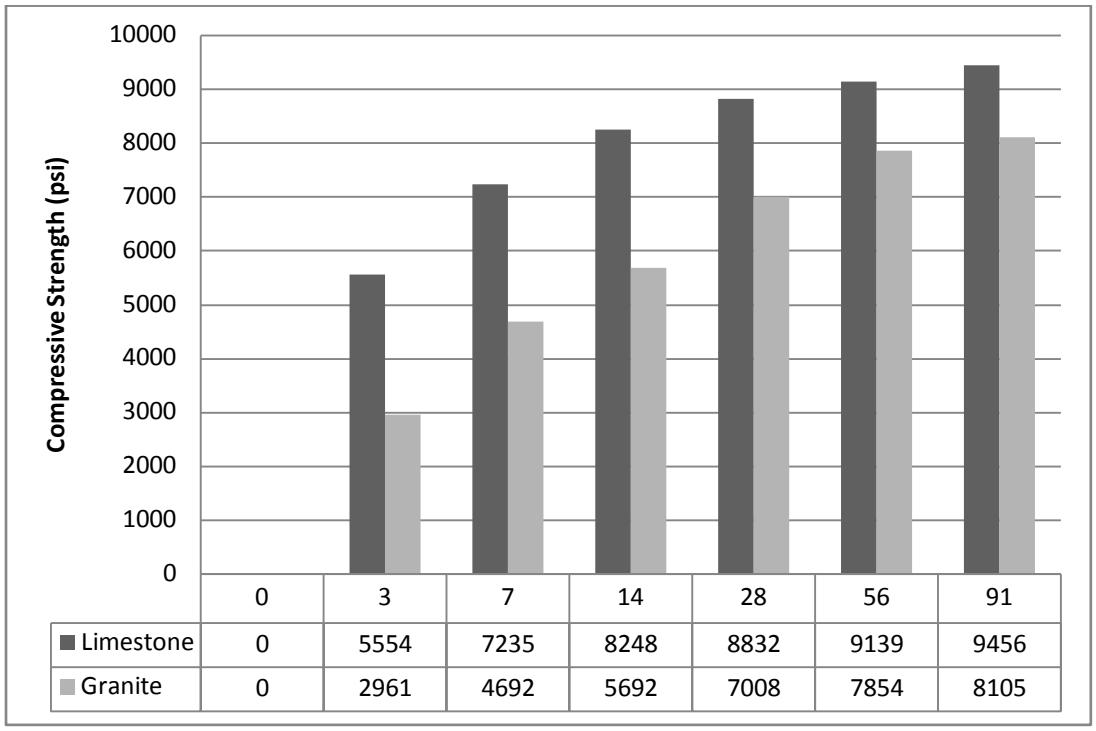

	0	3	7	14	28	56	91
Limestone	0	5554	7235	8248	8832	9139	9456
Granite	0	2961	4692	5692	7008	7854	8105

Figure 5-10. Effects of coarse aggregate type on compressive strength of Mix-5Sand Mix-5GS

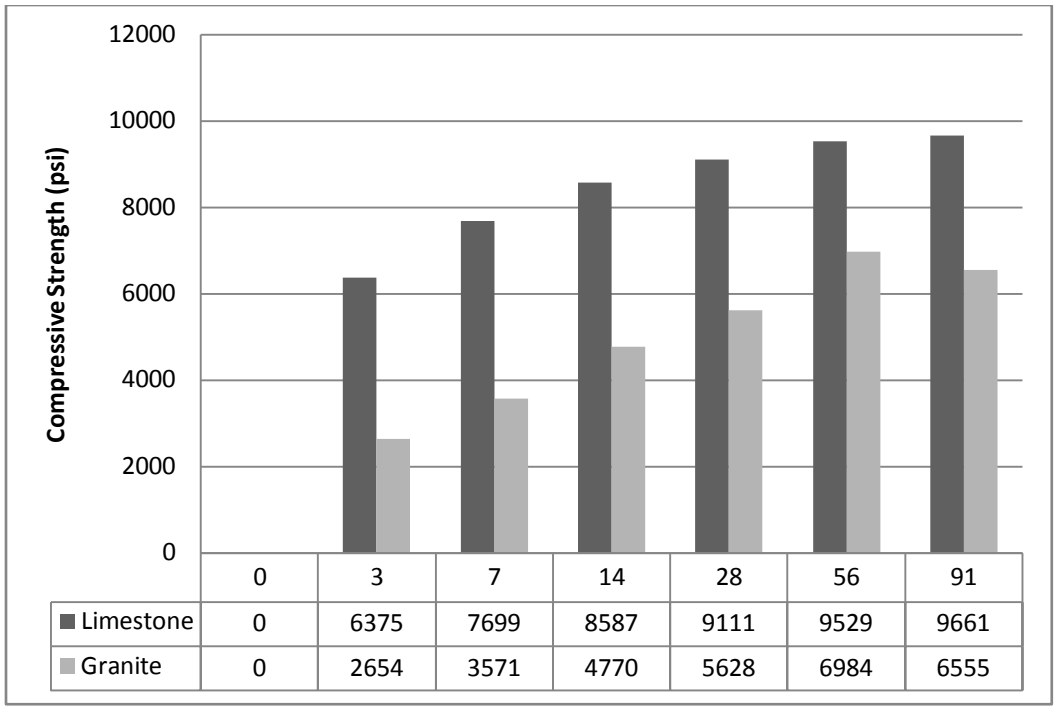

	0	3	7	14	28	56	91
Limestone	0	6375	7699	8587	9111	9529	9661
Granite	0	2654	3571	4770	5628	6984	6555

Figure 5-11. Effects of coarse aggregate type on compressive strength of Mix-6S and Mix-6GS

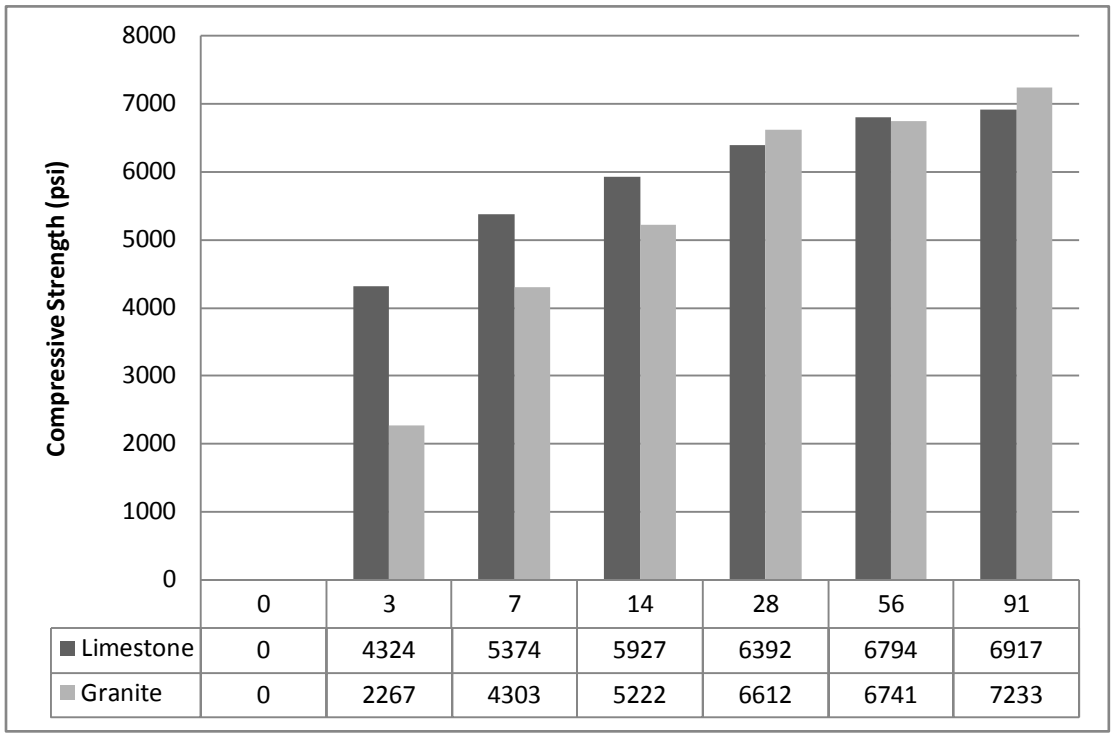

	0	3	7	14	28	56	91
Limestone	0	4324	5374	5927	6392	6794	6917
Granite	0	2267	4303	5222	6612	6741	7233

Figure 5-12. Effects of coarse aggregate type on compressive strength of Mix-7S and Mix-7GS

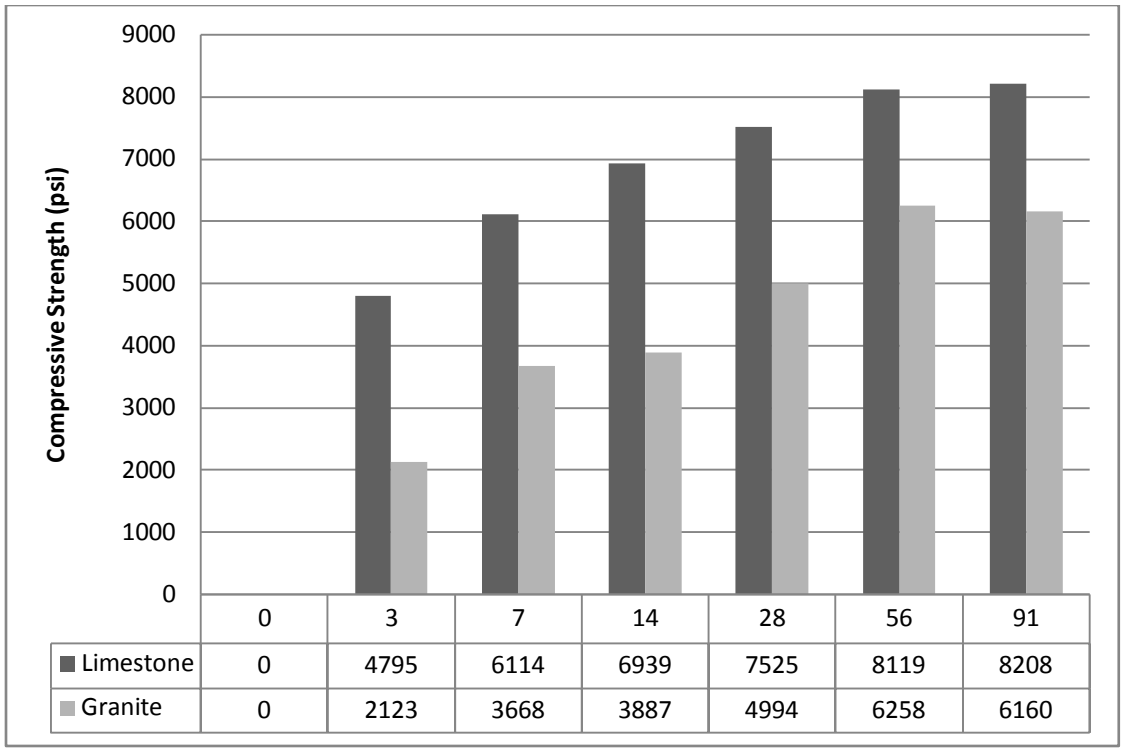

	0	3	7	14	28	56	91
Limestone	0	4795	6114	6939	7525	8119	8208
Granite	0	2123	3668	3887	4994	6258	6160

Figure 5-13. Effects of coarse aggregate type on compressive strength of Mix-8S and Mix-8GS

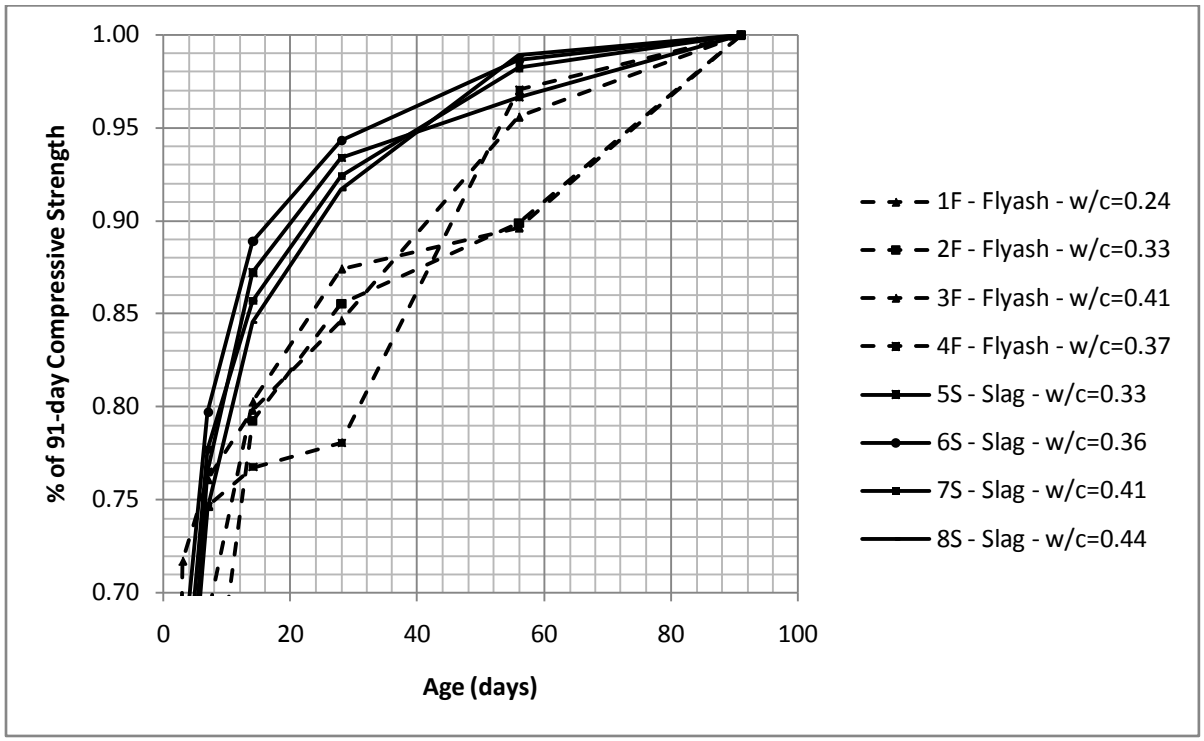

Figure 5-14. Effects of fly ash and slag on compressive strength of concrete

5.2.4 Prediction of Compressive Strength Development

The compressive strength is one of the most important properties of concrete. It depends largely on degree of hydration, curing conditions, water to cement ratio, porosity, and age of the concrete. The prediction of compressive strength development is even more important, especially when a structure is subjected to loading when in service.

ACI 209R-4 recommends the following general equation for predicting compressive strengths at any age:

$$(f_c^{'})t = \frac{t}{a + \beta t}(f_c^{'})_{28}$$

where a in days and β are constants, $(f_c^{'})_{28}$ = 28-day strength and t in days is the age of concrete. Constants a and β depend on the type of cement used and the curing methods employed.

The previous equation can be transformed into

$$(f_c^{'})t = \frac{t}{\frac{a}{\beta} + t}(f_c^{'})_u$$

where $\frac{a}{\beta}$ is age of concrete in days at which one half of the ultimate (in time) compressive strength of concrete $(f_c^{'})_u$ is reached.

According to ACI 209, the ranges of a and β are: a = 0.05 to 9.25, β = 0.67 to 0.98 for normal weight, sand lightweight, and all lightweight concretes using both steam and moist curing, and types I and III cement. For 6x12 specimens, type I cement, and moist curing conditions, a and β become 4.0 and 0.85 respectively.

Table 5-2 shows the values for both a and β as a result of regression analysis performed on the results of compressive strength of 648 specimens. Detailed results of this analysis are

presented in Table 5-3. Table 5-4 presents the values for the time-ratios $\frac{f_c^{'}(t)}{f_{c\,28}^{'}}$ and $\frac{f_c^{'}(t)}{f_{cu}^{'}}$ at 3, 7, 14, 28, 56, and 91 days.

According to the results presented in Table 5-2, there seems to be no apparent relationship between constants α and β, but the average value of α lower than the value by given by ACI and so is the average value of β. α has an average value of 3.21 versus 4.0 by ACI, while β has a value of 0.89 versus 0.85 by ACI. A more careful observation shows that mixes containing Miami Oolite limestone has average values of 2.33 for α which is significantly lower than 4.0 as given by ACI, and 0.92 for β which is slightly higher than 0.85 given by ACI. Figure 5-15 shows that that the concrete mixes containing Miami Oolite limestone develop strength faster than the mixes as predicted by ACI 209.

The mixes containing Georgia granite have average values of 4.66 and 0.86 for α and β respectively, very closed as compared to 4.0 and 0.85 as recommended by ACI. Figure 5-15 shows that mixes containing Georgia granite develop strength similarly as predicted by ACI 209.

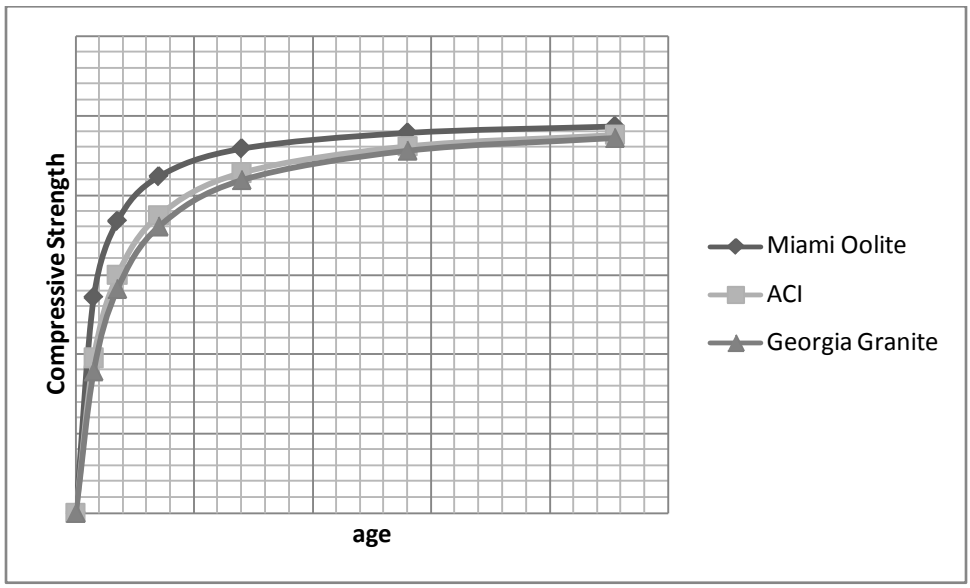

Figure 5-15. Comparison of strength development on mixes containing Miami Oolite limestone, Georgia granite, and constants given by ACI 209

Table 5-2. Results of regression analysis for prediction of compressive strength development using ACI 209 equation

Mix	α	α by ACI	β	β by ACI	Square root of Absolute sum of squares by Modified ACI Equation	Square root of Absolute sum of squares by ACI Equation
1F	1.40		0.91		924.5	1646.2
2F	2.13		0.89		925.1	1153.3
3F	2.66		0.86		520.3	772.8
4F	2.09		0.85		584.2	1108.9
5S	1.69	4.0	0.93	0.85	1581.9	1853.7
6S	2.11		1.03		1483.9	1820.1
7S	3.30		1.02		1232.9	1486.8
8S	3.26		0.83		1479.8	1528.5
9LF	3.80		0.84		519.6	534.9
10LS	6.79		0.75		1103.7	1196.1
1GF	0.80		0.98		495.9	1759.7
2GF	2.49		0.89		427.2	643.2
3GF	2.94		0.88		623.4	680.7
4GF	1.88	4.0	0.92	0.85	465.2	939.1
5GS	4.12		0.85		936.5	941.4
6GS	4.24		0.85		540.8	514.0
7GS	5.20		0.86		686.9	769.8
8GS	5.18		0.80		415.6	519.8

5.3 Analysis of Splitting Tensile Strength Test Results

Table 5-5 presents the average values for the results of splitting tensile strength tests at various ages.

5.3.1 Effects of Water to Cement Ratio on Splitting Tensile Strength

Same as the effects of water to cement ratio on compressive strength, Figures 5-10 and 5-11 show that splitting tensile strength decreases as the water to cement ratio increases at 28 days and 91 days respectively.

Table 5-3. Results of regression analysis on the prediction of compressive strength development using ACI 209 equation

Mix / Results	1F	2F	3F	4F	5S	6S
α	1.399	2.125	2.660	2.089	1.6910	2.110
β	0.9126	0.8901	0.8633	0.8548	0.9270	1.0271
α (SE)	0.4299	0.6299	0.3549	0.3383	0.7124	0.8046
β (SE)	0.03443	0.04947	0.02461	0.02628	0.06293	0.06718
α (95%CI)	0.4412 to 2.3568	0.7385 to 3.5115	1.8787 to 3.4409	1.3445 to 2.8340	0.1878 to 3.1941	0.4043 to 3.8160
β (95%CI)	0.8359 to 0.9893	0.7812 to 0.9990	0.8091 to 0.9175	0.7969 to 0.9126	0.7939 to 1.0595	0.8847 to 1.1695
DOF	10	11	11	11	17	16
R^2	0.9291	0.8602	0.9638	0.9531	0.6451	0.7000
ASS	8546212	9414840	2977308	3754672	42540889	35229390
Sy.x	924.5	925.1	520.3	584.2	1581.9	1483.9
Points Analyzed	12	13	13	13	19	18

Mix / Results	7S	8S	M-9LF	M-10LS	1GF	2GF
α	3.2963	3.255	3.796	6.787	0.804	2.485
β	1.019	0.8328	0.8383	0.7524	0.9838	0.8874
α (SE)	1.1865	1.0876	0.5756	2.4062	0.4934	0.8442
β (SE)	0.07859	0.07012	0.03252	0.09209	0.0598	0.0614
α (95%CI)	0.7931 to 5.7996	0.9491 to 5.5604	2.529 to 5.0633	1.4910 to 12.0831	0.3104 to 1.2972	1.6410 to 3.3293
β (95%CI)	0.8535 to 1.1851	0.6842 to 0.9815	0.7668 to 0.9099	0.5497 to 0.9551	0.9240 to 1.0436	0.8260 to 0.9488
DOF	17	16	11	11	10	11
R^2	0.6609	0.6895	0.9484	0.7694	0.9591	0.9541
ASS	25841965	3503662	2969920	13400762	2459650	2007330
Sy.x	1232.9	1479.8	519.6	1103.7	495.9	427.2
Points Analyzed	19	18	13	13	12	13

Table 5-3. Continued

Mix / Results	3GF	4GF	5GS	6GS	7GS	8GS
α	2.9364	1.8807	4.118	4.244	5.200	5.1840
β	0.8763	0.9184	0.8542	0.8516	0.8566	0.7970
α (SE)	1.2774	0.8342	1.2300	1.7286	1.1516	2.1524
β (SE)	0.0848	0.0863	0.06557	0.0842	0.05423	0.0836
α (95%CI)	1.6589 to 4.2138	1.0465 to 2.7149	1.411 to 6.8256	2.516 to 5.973	2.6657 to 7.7350	3.0315 to 7.3364
β (95%CI)	0.7914 to 0.9611	0.8378 to 0.9991	0.7098 to 0.9985	0.7674 to 0.9357	0.7372 to 0.9759	0.7134 to 0.8806
DOF	11	9	11	10	11	9
R^2	0.9215	0.9504	0.8346	0.9436	0.8989	0.9540
ASS	4275173	1947959	9647989	2924610	5190422	1554520
Sy.x	623.4	465.2	936.5	540.8	686.9	415.6
Points Analyzed	13	11	13	12	13	11

Table 5-4. Values of the constants,α, β and α/β and the time ratios

Time Ratio	Type of Curing	Cement Type	Aggregate type	α, β and α/β	Concrete ages (days) 3	7	14	28	56	91	Ultimate in time
$\frac{f_c'(t)}{f_{c\ 28}'}$	Moist cured	I/II	ACI 209R-4	α=4.00 β=0.85	0.45	0.70	0.87	1	1.08	1.11	1.17
			Miami Oolite Limestone	α=2.33 β=0.92	0.59	0.80	0.92	1	1.04	1.06	1.09
			Granite	α=3.36 β=0.88	0.50	0.74	0.89	1	1.06	1.09	1.14
			Stalite	α=5.50 β=0.78	0.38	0.63	0.84	1	1.11	1.15	1.24
$\frac{f_c'(t)}{f_{cu}'}$	Moist cured	I/II	ACI 209R-4	α/β=4.71	0.39	0.60	0.75	0.86	0.92	0.95	1
			Miami Oolite	α/β=2.53	0.54	0.73	0.85	0.92	0.96	0.97	1
			Granite	α/β=3.82	0.44	0.65	0.79	0.88	0.94	0.96	1
			Stalite	α/β=6.63	0.31	0.51	0.68	0.81	0.89	0.93	1

Table 5-5. Splitting tensile strengths of the concrete mixtures evaluated (psi)

Mix		Fly		Age of Testing (days)					
Number	W/C	ash	Slag	3	7	14	28	56	91
1F(1y)	0.24	20%		592	628	715	795	834	849
2F(1y)	0.33	20%		408	484	528	542	621	659
3F(1y)	0.41	20%		513	539	562	624	674	731
4F(1y)	0.37	20%		457	520	566	670	759	770
5S(1y)	0.33		50%	454	476	621	614(27)*	646	664(105)*
5S(3m)	0.33		50%	442	574	634	689	711	738
6S(1y)	0.36		50%	668(6)*	562	605	641(30)*	624(69)*	530(94)*
6S(3m)	0.36		50%	570	602	648	672	690	718
7S(1y)	0.41		70%	367(6)*	431	455	444	490(69)*	496(94)*
7S(3m)	0.41		70%	426	473	518	548	590	596
8S(1y)	0.44		50%	399	389	536	496	480(57)*	465(106)*
8S(3m)	0.44		50%	372	499	550	633	693	703
9LF(1y)	0.31	20%		350	404	448	490	551	577
10LS(1y)	0.39		60%	212	288	364	405	418	430
1GF(1y)	0.24	20%		628(5)*	676	666	693	786(89)*	-
1GF(3m)	0.24	20%		485	560	622	655	688	744
2GF(1y)	0.33	20%		352	421	488	529	548	595
2GF(3m)	0.33	20%		416	463	498	528	606	623
3GF(1y)	0.41	20%		382	409	503	561	599	651
3GF(3m)	0.41	20%		391	421	459	507	559	607
4GF(1y)	0.37	20%		449(5)*	447	535	562	654(90)*	-
4GF(3m)	0.37	20%		429	455	486	612	620	649
5GS(1y)	0.33		50%	282	420	462	525	591	649
5GS(3m)	0.33		50%	293	464(10)*	362	518	479	535
6GS(1y)	0.36		50%	273	378	440	514	464	500(92)*
6GS(3m)	0.36		50%	-	454	555	-	634	572
7GS(1y)	0.41		70%	245	362	430	504	554	577
7GS(3m)	0.41		70%	261	366(10)*	417	392	471(54)*	432
8GS(1y)	0.44		50%	217	312(8)*	401(16)*	475	432	432(92)*
8GS(3m)	0.44		50%	-	350	441	454	486	478

Note: number in parenthesis ( ) indicates actual age in days of samples when tested.*

5.3.2 Effects of Coarse Aggregate Type on Splitting Tensile Strength

Figures 5-12 through 5-17 show the effects of types of coarse aggregates on the splitting tensile strength. Each graph shows mixes with identical mix proportions except that the aggregate has been replaced by volume. The mixes containing the letter "G" are the mixes containing Georgia Granite as coarse aggregate. For example, Figure 5-12 shows the strength development of mixes 2F made with Miami Oolite limestone, and 2GF made with Georgia granite. In general, the splitting tensile strengths of mixes containing Georgia granite are weaker as compared to mixes containing Miami Oolite limestone. For example, mixes Mix-2F has a

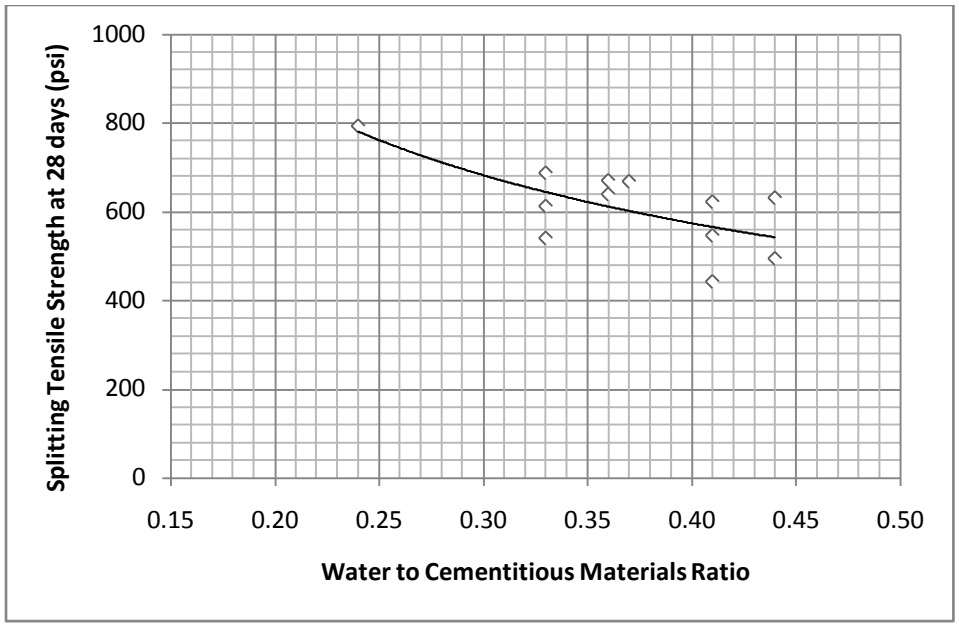

Figure 5-16. Effects of water to cement ratio on splitting tensile strength at 28 days

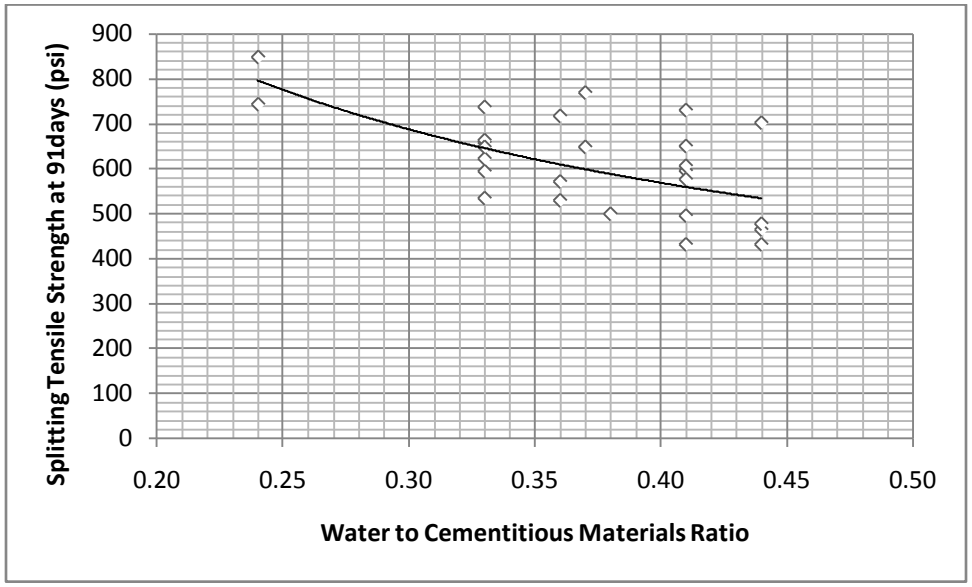

Figure 5-17. Effects of water to cement ratio on splitting tensile strength at 91 days

splitting tensile strength of 659 psi versus 595 psi for Mix-2GF. Mix-3F has a splitting tensile strength of 731 psi versus 561 psi for Mix-3GF. Mix-5S has a splitting tensile strength of 738 psi versus 649 psi for Mix-5GS. Mix-6S has a splitting tensile strength of 718 psi versus 500 psi for

Mix-6GS. Mix-7S has a splitting tensile strength of 596 psi versus 577 psi for Mix-7GS. Mix-8S has a splitting tensile strength of 703 psi versus 432 psi for Mix-8GS.

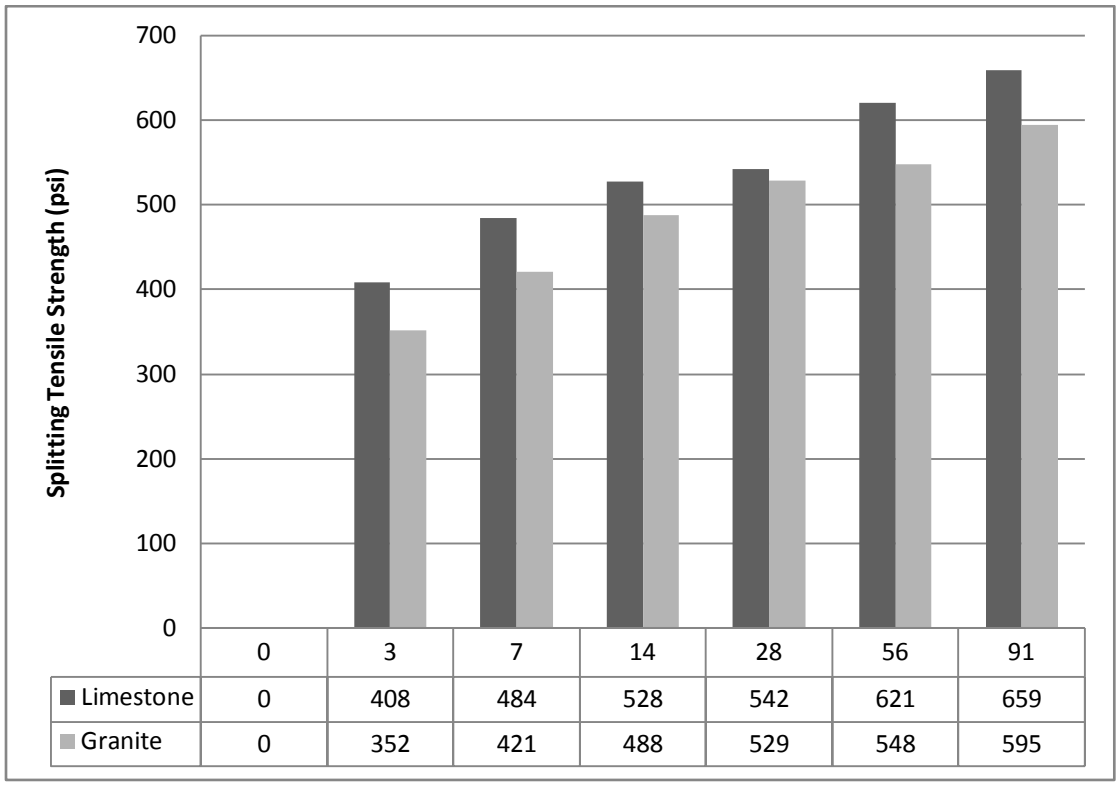

	0	3	7	14	28	56	91
Limestone	0	408	484	528	542	621	659
Granite	0	352	421	488	529	548	595

Figure 5-18. Effects of aggregate type on splitting tensile strength of Mix-2F and Mix-2GF

5.3.3 Effects of Fly Ash and Slag on Splitting Tensile Strength of Concrete

To analyze the effects of fly ash and slag on splitting tensile strength of concrete, the strength development has been plotted as a ratio of the 91-day splitting tensile strength for each mix. Figure 5-18 shows similarities as far as how rapidly both mixes develop strength relative to each other. Concrete specimens containing slag seem to reach 90% of their corresponding 91-day strength at just 28 days after being demolded. Concrete specimens containing fly ash reach 90% of their strength at around 50 days after being demolded. It can be also noted that concrete specimens containing fly ash reach 85% of the 91-day strength at 28 days. For example, the splitting tensile strength for Mix-3F has a 17.1% increase from 28-day splitting tensile strength of 624 psi to 91-day strength of 731 psi. Mix-3GF has a slightly bigger increase for the

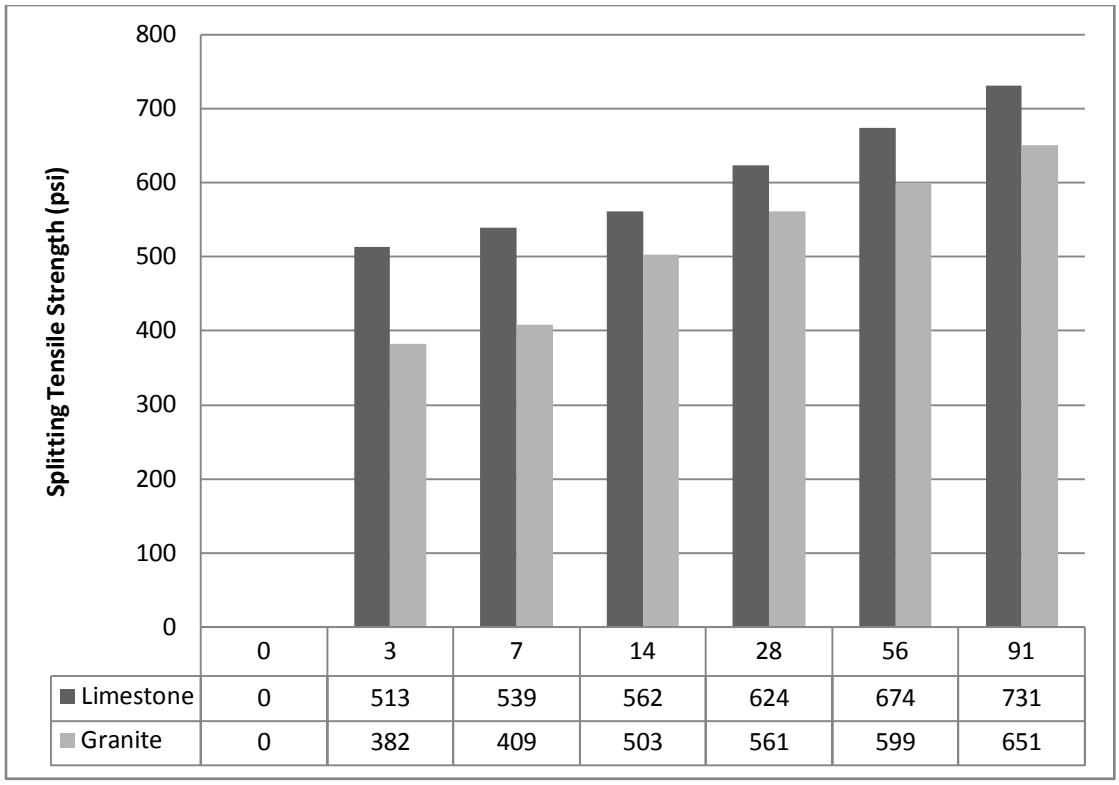

	0	3	7	14	28	56	91
Limestone	0	513	539	562	624	674	731
Granite	0	382	409	503	561	599	651

Figure 5-19. Effects of aggregate type on splitting tensile strength of Mix-3F and Mix-3GF

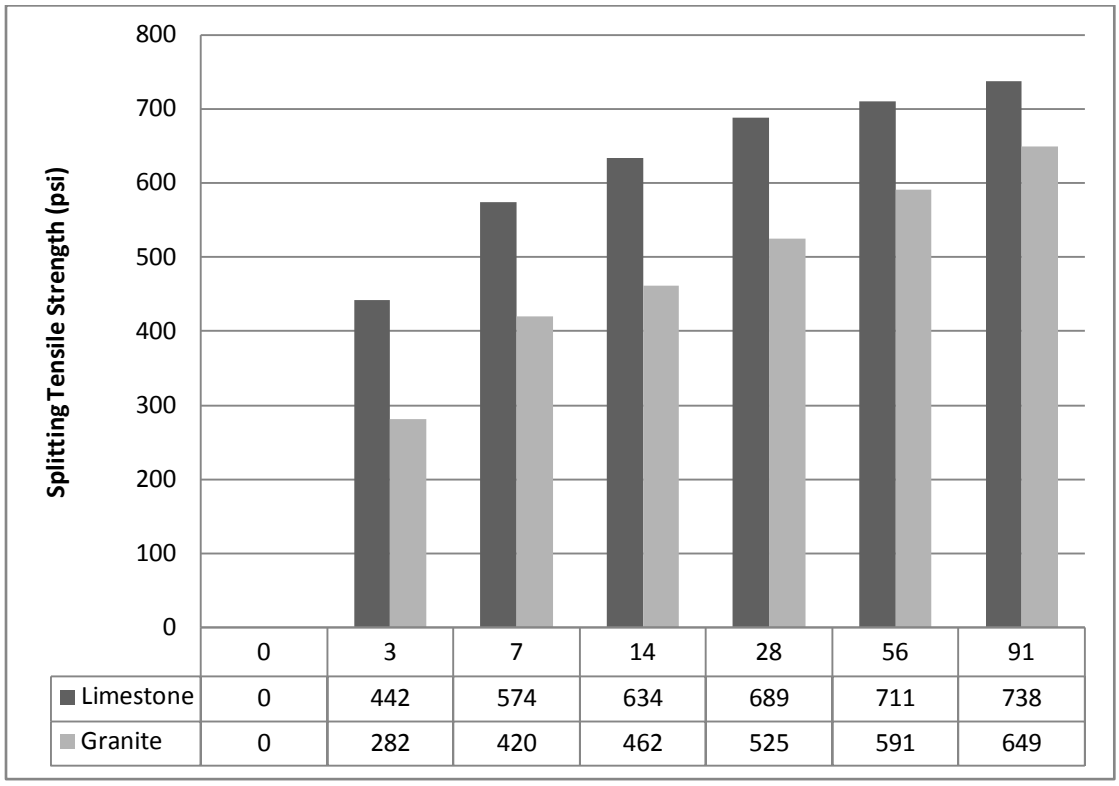

	0	3	7	14	28	56	91
Limestone	0	442	574	634	689	711	738
Granite	0	282	420	462	525	591	649

Figure 5-20. Effects of aggregate type on splitting tensile strength of Mix-5S and Mix-5GS

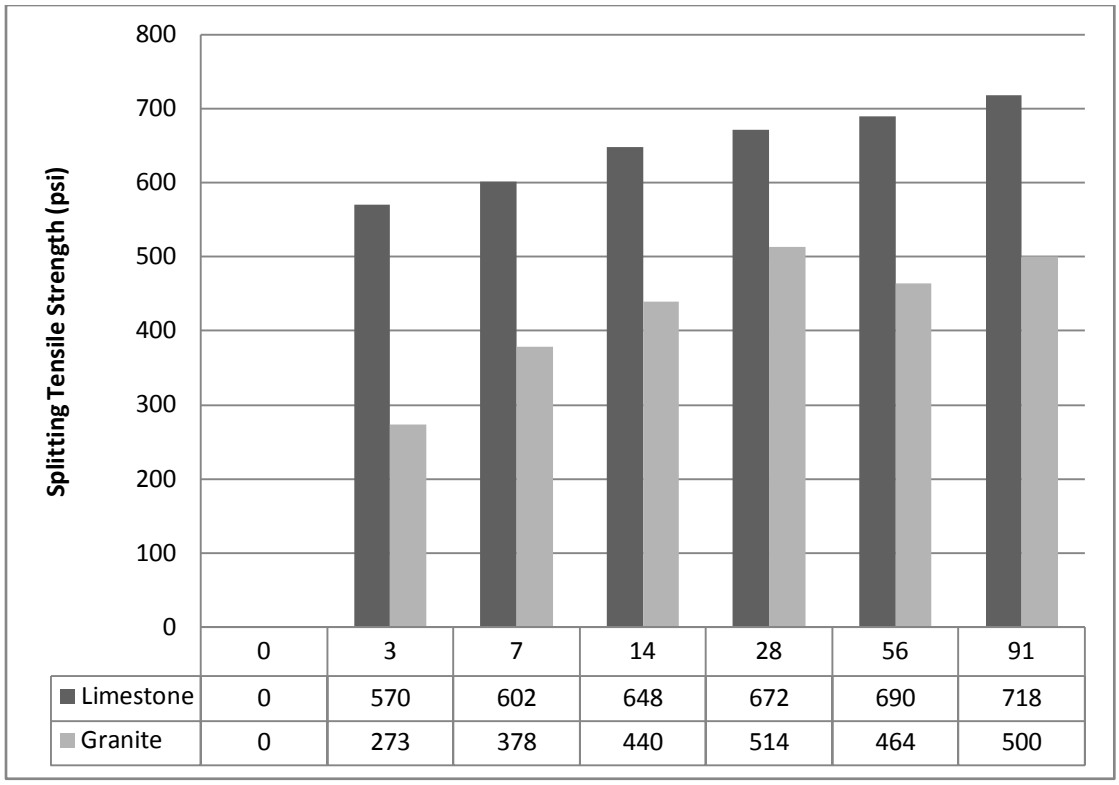

	0	3	7	14	28	56	91
Limestone	0	570	602	648	672	690	718
Granite	0	273	378	440	514	464	500

Figure 5-21. Effects of aggregate type on splitting tensile strength of Mix-6S and Mix-6GS

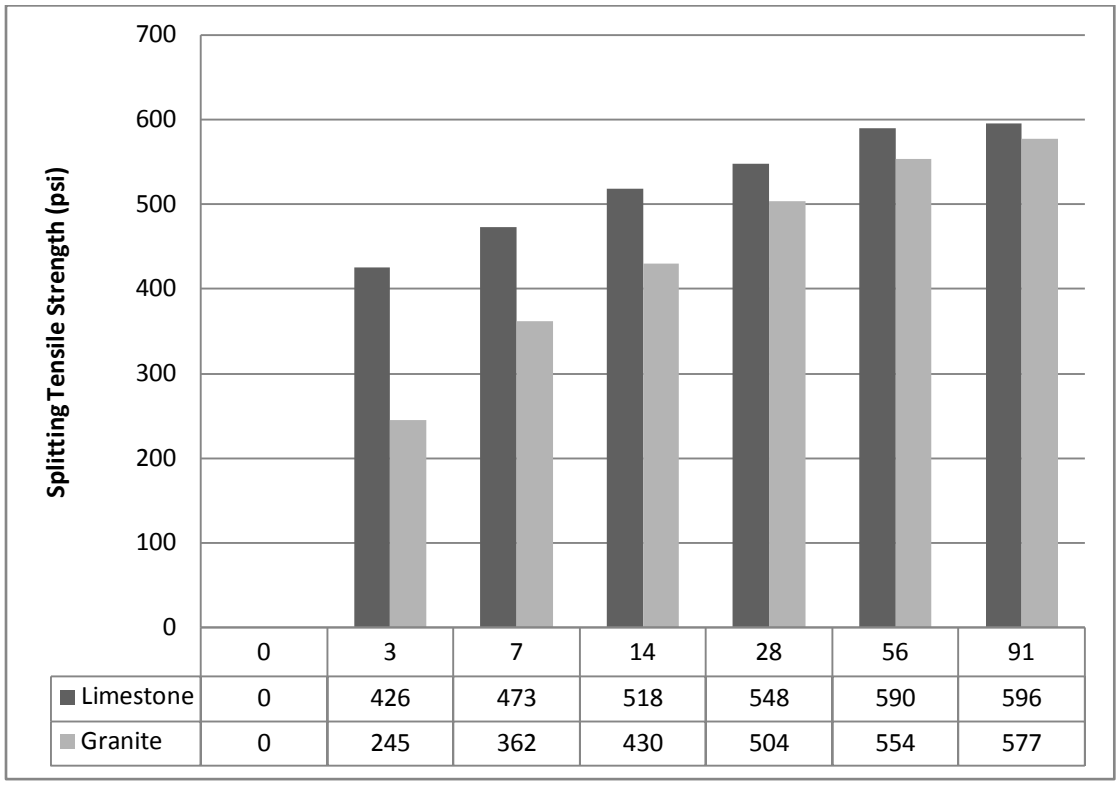

	0	3	7	14	28	56	91
Limestone	0	426	473	518	548	590	596
Granite	0	245	362	430	504	554	577

Figure 5-22. Effects of aggregate type on splitting tensile strength of Mix-7S and Mix-7GS

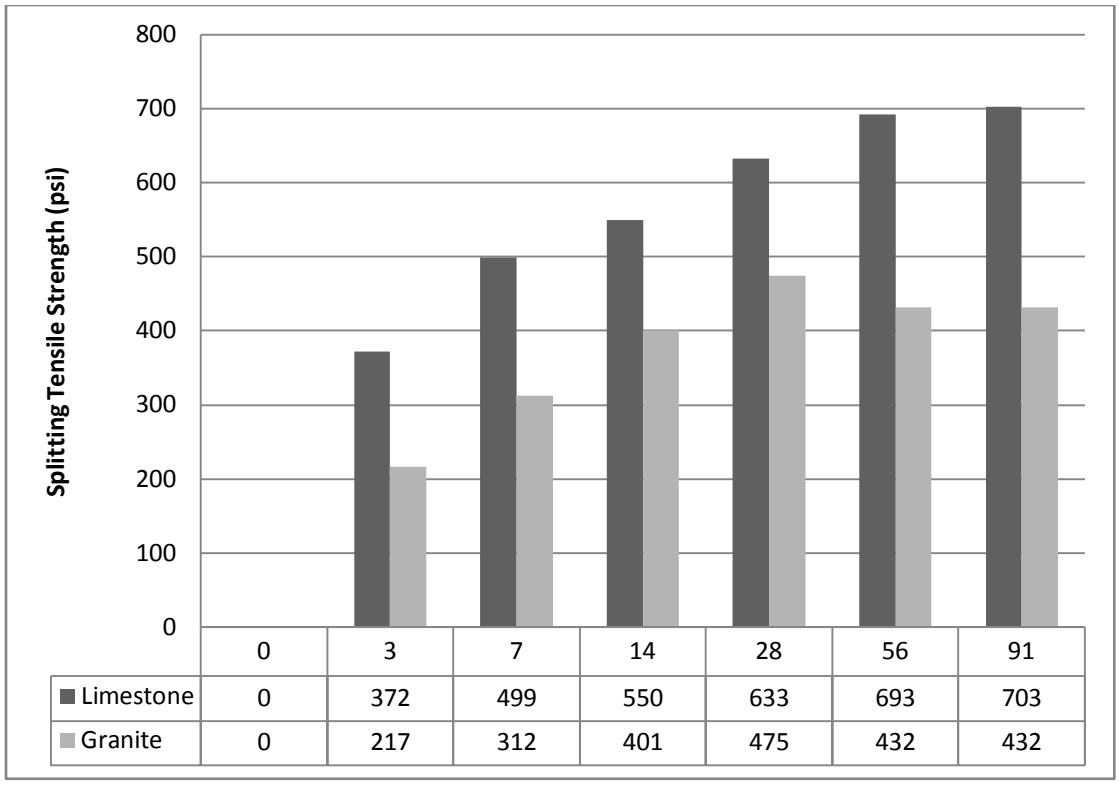

Figure 5-23. Effects of aggregate type on splitting tensile strength of Mix-8S and Mix-8GS

same time interval of 19.7% from 507 psi to 607 psi. The splitting tensile strength for Mix-5S has a 8.1% increase from 28-day splitting tensile strength of 614 psi to 91-day strength of 664 psi. Mix-5GS has a considerably bigger increase for the same time interval of 23.6% from 525 psi to 649 psi. The splitting tensile strength for Mix-7S has a 11.7% increase from 28-day splitting tensile strength of 444 psi to 91-day strength of 496 psi. Mix-7GS has a noticeably higher increase for the same time interval of 14.5% from 504 psi to 577 psi. In general, it seems that mixes containing slag and Miami Oolite limestone aggregate have an almost insignificant increase in splitting tensile strength from 28 days to 91 days. This seems to be also the case when the aggregate type is replaced by volume to Georgia granite. The increase in strength is not very pronounced when the mix contains slag and Georgia granite. Mixes containing Miami Oolite, or Georgia granite coarse aggregates and fly ash seem to have a more pronounced increase in strength.

The following figure shows the mixes analyzed in this study and their strength development as a ratio of their 91-day splitting tensile strength.

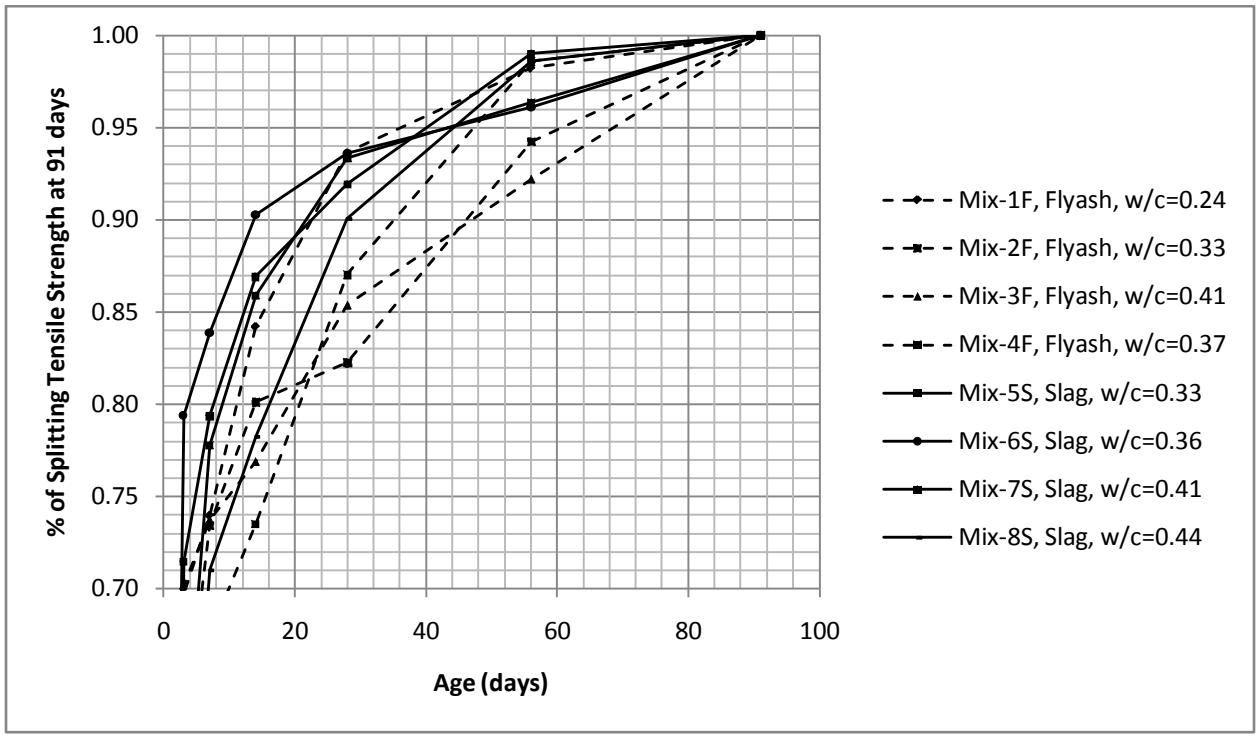

Figure 5-24. Effects of fly ash and slag on splitting tensile strength of concrete

5.4 Relationship between Compressive Strength and Splitting Tensile Strength

The splitting tensile strength of concrete can be related to its compressive strength. Figure 5-19 shows the values for the compressive strengths plotted against the corresponding splitting tensile strengths. ACI has established that splitting tensile strength is proportional to the square root of its compressive strength times a coefficient as presented by the next model published in ACI building code:

$$f_{ct} = A\sqrt{f_c'}$$

where f_{ct} is the splitting tensile strength in psi, f_c' is the compressive strength in psi, and A is a coefficient obtained through regression analysis.

ACI 318-89 established that this coefficient A is equal to 6.7 which makes the above mentioned model become:

$$f_{ct} = 6.7\sqrt{f_c'} \text{ (psi)}$$

The Committé Euro-Internationál du Beton (CEB) recommends a coefficient of 0.273 times the compressive strength raised to the 0.667 power, which makes the ACI model become:

$$f_{ct} = 0.273(f_c')^{0.667} \text{ (psi)}$$

Carino and Lew performed a statistical analysis on 124 published data points and concluded that the splitting tensile strength is proportional to the compressive strength to the 0.71 power times a coefficient equal to 1.15, and proposed that the ACI model should become:

$$f_{ct} = 1.15(f_c')^{0.71} \text{ (psi)}$$

Results from the regression analysis are shown in Table 5-6. For the ACI model, the coefficient A was found to be 7.02 which is slightly higher than the value of 6.7 by ACI. For the Carino and Lew model A was found to be 2.40 which is higher than the value of 1.15, and B was found to be 0.70, which is slightly lower than the value of 0.71. Figure 5-19 shows the measured values and both modified models plotted. It seems that the Carino and Lew model give a slightly better fit, especially at low compressive strengths. It also seems that the ACI model underestimates the splitting tensile strength values, especially at high compressive strengths.

Table 5-6. Results of regression analysis for relating compressive strength to splitting tensile strength

Equation	Curing condition	Coefficient A or B	Standard Error	Standard Error of the Estimate
ACI Code $f_{ct} = A\sqrt{f_c'}$	Moist curing	A=7.02	0.09529	63.3
Carino and Lew model $f_{ct} = A(f_c')^B$	Moist curing	A=2.40 B=0.62	1.0926	61.1

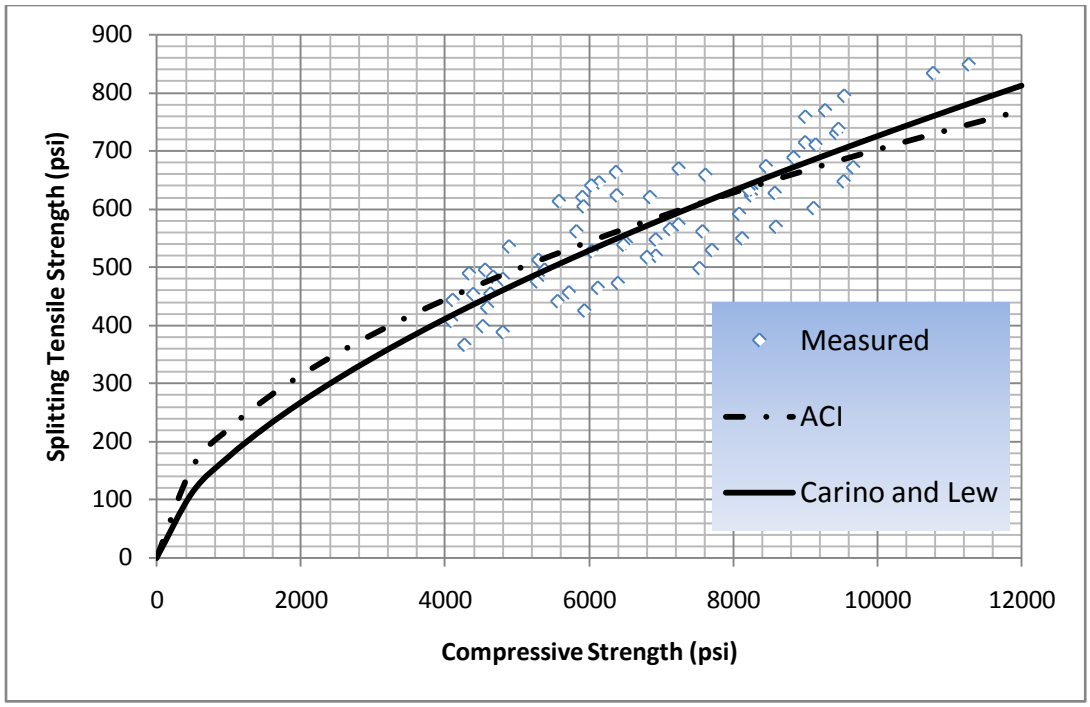

Figure 5-25. Relationship between compressive strength and splitting tensile strength

5.5 Analysis of Elastic Modulus Test Results

The results for the elastic modulus test for all mixes involved in this study are presented in Table 5-7. These results are the average of 4 values for every curing age. More detailed data is presented in Table A-3 in Appendix A.

Table 5-7. Elastic modulus of the concrete mixtures evaluated ($\times 10^6$ psi)

Mix Number	W/C	Fly ash	Slag	Age of Testing (days) 3	7	14	28	56	91
1F(1y)	0.24	20%		4.74	4.93	5.23	5.40	5.54	5.58
2F(1y)	0.33	20%		3.43	3.77	4.08	4.31	4.43	4.67
3F(1y)	0.41	20%		4.40	4.85	5.05	5.14	5.28	5.70
4F(1y)	0.37	20%		4.49	4.61	4.88	5.01	5.15	5.29
5S(1y)	0.33		50%	3.63	3.93	4.03	4.45(27)*	4.36	4.35
5S(3m)	0.33		50%	4.11	4.66	4.88	5.09	5.23	5.23
6S(1y)	0.36		50%	4.06(6)*	4.20	4.29	4.44(30)*	---	---
6S(3m)	0.36		50%	4.27	4.92	5.18	5.45	5.62	5.66
7S(1y)	0.41		70%	3.18(6)*	3.43	3.55	3.46(30)*	3.68(56)*	4.15(94)*
7S(3m)	0.41		70%	3.90	4.30	4.52	4.60	4.73	4.76
8S(1y)	0.44		50%	3.10	3.30	3.60	3.86	4.10(57)*	4.05
8S(3m)	0.44		50%	3.96	4.39	4.84	5.00	5.13	5.16
9LF(1y)	0.31	20%		2.76	2.92	3.13	3.27	3.40	3.50
10LS(1y)	0.39		60%	1.75	1.88	2.36	2.69	3.01	3.04

Table 5-7. Continued

1GF(1y)	0.24	20%		5.20	5.29	5.46	5.74	5.78(89)*	---
1GF(3m)	0.24	20%		5.04	5.41	5.61	5.50	5.60	5.74
2GF(1y)	0.33	20%		3.80	4.22	4.61	4.96	5.06	5.19
2GF(3m)	0.33	20%		4.06	4.39	4.50	4.99	5.06	5.53
3GF(1y)	0.41	20%		4.15	4.62	5.52	5.61	5.93	5.96
3GF(3m)	0.41	20%		4.24	4.55	4.85	5.10	5.55	5.66
4GF(1y)	0.37	20%		4.30	4.41	4.64	4.93	5.34(89)*	---
4GF(3m)	0.37	20%		4.49	4.10	4.85	5.10	5.36	5.71
5GS(1y)	0.33		50%	3.15	3.82	4.65	5.17	5.37	5.56
5GS(3m)	0.33		50%	2.85	3.91(10)*	4.20	4.16	4.41	4.10
6GS(1y)	0.36		50%	2.80	3.49	4.15(16)*	4.78	5.35	5.65(92)*
6GS(3m)	0.36		50%	---	4.35	5.03	5.41	5.63	5.73
7GS(1y)	0.41		70%	2.69	3.38	4.10	5.25	5.60	5.73
7GS(3m)	0.41		70%	2.43	3.35(10)*	3.76	4.46	4.90(54)*	4.73(100)*
8GS(1y)	0.44		50%	2.66	---	3.89(16)*	4.15	4.85	5.20(92)*
8GS(3m)	0.44		50%	---	3.55	4.35	4.88	5.00	4.88

Note: number in parenthesis ( ) indicates actual age in days of samples when tested.*

It can be appreciated from Table 5-7 that the elastic modulus of mixes containing Miami Oolite limestone range from 3.10×10^6 to 5.70×10^6 psi, mixes containing lightweight aggregate range in values from 1.75×10^6 to 3.50×10^6 psi, and mixes containing Georgia granite have the widest range with values from 2.43×10^6 to 5.96×10^6 psi.

Graphs Figure 5-20 through Figure 5-25 show the effects of aggregate type on the elastic modulus of comparable mixes. Each graph shows mixes with identical mix proportions except that the aggregate has been replaced by volume. The mixes containing the letter "G" are the mixes containing Georgia Granite as coarse aggregate. For example, Figure 5-20 shows the strength development of mixes 2F made with Miami Oolite limestone, and 2GF made with Georgia granite. In general, the elastic moduli of mixes containing Georgia granite are higher as compared to mixes containing Miami Oolite limestone. For example, by comparing the elastic moduli at 91 days of mixes Mix-2F and Mix-2GF, it can be seen that 2F is 4.67×10^6 psi versus 5.19×10^6 psi for Mix-2GF. This is also the case for the 91-day elastic moduli for Mix-3F and Mix-3GF: 5.70×10^6 psi versus 5.96×10^6 psi. Figure 5-22 shows 5.23×10^6 psi versus 5.56×10^6 psi for Mix-5S and Mix-5GS respectively, Figure 5-24 shows 4.76×10^6 psi versus 5.73×10^6 psi for

Mix-7S and Mix-7GS respectively, and Figure 5-25 shows 5.16×10^6 psi versus 5.20×10^6 psi for Mix-8S and Mix-8GS respectively.

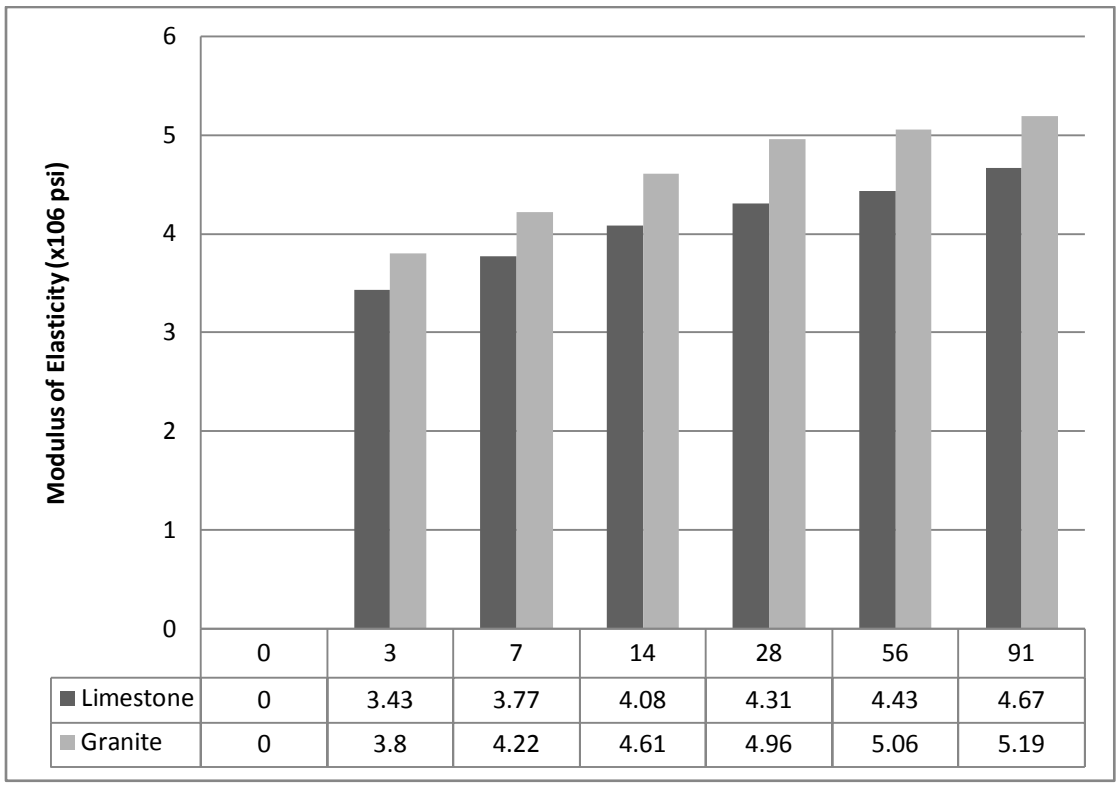

	0	3	7	14	28	56	91
Limestone	0	3.43	3.77	4.08	4.31	4.43	4.67
Granite	0	3.8	4.22	4.61	4.96	5.06	5.19

Figure 5-26. Effects of coarse aggregate type on modulus of elasticity of Mix-2F and Mix-2GF

5.6 Relationship between Compressive Strength and Elastic Modulus

The determination of modulus of elasticity is obtained by means of a complicated test, and it is known that the elastic modulus of concrete is sensitive to the modulus of the aggregate. Therefore, it is useful to find a correlation between relatively easier strength tests, such as the compressive strength test, so that this value can be used to determine this nonstrength property in question. ACI 318-95 recommends that the elastic modulus of normal weight concrete can be related to its compressive strength by the following expression:

$$E_c = \alpha\sqrt{f_c'}$$

where α is a coefficient obtained through regression analysis, f_c' is the compressive

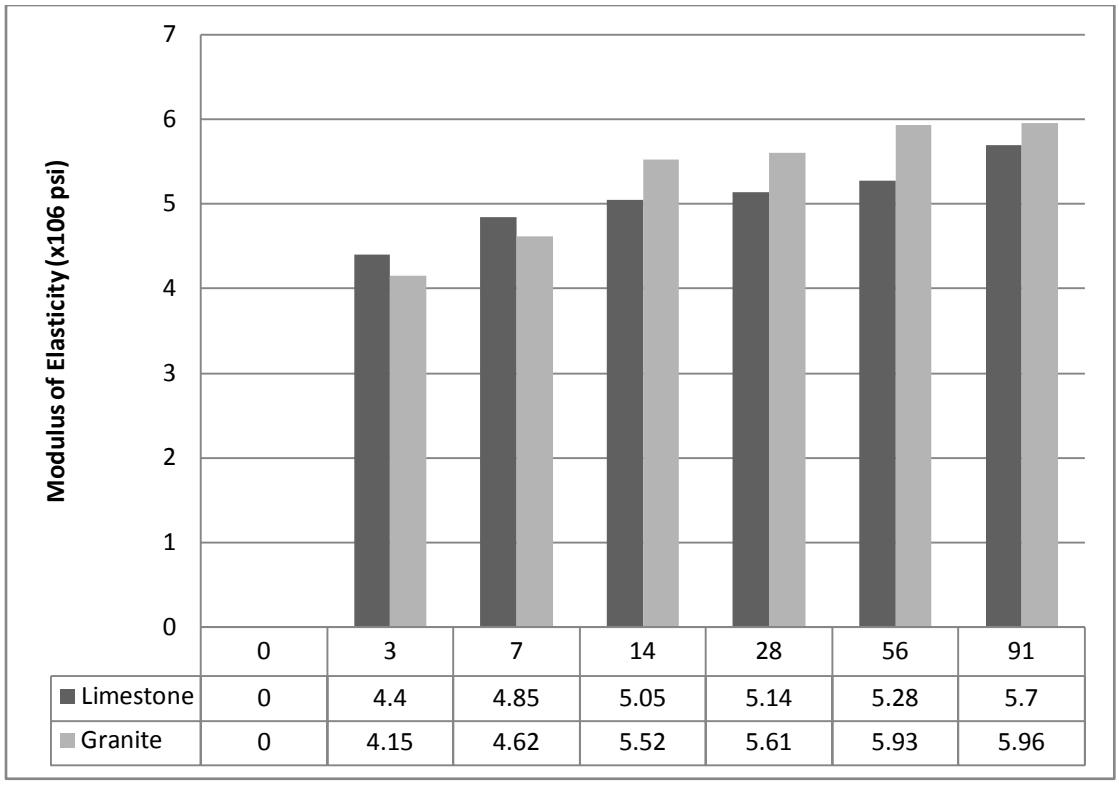

	0	3	7	14	28	56	91
Limestone	0	4.4	4.85	5.05	5.14	5.28	5.7
Granite	0	4.15	4.62	5.52	5.61	5.93	5.96

Figure 5-27. Effects of coarse aggregate type on modulus of elasticity of Mix-3F and Mix-3GF

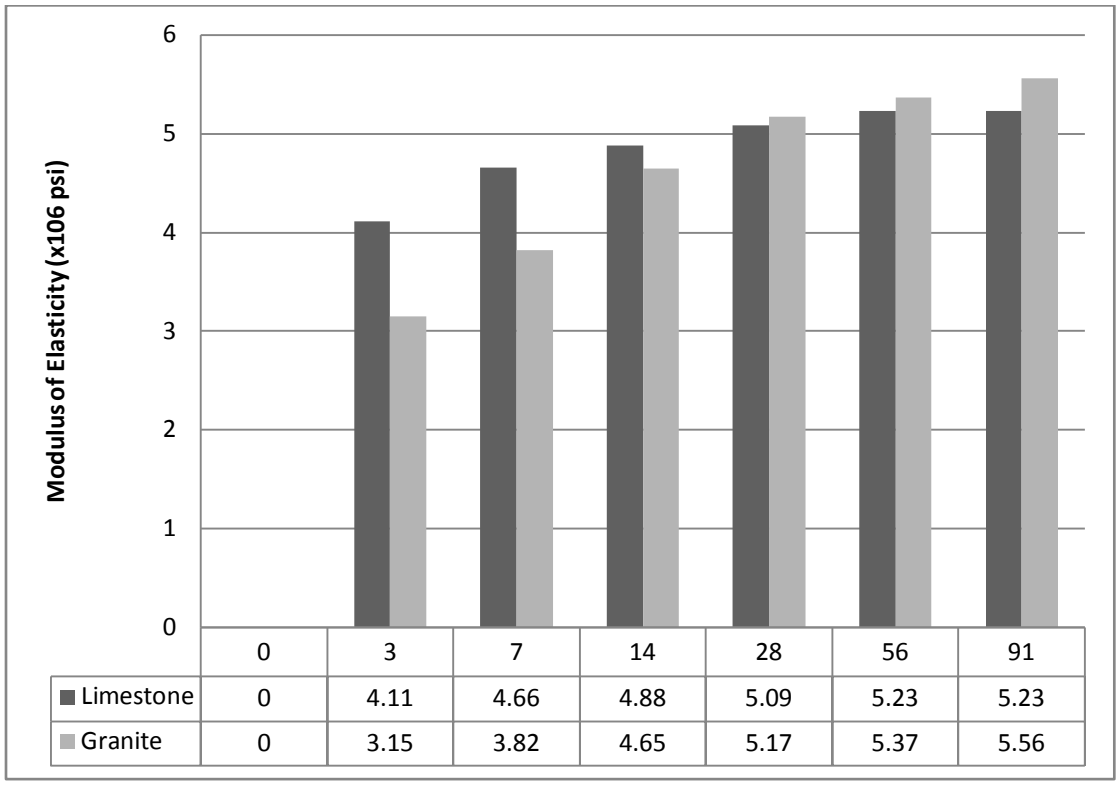

	0	3	7	14	28	56	91
Limestone	0	4.11	4.66	4.88	5.09	5.23	5.23
Granite	0	3.15	3.82	4.65	5.17	5.37	5.56

Figure 5-28. Effects of coarse aggregate type on modulus of elasticity of Mix-5S and Mix-5GS

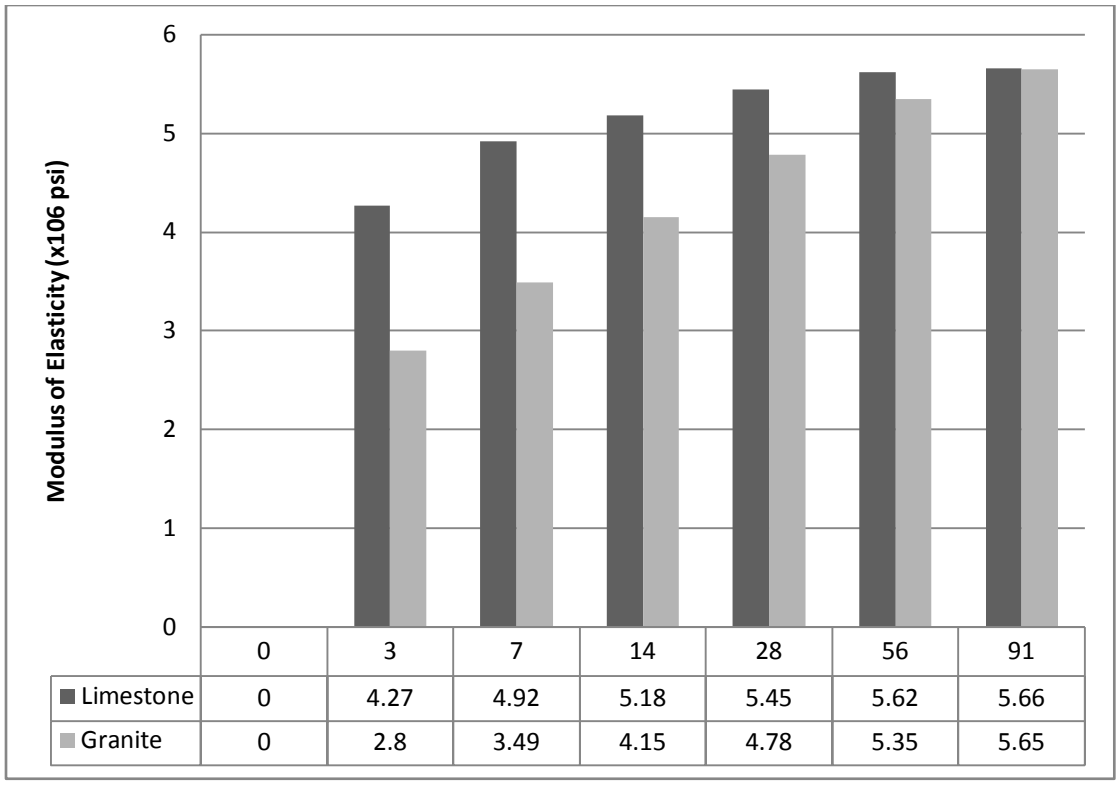

	0	3	7	14	28	56	91
Limestone	0	4.27	4.92	5.18	5.45	5.62	5.66
Granite	0	2.8	3.49	4.15	4.78	5.35	5.65

Figure 5-29. Effects of coarse aggregate type on modulus of elasticity of Mix-6S and Mix-6GS

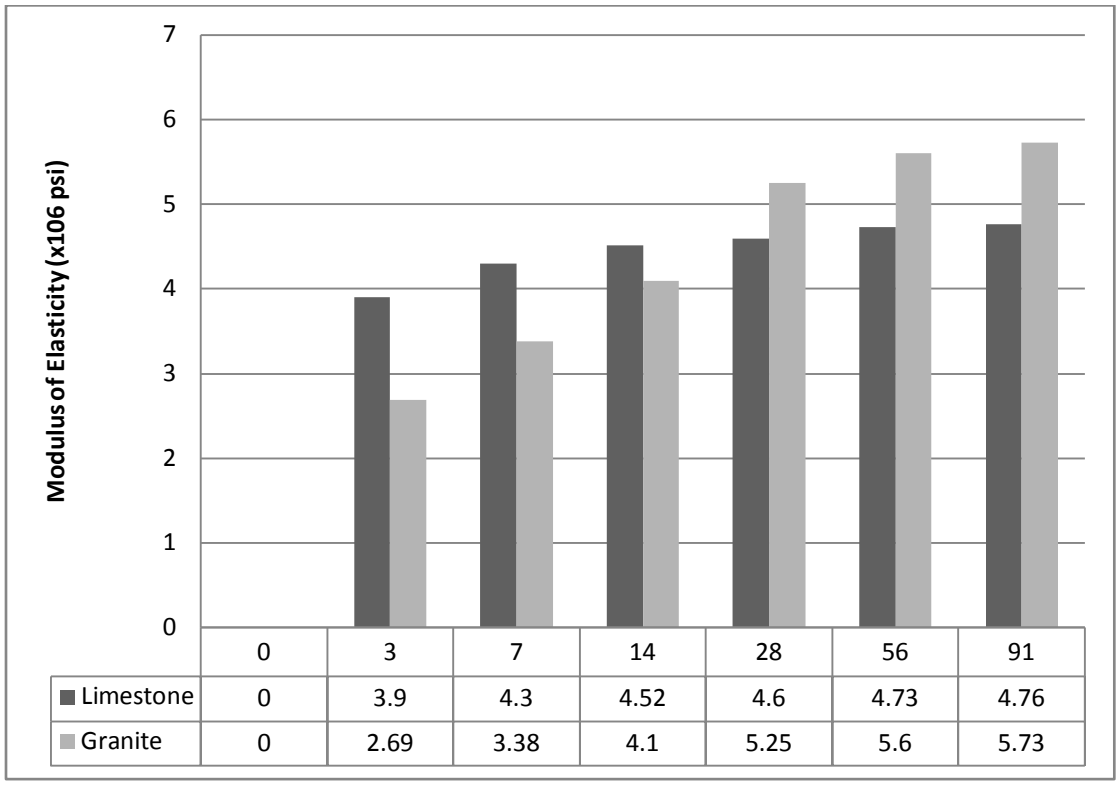

	0	3	7	14	28	56	91
Limestone	0	3.9	4.3	4.52	4.6	4.73	4.76
Granite	0	2.69	3.38	4.1	5.25	5.6	5.73

Figure 5-30. Effects of coarse aggregate type on modulus of elasticity of Mix-7S and Mix-7GS

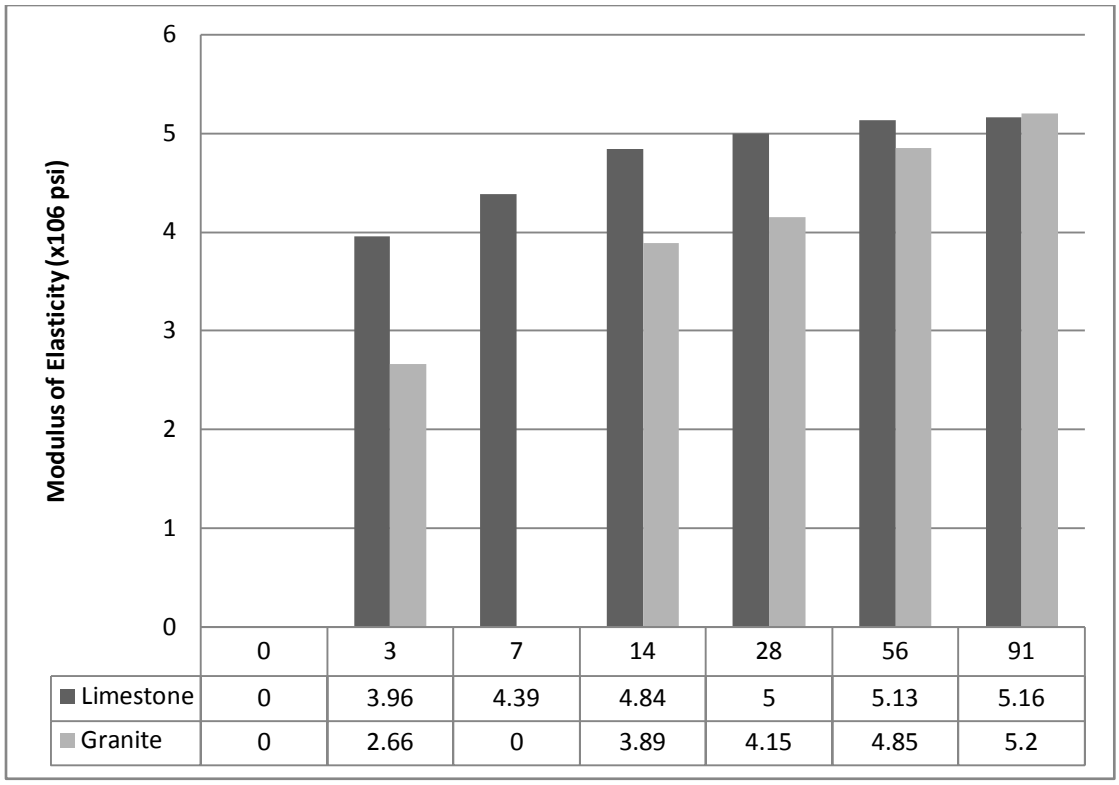

Figure 5-31. Effects of coarse aggregate type on modulus of elasticity of Mix-8S and Mix-8GS

strength of concrete in psi, and E_c is the elastic modulus in psi. ACI recommends a value of 57,000 for α which makes the above equation become:

$$E_c = 57{,}000\sqrt{f_c'}$$

For concretes with unit weight ranging from 90 to 155 lb/ft^3, ACI 318-95 recommends that the modulus of elasticity of concrete should be determined by the following formula:

$$E_c = A \cdot w_c^{1.5}\sqrt{f_c'}$$

where E_c is the elastic modulus in psi, A is a coefficient to be determined through regression analysis, w_c is the unit weight of concrete in lb/ft^3, and f_c' is the compressive strength of concrete in psi. ACI recommends a value of 33.0 for the coefficient A which makes the above formula become:

$$E_c = 33.0 \cdot w_c^{1.5}\sqrt{f_c'}$$

Figure 5-26 shows the measured results of the elastic modulus plotted against the compressive strength of all the mixes involved in this study. The results are very clear; the aggregate type has significant effects on the elastic modulus of concrete. Concretes containing Georgia granite will exhibit higher elastic modulus for the same compressive strength as compared to concretes made with Miami Oolite limestone or lightweight aggregate. Concretes made with Miami Oolite limestone will display higher elastic modulus as compared to concretes made with lightweight aggregate. Regression analysis has been performed on these measured values, and the results are presented in Table 5-8. From this table it can be seen that the value of 57,000 recommended by ACI for normal weight concrete is close to the regression analysis on concretes containing Miami Oolite limestone, which yields a value for α of 55,824. But well below the value obtained for concretes containing Georgia granite (α = 63,351) and well above the values obtained for concretes made with lightweight aggregate (α = 43,777).

Then all the results for the elastic moduli were plotted against $w_c^{1.5}\sqrt{f_c'}$ to establish a linear relationship and therefore perform a linear regression analysis, using as model the one recommended by ACI318-95 for concretes with unit weight ranging from 90 to 155 lb/ft^3; these results are presented on Table 5-9 and a plot can be seen in Figure 5-27. The value obtained for coefficient A of 33.6 which is almost the same as the value recommended by ACI318-95, which is equal to 33.0. But by plotting the model on the measured data, it is obvious that a constant must be added for a better approximation of the model. The modified ACI equation then has the form:

$$E_c = A \cdot w_c^{1.5}\sqrt{f_c'} + C$$

where E_c is the elastic modulus in psi, A is a coefficient to be determined through regression analysis, w_c is the unit weight of concrete in lb/ft^3, f_c' is the compressive

strength of concrete in psi, and C is a constant determined through regression analysis.

Regression analysis was performed on this modified model, and the results are presented in Table 5-9. The constant for A is determined to be equal to 31.92 which is slightly lower than the value recommended by ACI318-95, which is equal to 33.0, but because of the added constant, this model gives a much better approximation of the data. The modified equation is presented below; this equation can be used to predict the elastic modulus of the concretes investigated in this study:

$$E_c = 31.92 \cdot w^{1.5} \cdot \sqrt{f_c'} + 345{,}328$$

Table 5-8. Results of regression analysis for prediction of elastic modulus using the equation recommended by ACI 318-89

Aggregate type / Results	Granite	Lightweight	Limestone
α (Best-fit values)	63351	43777	55824
α (Standard Error)	811.3	692.3	292.5
α (95% confidence intervals)	62540 to 64162	42253 to 45301	55240 to 56407
Degrees of Freedom	91	11	69
R^2	0.9067	0.922	0.9088
Absolute Sum of Squares	7.863E+12	2.693E+11	2.77E+12
Sy.x	293944	156461	200295
Number of points Analyzed	92	12	70

Table 5-9. Results of regression analysis for prediction of elastic modulus using ACI 318-95 equation

Best-fit values	With equation going through the origin	Without forcing the equation to go through the origin
Slope	33.64 ± 0.1625	31.92 ± 0.7781
Y-intercept when X=0.0	0.0000	345328 ± 101545
X-intercept when Y=0.0	0.0000	-16048
1/slope	0.02973	0.03313
95% Confidence Intervals		
Slope	34.19 to 34.83	30.38 to 33.45
Sy.x	264919	256327

5.7 Summary of Findings

The summary of the results of this chapter are presented next in page 106. The information is presented as a review of the most important findings from testing results and data analysis.

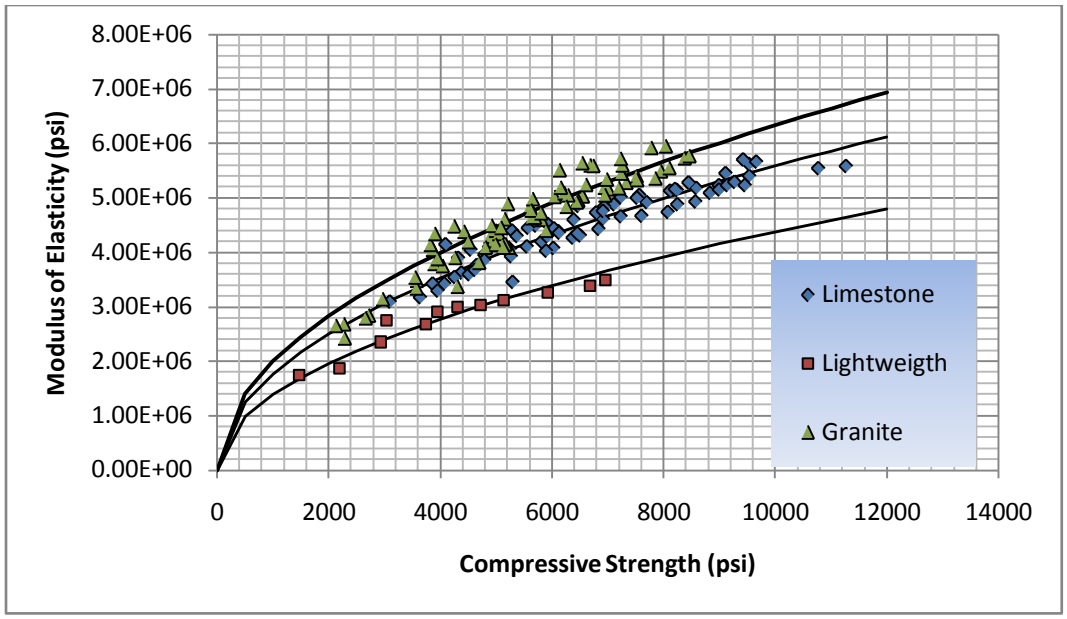

Figure 5-32. Relationship between compressive strength and elastic modulus based on ACI Code

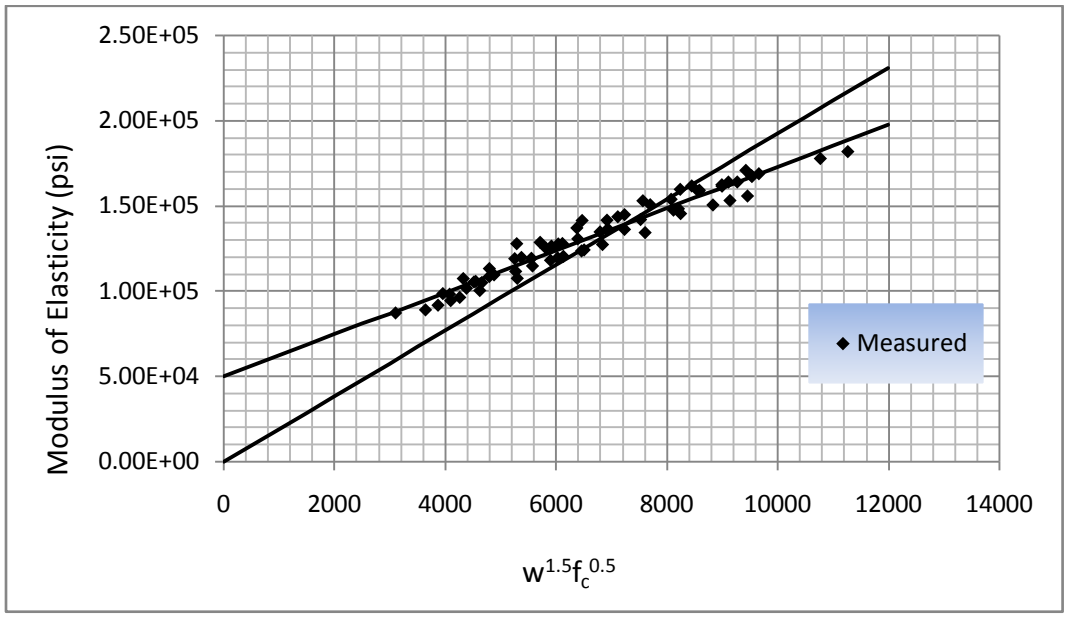

Figure 5-33. Plot of elastic modulus against $w_c^{1.5}\sqrt{f_c'}$ for all aggregate types and curing conditions

Table 5-10. Results of regression analysis for prediction of elastic modulus using the ACI 318-95 equation

Results \ Age	overall	3-day	7-day	14-day	28-day	56-day	91-day
Slope	31.92 ± 0.7781	32.37 ± 1.945	30.89 ± 1.931	31.15 ± 2.241	31.43 ± 1.735	28.85 ± 1.983	27.81 ± 2.413
Y-intercept when X=0.0	345328 ± 101545	204351 ± 214573	359969 ± 237124	469112 ± 290199	443749 to 238205	842096 ± 282142	1029259 ± 343315
X-intercept when Y=0.0	-10820	-6314	-11654	-15058	-14117	-29186	-37016
1/slope	0.03313	0.0309	0.0324	0.0321	0.0318	0.0347	0.0360
95% Confidence Intervals							
Slope	30.38 to 33.45	28.36 to 36.37	26.92 to 34.86	26.56 to 35.75	27.86 to 35.01	24.74 to 32.96	22.75 to 32.86
Y-intercept when X=0.0	144726 to 545930	-237652 to 646264	-127439 to 847378	-126318 to 1064542	-46833 to 934332	256961 to 1427231	310702 to 1747816
X-intercept when Y=0.0	-17970 to -4327	-22789 to 6531	-31479 to 3656	-40087 to 3533	-33536 to 1338	-57686 to -7795	-76812 to -9456
Goodness of Fit							
r^2	0.9162	0.9172	0.9077	0.8774	0.9292	0.9059	0.8748
Sy.x	256327	252444	236042	262646	201179	235995	289701
Is slope significantly non-zero?							
F	1682.6	276.8	255.8	193.3	328.3	211.8	132.7
DFn, DFd	1, 154	1, 24	1, 25	1, 26	1, 24	1, 21	1, 18
P value	< 0.0001	< 0.0001	< 0.0001	< 0.0001	< 0.0001	< 0.0001	< 0.0001
Deviation from zero?	Significant	Significant	Significant	Significant	Significant	Significant	Significant
Data							
Number of X values	156	26	27	28	26	23	20
Maximum number of Y replicates	1	1	1	1	1	1	1
Total number of values	156	26	27	28	26	23	20

(1) The compressive strengths of concrete mixes containing Miami Oolite limestone aggregate are overall greater in magnitude than those mixes containing Georgia granite or lightweight aggregate. This can be attributed to differences in physical properties between the aggregates.

(2) The splitting tensile strengths of the concrete mixes containing Miami Oolite limestone aggregate are overall greater in magnitude than those mixes containing Georgia granite or lightweight aggregate. This can also be attributed to differences in physical properties between the aggregates.

(3) Mixes containing Georgia granite aggregate produce concretes with higher elastic moduli as compared to mixes containing Miami Oolite limestone or lightweight aggregate.

(4) Mixes containing slag will develop strength at early days much faster than mixes containing fly ash. Mixes containing slag reach 90% of their 91-day strength at around 20 days, while mixes containing fly ash reach 90% of their 91-day strength at around 50 days.

(5) The model recommended by ACI to predict the compressive strength of concrete at various ages was modified to give a better approximation of the mixes involved in this study. The general expression is presented next:

$$(f_c^{'})t = \frac{t}{a + \beta t}(f_c^{'})_{28}$$

The following equation is recommended by ACI 209R-5:

$$(f_c^{'})t = \frac{t}{4.00 + 0.85t}(f_c^{'})_{28}$$

The modified equation to predict concretes made with Miami Oolite aggregate is presented next:

$$(f_c^{'})t = \frac{t}{2.33 + 0.92t}(f_c^{'})_{28}$$

The modified equation to predict concretes made with Georgia granite aggregate is presented next:

$$(f_c^{'})t = \frac{t}{3.36 + 0.88t}(f_c^{'})_{28}$$

Finally, the modified equation to predict concretes made with lightweight aggregate is presented next:

$$(f_c^{'})t = \frac{t}{5.50 + 0.78t}(f_c^{'})_{28}$$

(6) The model that relates compressive strength to splitting tensile strength recommend by ACI is presented next:

$$f_{ct} = A\sqrt{f_c^{'}}$$

ACI recommends a value of 6.7 for A, which makes the expression become:

$$f_{ct} = 6.7\sqrt{f_c'}$$

This expression was modified to the following equation:

$$f_{ct} = 7.02\sqrt{f_c'}$$

The model recommended by Carino and Lew is presented next:

$$f_{ct} = A(f_c')^B$$

Carino and Lew recommend values of 1.15 and 0.71 for A and B respectively. This expression is presented next:

$$f_{ct} = 1.15(f_c')^{0.71}$$

This expression was modified to the following equation:

$$f_{ct} = 2.40(f_c')^{0.62}$$

(7) ACI 318 recommends the following expression to relate compressive strength to elastic modulus. This expression is presented next:

$$E_c = \alpha\sqrt{f_c'}$$

ACI recommends a value equal to 57,000 for α. This expression is presented next:

$$E_c = 57{,}000\sqrt{f_c'}$$

The modified equation for mixes containing Georgia granite aggregate is presented next:

$$E_c = 63{,}351\sqrt{f_c'}$$

The modified equation for mixes containing Miami Oolite limestone aggregate is presented next:

$$E_c = 55{,}824\sqrt{f_c'}$$

The modified equation for mixes containing lightweight aggregate is presented next:

$$E_c = 43{,}777\sqrt{f_c'}$$

(8) Results of all measured data for all aggregate types is approximated by the following formula recommended by ACI, a constant is added to the model for a better estimate of the elastic modulus:

$$E_c = A \cdot w_c^{1.5} \sqrt{f_c'} + C$$

The modified equation for mixes containing all 3 aggregate types is presented next:

$$E_c = 31.92 \cdot w^{1.5} \cdot \sqrt{f_c'} + 345{,}328$$

CHAPTER 6
ANALYSIS OF SHRINKAGE TEST RESULTS

6.1 Introduction

The shrinkage strain results for all mixes are presented in this chapter. The preparation procedures of the specimens to be tested in shrinkage strain are explained, as well as the curing methods and time. The shrinkage strains were calculated by means of an equation presented later in the chapter. DataFit was used to perform regression analysis on the results so a relationship can be established between shrinkage strain and the different factors that have an effect on it. A relationship between the compressive strength of concrete and shrinkage strain is established, and well as a relationship between the elastic modulus and the shrinkage strain. An evaluation of the current shrink prediction model is discussed, and a model to predict ultimate shrinkage strains is presented as well. Data from Dr. Liu's dissertation was combined with the data collected in this part of the studied and both were analyzed.

6.2 Results and Analysis of Shrinkage Tests

The following table shows the shrinkage strains of the concrete mixtures evaluated at various curing ages. Each mix has samples cured under two different conditions: in the first condition, the samples were moist cured for 7 days and then moved to a 50% moisture room for the rest of the time until ready to be tested, and the second condition involves moist curing for 14 days and then 50% moist curing until the samples are ready to be tested.

Table 6-1. Shrinkage strains of the concrete mixtures evaluated at various curing ages

		Age of testing (days)						
Mix	Moist Curing Time	3	7	14	28	56	91	Predicted ultimate shrinkage strain
Mix-1F(1y)	7-day	2.00E-05	4.40E-05	7.50E-05	1.18E-04	1.63E-04	2.02E-04	2.66E-04
	14-day	1.40E-05	3.50E-05	6.10E-05	1.00E-04	1.36E-04	1.67E-04	2.27E-04
Mix-2F(1y)	7-day	5.10E-05	9.70E-05	1.54E-04	2.10E-04	2.61E-04	2.86E-04	3.39E-04
	14-day	3.10E-05	6.90E-05	1.12E-04	1.73E-04	2.33E-04	2.58E-04	3.20E-04

Table 6-1. Continued

Mix-3F(1y)	7-day	4.00E-05	7.30E-05	1.24E-04	1.77E-04	2.21E-04	2.48E-04	3.03E-04
	14-day	2.40E-05	5.00E-05	8.70E-05	1.37E-04	1.84E-04	2.16E-04	2.85E-04
Mix-4F(1y)	7-day	3.70E-05	7.10E-05	1.18E-04	1.76E-04	2.33E-04	2.67E-04	3.64E-04
	14-day	3.10E-05	5.30E-05	9.20E-05	1.42E-04	1.97E-04	2.31E-04	3.44E-04
Mix-5S(3m)	7-day	4.40E-05	8.80E-05	1.30E-04	1.70E-04	2.01E-04	2.16E-04	2.46E-04
	14-day	4.30E-05	7.40E-05	1.10E-04	1.49E-04	1.78E-04	1.93E-04	2.29E-04
Mix-5S(1y)*	7-day	4.78E-05	8.86E-05	1.30E-04	1.70E-04	2.01E-04	2.16E-04	2.55E-04
	14-day	4.25E-05	7.46E-05	1.09E-04	1.46E-04	1.77E-04	1.94E-04	2.29E-04
Mix-6S(3m)	7-day	4.20E-05	8.40E-05	1.23E-04	1.56E-04	1.83E-04	1.95E-04	2.16E-04
	14-day	3.30E-05	7.10E-05	1.12E-04	1.41E-04	1.64E-04	1.76E-04	1.93E-04
Mix-6S(1y)*	7-day	4.96E-05	8.75E-05	1.21E-04	1.55E-04	1.98E-04	2.41E-04	2.05E-04
	14-day	4.44E-05	7.33E-05	1.08E-05	1.51E-04	1.75E-04	1.98E-04	1.99E-04
Mix-7S(3m)	7-day	3.90E-05	8.10E-05	1.26E-04	1.70E-04	2.02E-04	2.23E-04	2.55E-04
	14-day	3.80E-05	7.30E-05	1.11E-04	1.48E-04	1.84E-04	2.04E-04	2.40E-04
Mix-7S(1y)*	7-day	4.46E-05	7.75E-05	1.11E-04	1.53E-04	2.01E-04	2.54E-04	2.65E-04
	14-day	4.93E-05	6.78E-05	7.45E-05	9.28E-05	1.21E-04	2.03E-04	2.61E-04
Mix-8S(1y)*	7-day	5.08E-05	9.82E-05	1.54E-04	2.18E-04	2.76E-04	3.08E-04	5.52E-04
	14-day	3.13E-05	6.60E-05	1.05E-04	1.43E-04	1.74E-04	1.90E-04	4.58E-04
Mix-8S(3m)	7-day	7.30E-05	1.23E-04	1.61E-04	1.94E-04	2.28E-04	2.50E-04	2.43E-04
	14-day	5.00E-05	9.80E-05	1.36E-04	1.69E-04	2.02E-04	2.30E-04	2.20E-04
Mix-9LF(1y)	7-day	4.90E-05	9.60E-05	1.34E-04	2.25E-04	2.87E-04	3.22E-04	3.95E-04
	14-day	4.60E-05	8.30E-05	1.34E-04	1.84E-04	2.41E-04	2.76E-04	3.49E-04
Mix-10LS(1y)	7-day	6.70E-05	1.30E-04	1.98E-04	2.60E-04	3.20E-04	3.58E-04	4.22E-04
	14-day	3.80E-05	9.00E-05	1.52E-04	2.09E-04	2.80E-04	3.17E-04	3.96E-04
Mix-1GF(1y)*	7-day	1.18E-04	6.76E-05	1.52E-05	1.22E-04	1.69E-04	2.30E-04	2.23E-04
	14-day	1.99E-04	6.78E-05	9.24E-05	1.38E-04	1.77E-04	2.32E-04	1.98E-04
Mix-1GF(3m)*	7-day	9.90E-05	1.50E-04	3.50E-05	7.67E-05	1.47E-04	1.65E-04	2.23E-04
	14-day	2.16E-05	4.42E-05	6.83E-05	1.00E-04	1.32E-04	1.51E-04	1.98E-04
Mix-2GF(1y)	7-day	---	---	---	---	---	---	---
	14-day	3.20E-05	6.10E-05	1.09E-04	1.61E-04	2.04E-04	2.31E-04	2.83E-04
Mix-2GF(3m)	7-day	3.34E-05	5.00E-05	8.34E-05	1.33E-04	2.08E-04	2.32E-04	3.18E-04
	14-day	2.78E-05	2.56E-05	7.23E-05	1.11E-04	1.91E-04	2.20E-04	3.08E-04
Mix-3GF(1y)	7-day	---	---	---	---	---	---	---
	14-day	2.90E-05	5.40E-05	8.40E-05	1.23E-04	1.57E-04	1.82E-04	2.62E-04
Mix-3GF(3m)*	7-day	2.08E-05	4.33E-05	7.34E-05	1.13E-04	1.55E-04	1.81E-04	2.49E-04
	14-day	2.03E-05	4.04E-05	6.76E-05	1.05E-04	1.48E-04	1.77E-04	2.70E-04
Mix-4GF(1y)*	7-day	4.11E-05	9.32E-05	1.19E-04	1.61E-04	1.96E-04	2.39E-04	2.89E-04
	14-day	6.79E-05	1.07E-04	2.14E-04	1.92E-04	3.03E-04	2.77E-04	3.38E-04
Mix-4GF(3m)	7-day	5.46E-05	9.02E-05	1.25E-04	1.60E-04	2.21E-04	2.35E-04	2.89E-04
	14-day	9.25 E-05	1.34E-04	2.14E-04	2.79E-04	3.41E-04	2.53E-04	3.38E-04
Mix-5GS(3m)*	7-day	7.90E-05	9.33E-05	1.18E-04	1.49E-04	1.88E-04	2.25E-04	2.35E-04
	14-day	5.68E-05	7.56E-05	1.05E-04	1.40E-04	1.86E-04	2.20E-04	2.35E-04
Mix-6GS(1y)*	7-day	8.91E-06	5.53E-05	9.36E-05	1.29E-04	1.41E-04	2.35E-04	1.23E-04
	14-day	3.12E-05	5.77E-05	1.04E-04	1.38E-04	2.04E-04	2.64E-04	1.50E-04

Table 6-1. Continued

Mix-6GS(3m)	7-day	2.45E-05	3.45E-05	5.56E-05	8.12E-05	1.76E-04	1.84E-04	1.23E-04
	14-day	6.33E-05	9.34E-05	1.13E-04	1.29E-04	1.40E-04	1.60E-04	1.50E-04
Mix-7GS(1y)	7-day	---	---	---	---	---	---	---
	14-day	4.30E-05	7.40E-05	1.00E-04	1.31E-04	1.63E-04	1.81E-04	2.19E-04
Mix-7GS(3m)*	7-day	5.63E-05	8.30E-05	1.11E-04	1.43E-04	1.75E-04	1.95E-04	2.48E-04
	14-day	4.78E-05	7.07E-05	9.56E-05	1.26E-04	1.58E-04	1.80E-04	2.49E-04
Mix-8GS(1y)*	7-day	7.54E-05	7.03E-05	1.21E-05	1.43E-04	1.91E-04	2.30E-04	2.34E-04
	14-day	1.51E-05	3.14E-05	6.40E-05	8.29E-05	1.27E-04	1.53E-04	2.10E-04
Mix-8GS(3m)*	7-day	5.33E-05	8.82E-05	1.24E-04	1.34E-04	1.88E-04	2.03E-04	2.34E-04
	14-day	2.39E-05	4.57E-05	7.26E-05	1.06E-04	1.40E-04	1.60E-04	7.54E-05

**** Data has been modified***

6.2.1 Effects of Curing Conditions on Shrinkage Behavior of Concrete

Figure 6-1 shows the shrinkage strain at 91 for both curing conditions for the mixes containing Miami Oolite limestone as aggregate. It can be seen that moist curing samples for 14 days has a considerably lower shrinkage strain at 91 days relative to the samples that were moist cured for 7 days. For example, the percent difference between curing conditions for Mix-1F is of 19.0% for the 7 day shrinkage strain of 2.02×10^{-4} and the 14 day shrinkage strain of 1.67×10^{-4}. For Mix-2F the percent difference is 10.3% for the 7 day shrinkage strain of 2.86×10^{-4} and the 14 day shrinkage strain of 1.58×10^{-4}. For Mix-3F the percent difference is 13.8% for the 7 day shrinkage strain of 2.48×10^{-4} and the 14 day shrinkage strain of 2.16×10^{-4}. For Mix-4F the percent difference is 14.5% for the 7 day shrinkage strain of 2.67×10^{-4} and the 14 day shrinkage strain of 2.31×10^{-4}. For mixes containing slag, similar strains can be appreciated. For Mix-5S the percent difference is 11.2% for the 7 day shrinkage strain of 2.16×10^{-4} and the 14 day shrinkage strain of 1.93×10^{-4}. For Mix-6S the percent difference is 15.3% for the 7 day shrinkage strain of 2.18×10^{-4} and the 14 day shrinkage strain of 1.87×10^{-4}. For Mix-6S the percent difference is 15.3% for the 7 day shrinkage strain of 2.18×10^{-4} and the 14 day shrinkage strain of 1.87×10^{-4}. For Mix-7S the percent difference is 15.8% for the 7 day shrinkage strain of 2.39×10^{-4} and the

14 day shrinkage strain of 2.04×10^{-4}. For Mix-8S the percent difference is 28.2% for the 7 day shrinkage strain of 2.79×10^{-4} and the 14 day shrinkage strain of 2.10×10^{-4}.

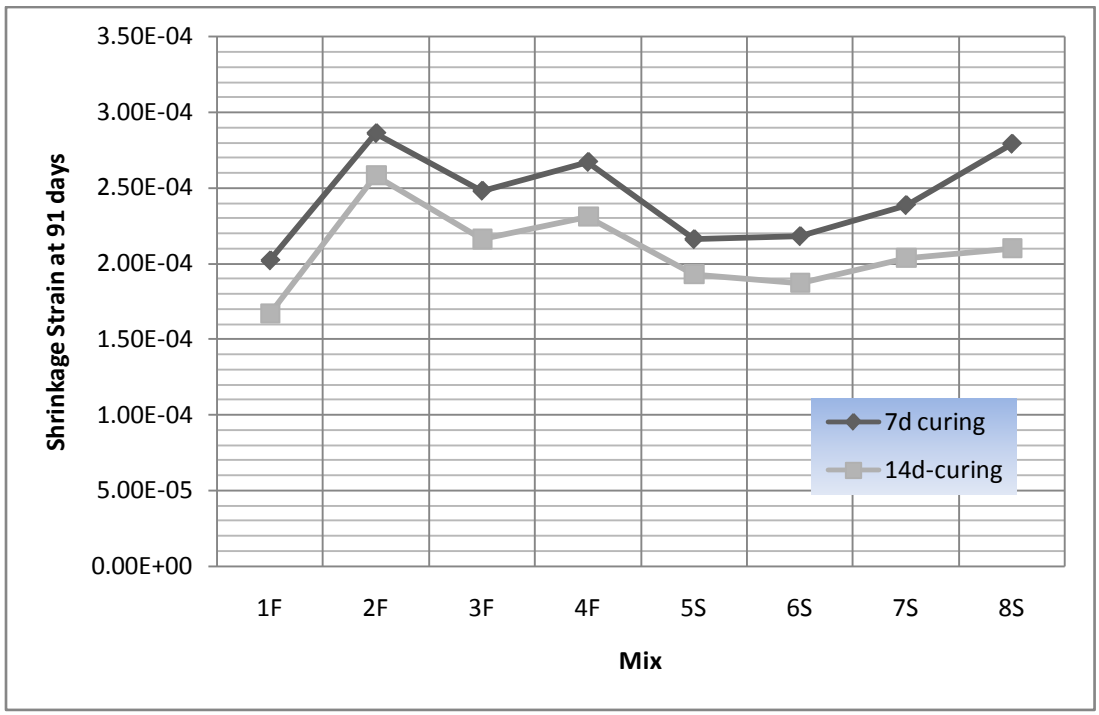

Figure 6-1. Effects of curing condition on shrinkage strain of concrete mixtures containing Miami Oolite limestone aggregate at 91 days

Figure 6-2 shows the shrinkage strain at 91 for both curing conditions for the mixes containing Georgia granite as aggregate. The effects of the curing conditions at 91 days seem to be less pronounced as compared to mixes containing Miami Oolite limestone. For example, the percent difference between curing conditions for Mix-1GF is of 3.1% for the 7 day shrinkage strain of 1.98×10^{-4} and the 14 day shrinkage strain of $1.92\text{x}10^{-4}$. For Mix-2GF the percent difference is 2.8% for the 7 day shrinkage strain of 2.32×10^{-4} and the 14 day shrinkage strain of 2.26×10^{-4}. For Mix-3GF the percent difference is 0.8% for the 7 day shrinkage strain of 1.81×10^{-4} and the 14 day shrinkage strain of 1.80×10^{-4}. For Mix-5GS the percent difference 2.2% for the 7 day shrinkage strain of 2.25×10^{-4} and the 14 day shrinkage strain of 2.20×10^{-4}. For Mix-7GS the percent difference is a bit higher in the order of 1.95% for the 7 day shrinkage strain of

1.81×10^{-4} and the 14 day shrinkage strain of 2.20×10^{-4}. And, similarly to Mix-8S, Mix-8GS has the highest percent difference in the order of 32.2% for the 7 day shrinkage strain of 2.17×10^{-4} and the 14 day shrinkage strain of 1.57×10^{-4}. Mixes Mix-4GF and Mix-6GS show that the shrinkage strain for the 7 day curing condition is lower than the 14 day curing condition; while these results might not be what is expected, it must be noted that these are only the results of readings of that specific date, meaning that the readings might have been off. From these results it seems that curing condition does not have a significant effect on mixes containing Georgia granite. Moreover, when comparing the shrinkage strain at 91-days for both mixes, the mixes containing Georgia granite exhibit a much lower shrinkage strain. This could be explained by analyzing the properties of the fresh concrete, the environmental conditions when the samples were transferred from the storage to the lab, and the modulus of elasticity of the concretes. Chapter 5 showed the non-strength results of both mixes, and the mixes containing Georgia granite aggregate had considerably higher elastic modulus.

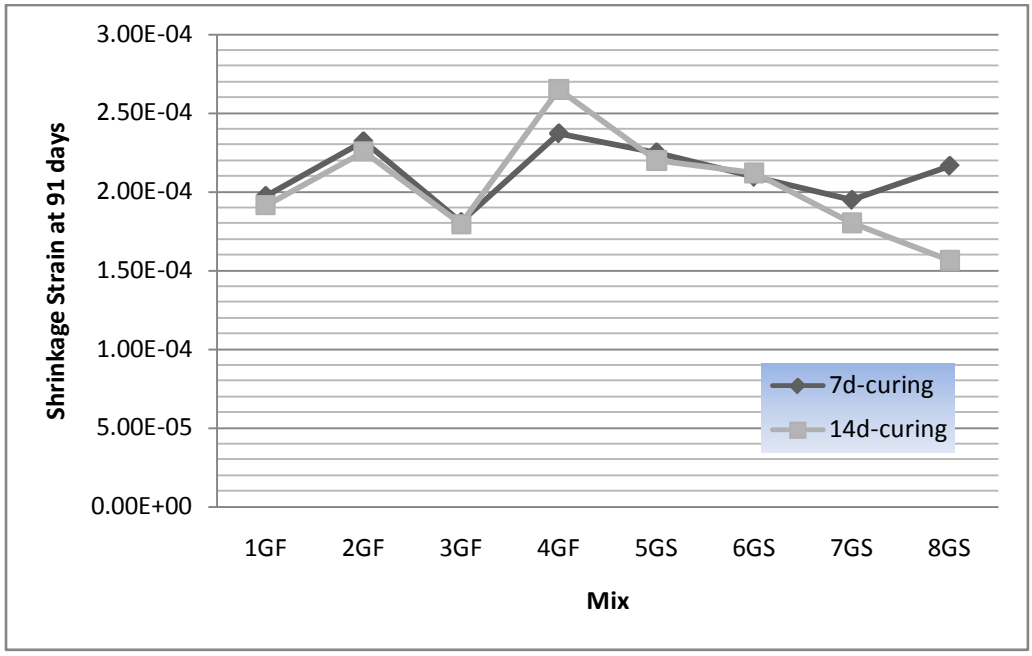

Figure 6-2. Effects of curing condition on shrinkage strain of concrete mixtures containing Georgia granite aggregate at 91 days

Figure 6-3 shows the shrinkage strain at 91 for both curing conditions for the two mixes containing lightweight aggregate, Mix-9LF and Mix-10-LS. For Mix-9LF the percent difference is 15.4% for the 7 day shrinkage strain of 3.22×10^{-4} and the 14 day shrinkage strain of 2.76×10^{-4}. For Mix-10LS the percent difference is 12.1% for the 7 day shrinkage strain of 3.58×10^{-4} and the 14 day shrinkage strain of 3.17×10^{-4}. Overall, the mixes containing lightweight aggregate show the highest shrinkage strain at 91 days as compared to mixes containing Miami Oolite limestone or Georgia granite as aggregate.

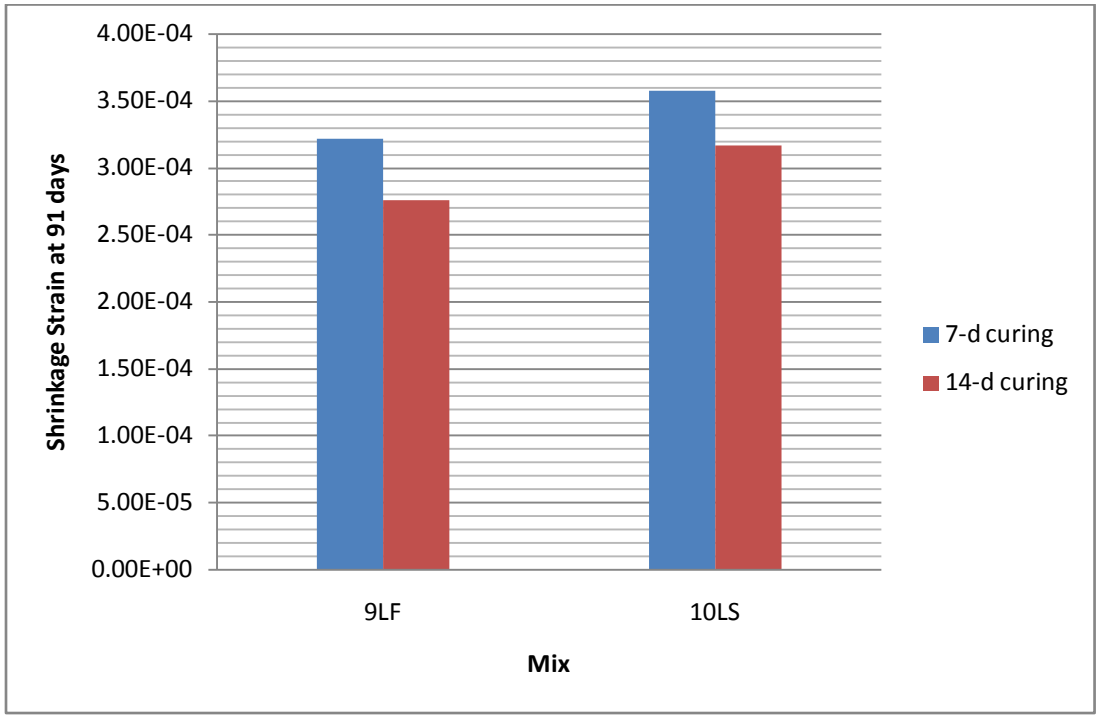

Figure 6-3. Effects of curing condition on shrinkage strain of concrete mixtures containing lightweight aggregate at 91 days

6.2.2 Effects of Mineral Additives on Shrinkage Behavior

Further investigation of Figure 6-1 shows an interesting finding in the effects of mineral additives on shrinkage behavior of concrete: by comparing mixes with the same water to cementitious materials ratio, one can see that mixes that contain slag seem to experience lower shrinkage strains at 91 days as compared to concrete mixtures containing fly ash. For example,

mixes Mix-2F and Mix-5S both have a water to cementitious materials ratio of 0.33. But for 7 day curing condition, Mix2F exhibits a shrinkage strain of 2.86×10^{-4} at 91 days while Mix-5S exhibits a shrinkage strain of 2.16×10^{-4} at 91 days; a 27.9% difference. For 14 days curing condition, this percent difference is of 28.8% between 2.58×10^{-4} at 91 days for Mix-2F and 1.93×10^{-4} at 91 days for Mix-5S. Mixes Mix-3F and Mix-7S also have similar water to cementitious materials ratio of 0.41. But for 7 day curing condition, Mix3F exhibits a shrinkage strain of 2.48×10^{-4} at 91 days while Mix-7S exhibits a shrinkage strain of 2.39×10^{-4} at 91 days; a 3.9% difference. For 14 days curing condition, this percent difference is of 6.0% between 2.16×10^{-4} at 91 days for Mix-3F and 2.04×10^{-4} at 91 days for Mix-7S. Similar results are found in the case of mixes Mix-2GF and Mix-5GS. For 7 day curing condition, Mix2GF exhibits a shrinkage strain of 2.32×10^{-4} at 91 days while Mix-5GS exhibits a shrinkage strain of 2.25×10^{-4} at 91 days; a 3.1% difference. For 14 days curing condition, this percent difference is of 2.5% between 2.26×10^{-4} at 91 days for Mix-2GF and $2.20\text{x}10^{-4}$ at 91 days for Mix-5GS. For mixes Mix-3GF and Mix-7GS, this is not the case. For 7 day curing condition, Mix3GF exhibits a shrinkage strain of 1.80×10^{-4} at 91 days while Mix-7GS exhibits a shrinkage strain of 1.95×10^{-4} at 91 days; a 7.4% difference. For 14 days curing condition, this percent difference is of 0.6% between 1.80×10^{-4} at 91 days for Mix-3GF and 1.81×10^{-4} at 91 days for Mix-7GS.

6.2.3 Effects of Water Content on Shrinkage Behavior

Figure 6-4 shows a plot of the shrinkage strain at 91 days for each mix against its corresponding water content in pounds per cubic yard. The results do not seem to be very conclusive: While it would be expected that the higher the water content the more water the concrete will lose to the environment leading higher the shrinkage strain, the data seem to be scattered with some points well below the trend line that do not seem to follow this general trend.

This could possibly mean that the shrinkage strain is not entirely dependent on the water content of concrete, but rather a combination of other factors. The addition of supplementary data could be helpful to establish a more solid relationship between water content and shrinkage strain.

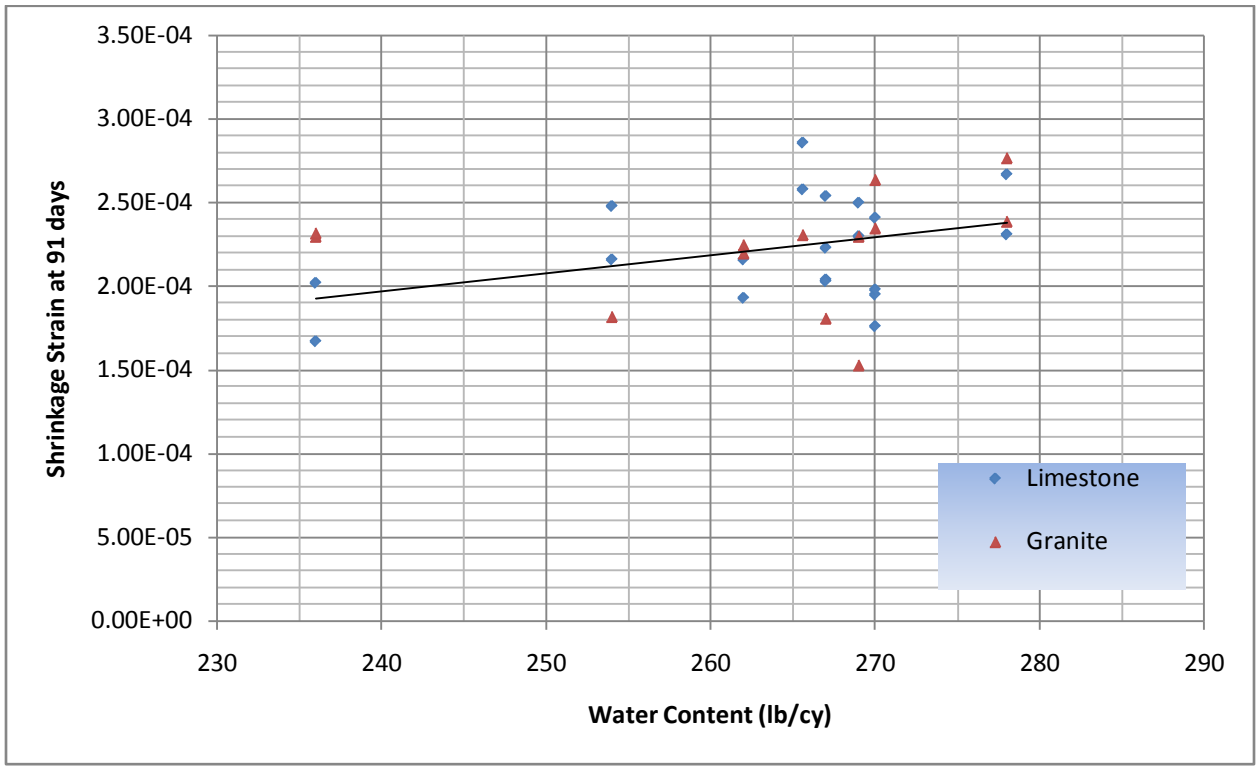

Figure 6-4. Effects of water content on shrinkage strain at 91 days

6.2.4 Effects of Aggregate Types on Shrinkage Behavior

Figure 6-5 shows the shrinkage strain at 91 days for each mix for both types of aggregate: Miami Oolite limestone and Georgia granite aggregate. The results show mixed results, half of the mixes containing Georgia granite shrink less than the identical mixes with the coarse aggregate replaced with Miami Oolite limestone aggregate and some shrink more. An important fact should be mention and it is that the results graphed are the calculated shrinkage strains from the actual readings, which means that the readings could have been a bit high or low. It is more important and more useful to examine the regression analysis for all data pertaining to each mix. A quick observation of the difference in shrinkage strains between mixes shows that the

magnitude of the shrinkage strains for the Georgia granite mixes that shrink more than the limestone mixes, is much lower than the magnitude of those who shrink more. For example, Mix-1GF is 22.4% higher in shrinkage strain than Mix-1F. At 91 days Mix-1F has a shrinkage strain of 1.85×10^{-4} while Mix-1GF has a shrinkage strain of 2.31×10^{-4}. Mix-2GF is 16.3% lower in shrinkage strain than Mix-2F. At 91 days Mix-2F has a shrinkage strain of 2.72×10^{-4} while Mix-2GF has a shrinkage strain of 2.31×10^{-4}. Mix-3GF is 24.2% lower in shrinkage strain than Mix-3F. At 91 days Mix-3F has a shrinkage strain of 2.32×10^{-4} while Mix-3GF has a shrinkage strain of 1.82×10^{-4}. Mix-4GF is 3.6% higher in shrinkage strain than Mix-4F. At 91 days Mix-4F has a shrinkage strain of 2.49×10^{-4} while Mix-4GF has a shrinkage strain of 2.58×10^{-4}. Mix-5GS is 8.4% higher in shrinkage strain than Mix-5S. At 91 days Mix-5S has a shrinkage strain of 2.05×10^{-4} while Mix-5GS has a shrinkage strain of 2.23×10^{-4}. Mix-6GS is 20.8% higher in shrinkage strain than Mix-6S. At 91 days Mix-6S has a shrinkage strain of 2.03×10^{-4} while Mix-6GS has a shrinkage strain of 2.50×10^{-4}. Mix-7GS is 42.2% lower in shrinkage strain than Mix-7S. At 91 days Mix-7S has a shrinkage strain of 2.21×10^{-4} while Mix-7GS has a shrinkage strain of 1.44×10^{-4}. Mix-8GS is 50.7% lower in shrinkage strain than Mix-8S. At 91 days Mix-8S has a shrinkage strain of 3.22×10^{-4} while Mix-8GS has a shrinkage strain of 1.92×10^{-4}.

6.2.5 Relationship between Compressive Strength and Shrinkage Strain

It would be very useful to establish a relationship between the fundamental properties of concrete, such as compressive strength, and its shrinkage strain because of strength tests are relatively easier and much faster to perform than shrinkage strain. As will be discussed later on, the measurement of shrinkage strain can be very time consuming and these measurements should be performed by a single person only.

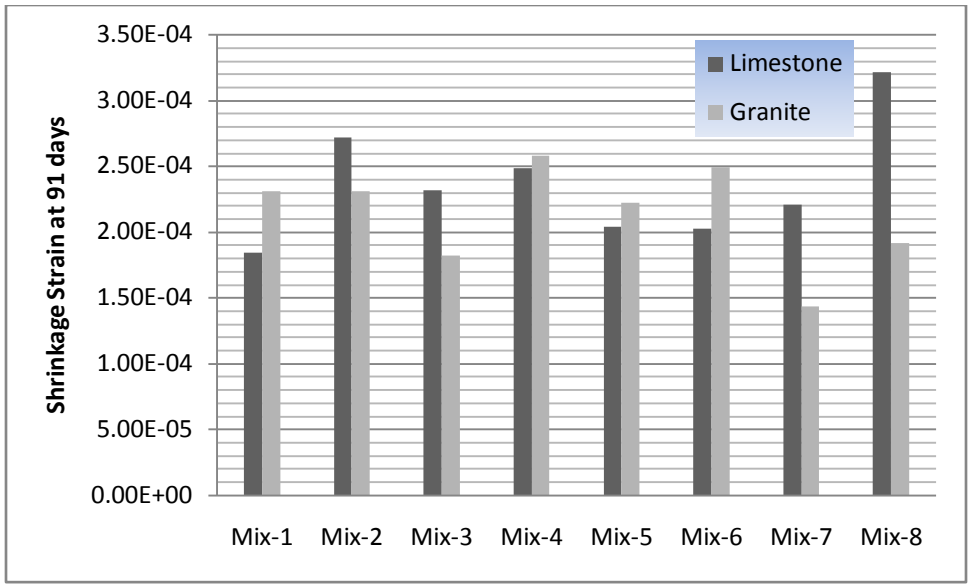

Figure 6-5. Effects of coarse aggregate type on shrinkage behavior of concrete

Figure 6-6 shows the shrinkage strain results at 91 days against their compressive strength at 28 days. According to Liu, this relationship can be approximated with a model of exponential form with two unknown parameters as follows:

$$\varepsilon_{sh} = \alpha \cdot e^{-\beta f_c}$$

where ε_{sh} is the shrinkage strain, f_c is the compressive strength of concrete at age of initial shrinkage test, and α and β are parameters obtained by regression analysis. Table 6-2 shows the results of this regression analysis and it indicates that best fit value of α is 4.139×10^{-4} and 7.454×10^{-5} for β, R^2 has a value of 0.6469. This regression line has been plotted on Figure 6-6 and it seems to be a fairly good estimation considering all the other components in concrete such as admixtures, aggregate type, as well as two different curing conditions.

It would be very useful to combine data from other data banks to develop a better and more representative model, especially because, as mentioned before, the shrinkage strain tests can be very time consuming.

6.2.6 Relationship between Elastic Modulus and Shrinkage Strain

If a relationship can be established between shrinkage strain and strength properties of concrete, a relationship could be established between shrinkage strain and non-strength properties of concrete, such as elastic modulus; this is safely assumed because as shown in Chapter 5, the compressive strength can be related to the elastic modulus.

Table 6-2. Results of regression analysis on relationship of compressive strength to shrinkage strain

Regression Results	Best-fit Value	Standard Error (SE)	95% Confidence Interval	R^2	Absolute Sum of Square Root due to Error (SSE)
α	4.139E-04	5.973E-05	3.54E-04~ 4.74 E-04	0.6469	7.067E-09
β	7.454E-05	1.194E-05	5.44E-05~ 9.47E-05		

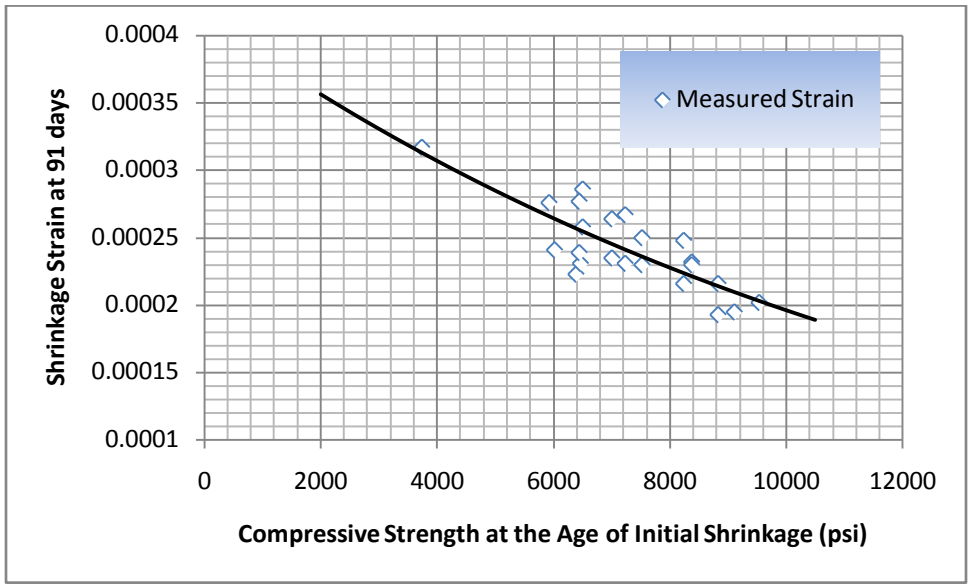

Figure 6-6. Relationship between compressive strength and shrinkage strain at 91 days

Figure 6-7 shows the shrinkage strain results at 91 days against its corresponding elastic modulus at 28 days. According to Liu, this relationship can be approximated with a model of exponential form with two unknown parameters as follows:

$$\varepsilon_{sh} = \alpha \cdot e^{-\beta E_c}$$

where ε_{sh} is the shrinkage strain, E_c is the elastic modulus of concrete at age of initial shrinkage test, and α and β are parameters obtained by regression analysis. Table 6-3 shows the results of this regression analysis and it indicates that best fit value of α is 5.616×10^{-4} and 1.916×10^{-7} for β, R^2 has a value of 0.7065. This regression line has been plotted on Figure 6-7 and it seems to be a fairly good estimation considering all the other components in concrete such as admixtures, aggregate type, as well as two different curing conditions. Data is less scattered as compared to the results from the regression analysis done on the compressive strength and the shrinkage strain.

It would be very useful to combine data from other data banks to develop a better and more representative model, especially because, as mentioned before in the previous model, the shrinkage strain tests can be very time consuming.

Table 6-3. Results of regression analysis on relationship of elastic modulus to shrinkage strain

Regression Results	Best-fit Value	Standard Error (SE)	95% Confidence Interval	R^2	(SSE)	
α	5.616E-04	1.024E-04	4.592E-04~ 6.460E-04	0.7065		2.136E-08
β	1.916E-07	4.0102E-08	1.515E-07~ 2.317E-07			

6.3 Evaluation on Shrinkage Prediction Models

The models for predicting shrinkage of concrete evaluated in this study are the ACI 209 and the C.E.B-F.I.P model.

6.3.1 ACI-209 model

ACI 209R-5 recommends that the following model is to be used for the prediction of shrinkage of concrete:

$$(\varepsilon_{sh})_t = \frac{t^{\alpha}}{f + t^{\alpha}} \cdot (\varepsilon_{sh})_u$$

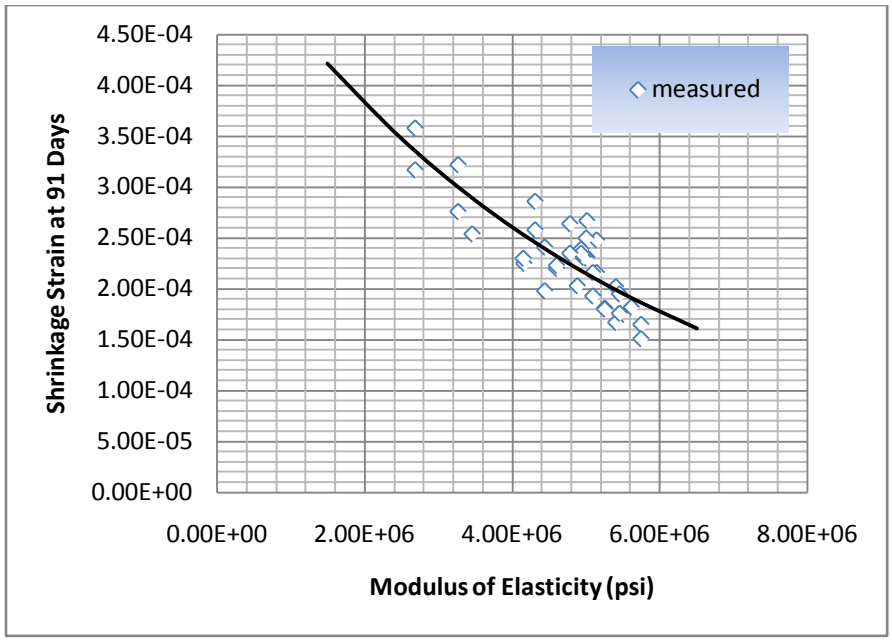

Figure 6-7. Relationship between shrinkage strain at 91 days and modulus of elasticity

where $(\varepsilon_{sh})_t$ is the time dependent shrinkage strain, $(\varepsilon_{sh})_u$ is the ultimate shrinkage strain, f is in days, t is the time after loading, and α is considered a constant for a given member shape and size which defines the time-ratio part. Values of $(\varepsilon_{sh})_u$, f, and α can be determined by fitting the data obtained from tests performed in accordance to ASTM C152. ACI209R-5 lists the normal ranges for these variables as follows:

$(\varepsilon_{sh})_u$ = 415×10-6 to 1070×10-6 in./in., (m/m)

α = 0.90 to 1.10

f = 20 to 130 days

For unrestrained shrinkage strain at any time, including ultimate values, normal weight concrete, moist cured, and Type I cement used, ACI suggests that the shrinkage after 7 days can be approximated by the following model:

$$(\varepsilon_{sh})_t = \frac{t}{35 + t} \cdot (\varepsilon_{sh})_u$$

ACI 209R-5 also suggests that whenever there is absence f specific shrinkage data, $(\varepsilon_{sh})_u$ should be set equal to 780 γ_{sh} × 10-6 in./in. (m/m), where γ_{sh} represents the product of the applicable correction factors such as correction factors for curing conditions, loading age, ambient relative humidity, average-thickness, slump of fresh concrete, fine aggregate content, cement content, and air content; γ_{sh} is set equal to 1 under standard testing conditions. The formula to calculate γ_{sh} is the following:

$$\gamma_{sh} = \gamma_{la} \cdot \gamma_{\lambda} \cdot \gamma_{h} \cdot \gamma_{s} \cdot \gamma_{\psi} \cdot \gamma_{\alpha}$$

The calculated values for each of the correction factors for the ACI 209 model on shrinkage prediction are presented in Table 6-4.

Table 6-4. Correction factors for the ACI 209 model on shrinkage prediction

	γ_{la}							γ_{sh}	
Mix	7-day moist	14-day moist	γ_{λ}	γ_{s}	γ_{α}	γ_{h}	γ_{ψ}	7-day moist	14-day moist
1F	0.994	0.916	0.70	1.21	0.96	0.97	0.97	0.76	0.7
2F	0.994	0.916	0.70	1.13	1	0.97	0.97	0.74	0.68
3F	0.994	0.916	0.70	0.96	0.97	0.97	0.98	0.62	0.57
4F	0.994	0.916	0.70	1.01	0.96	0.97	0.97	0.63	0.58
5S	0.994	0.916	0.70	1.22	1	0.97	0.98	0.81	0.74
6S	0.994	0.916	0.70	1.03	0.98	0.97	0.98	0.67	0.62
7S	0.994	0.916	0.70	1.08	1	0.97	0.98	0.71	0.66
8S	0.994	0.916	0.70	1.06	0.99	0.97	0.98	0.69	0.64
9LF	0.994	0.916	0.70	1.02	0.98	0.97	0.99	0.67	0.62
10LS	0.994	0.916	0.70	1.02	0.99	0.97	0.98	0.67	0.62
1GF	0.994	0.916	0.70	0.95	0.97	0.97	0.96	0.6	0.55
2GF	0.994	0.916	0.70	1.12	0.99	0.97	0.96	0.72	0.66
3GF	0.994	0.916	0.70	1.11	0.97	0.97	0.97	0.7	0.65
4GF	0.994	0.916	0.70	1.12	0.97	0.97	0.97	0.71	0.66
5GS	0.994	0.916	0.70	1.17	1.01	0.97	0.97	0.77	0.71
6GS	0.994	0.916	0.70	1.03	0.97	0.97	0.97	0.65	0.6
7GS	0.994	0.916	0.70	1.05	0.98	0.97	0.97	0.67	0.62
8GS	0.994	0.916	0.70	1.15	0.99	0.97	0.97	0.75	0.69

6.3.2 CEB-FIP Model

CEB-FIP recommends that the following model is to be used for the prediction of shrinkage of concrete having a compressive strength between 12 to 80 MPa, having mean humidity between 40 to 100%, and having a mean temperature between 5 and 30°C:

$$\varepsilon_{cs}(t, t_s) = \varepsilon_{cs0} \cdot \beta_s(t - t_s)$$

where $\varepsilon_{cs}(t, t_s)$ is the total shrinkage strain. β_s can be computed with the following formula:

$$\beta_s(t) = \sqrt{\left(\frac{t}{203.23 + t}\right)}$$

and ε_{cs0} can be computed with the following formula:

$$\varepsilon_{cs0} = \left[160 + 10\beta_{sc}(9 - 0.1f_{cm})\right] \times 10^{-6} \times \beta_{RH}$$

and β_{RH} can be calculated with the following formula:

$$\beta_{RH} = 1.55\left(1 - \left(\frac{RH}{RH_0}\right)^3\right) \text{ for } 40\% \leq RH \leq 99\%$$

where RH is the relative humidity. For the lab conditions in this study, RH is equal to 75% and RH_0 is equal to 100%, which will make β_{RH} equal to:

$$\beta_{RH} = 1.55\left(1 - \left(\frac{.75}{1}\right)^3\right) = 0.8961$$

The total shrinkage strain can be then approximated by the following formula:

$$\varepsilon_{cs}(t, t_c) = \left[160 + 10\beta_{sc}(9 - 0.1f_{cm})\right] \times 10^{-6} \cdot 0.8961$$

where $\varepsilon_{cs}(t, t_c)$ is the time dependent total shrinkage strain, β_{sc} is a coefficient depending on the type of cement is equal to 5 for normal or rapid hardening cements, f_{cm} is the mean compressive strength of concrete at the age of initial shrinkage tests in MPa, A_c is the cross-sectional area in mm^2.

Replacing all constants into the original formula will give the following:

$$\varepsilon_{cs}(t, t_c) = [160 + 50 \cdot (9 - 0.1 f_{cm})] \times 10^{-6} \cdot 0.8961$$

Table 6-6 shows the results of the total shrinkage strain using the CEB-FIP model for all mixes involved in this study and Table 6-7 the results using the ACI 209 model in case of absent data. These results at 91 days are compared with the calculated shrinkage strain results from using the ACI 209R-5 model and plotted in Figure 6-8. The results are hard to analyze. The ACI model seems to overestimate the shrinkage strain results for most of the data. , In comparison with the parameters that are used to calculate the shrinkage strain for both models, the ACI model incorporates the modulus of elasticity at the time of loading, type of curing, volume-surface ratio, cement content, slump, percentage of fine aggregate by weight, percentage of air content by volume, and density of the concrete, while the CEB-FIP model does not. At the same time CEB-FIP model uses parameters such as cross-sectional area and parameter of the section in contact with the atmosphere, which the ACI 209 model does not take into consideration. Table 6-5 shows this comparison in the parameters that are accounted for shrinkage strain between the ACI 209 model and the CEB-FIP model.

Table 6-5. Comparison of Parameters Required for Prediction of Shrinkage in Concrete

Variables	Standard Codes	
	ACI 209R-5	CEB-FIP
Concrete strength at 28 days	√	√
Modulus of elasticity at the time of loading	√	X
Type of cement	√	√
Type of curing	√	X
Relative humidity	√	√
Age of concrete at loading	√	√
Age of concrete at curing	√	√
Volume-surface ratio	√	X
Cement content	√	X
Slump	√	X
Percentage of fine aggregates by weight	√	X

Table 6-5. Continued

Percentage of air content by volume	√	X
Concrete density	√	X
Shape of cross section	X	X
Water content	X	X
Water-cement ratio	X	X
Aggregate-cement ratio	X	X
Cross-sectional area	X	√
Parameter of the section in contact with the atmosphere	X	√

Table 6-6. Shrinkage strain results using the CEB-FIP model

Mix	$\beta_s(t)$	β_{RH}	ε_{cs0}	$\varepsilon_{sh}(t,t_c)$
1F	0.56	0.8959	2.21E-04	1.24E-04
2F	0.56	0.8959	3.24E-04	1.81E-04
3F	0.56	0.8959	2.97E-04	1.66E-04
4F	0.56	0.8959	3.01E-04	1.69E-04
5S	0.56	0.8959	2.94E-04	1.65E-04
6S	0.56	0.8959	2.48E-04	1.39E-04
7S	0.56	0.8959	3.30E-04	1.85E-04
8S	0.56	0.8959	3.31E-04	1.85E-04
9LF	0.56	0.8959	3.50E-04	1.96E-04
10LS	0.56	0.8959	3.93E-04	2.20E-04
1GF	0.56	0.8959	3.24E-04	1.81E-04
2GF	0.56	0.8959	3.59E-04	2.01E-04
3GF	0.56	0.8959	3.46E-04	1.94E-04
4GF	0.56	0.8959	3.51E-04	1.97E-04
5GS	0.56	0.8959	3.59E-04	2.01E-04
6GS	0.56	0.8959	3.52E-04	1.97E-04
7GS	0.56	0.8959	3.66E-04	2.05E-04
8GS	*0.56*	*0.8959*	*3.95E-04*	*2.21E-04*

Table 6-7 shows the results of the total shrinkage strain using the ACI 209 model for all mixes involved in this study in case of absent data on the next page.

Table 6-7. Shrinkage strain results using the ACI 209 model

	γ_{sh}		$(\varepsilon_{sh})_u$		$(\varepsilon_{sh})_t$	
Mix	7-day moist	14-day moist	7-day moist	14-day moist	7-day moist	14-day moist
1F	0.76	0.7	5.93E-04	5.46E-04	4.28E-04	3.94E-04

Table 6-7. Continued

2F	0.74	0.68	5.77E-04	5.30E-04	4.17E-04	3.83E-04
3F	0.62	0.57	4.84E-04	4.45E-04	3.49E-04	3.21E-04
4F	0.63	0.58	4.91E-04	4.52E-04	3.55E-04	3.27E-04
5S	0.81	0.74	6.32E-04	5.77E-04	4.56E-04	4.17E-04
6S	0.67	0.62	5.23E-04	4.84E-04	3.77E-04	3.49E-04
7S	0.71	0.66	5.54E-04	5.15E-04	4.00E-04	3.72E-04
8S	0.69	0.64	5.38E-04	4.99E-04	3.89E-04	3.61E-04
9LF	0.67	0.62	5.23E-04	4.84E-04	3.77E-04	3.49E-04
10LS	0.67	0.62	5.23E-04	4.84E-04	3.77E-04	3.49E-04
1GF	0.60	0.55	4.68E-04	4.29E-04	3.38E-04	3.10E-04
2GF	0.72	0.66	5.62E-04	5.15E-04	4.06E-04	3.72E-04
3GF	0.70	0.65	5.46E-04	5.07E-04	3.94E-04	3.66E-04
4GF	0.71	0.66	5.54E-04	5.15E-04	4.00E-04	3.72E-04
5GS	0.77	0.71	6.01E-04	5.54E-04	4.34E-04	4.00E-04
6GS	0.65	0.60	5.07E-04	4.68E-04	3.66E-04	3.38E-04
7GS	0.67	0.62	5.23E-04	4.84E-04	3.77E-04	3.49E-04
8GS	0.75	0.69	5.85E-04	5.38E-04	4.23E-04	3.89E-04

The results from both models for the shrinkage strains at 91 days for all mixes investigated in this study at 91 days are plotted in Figure 6-8 on the next page.

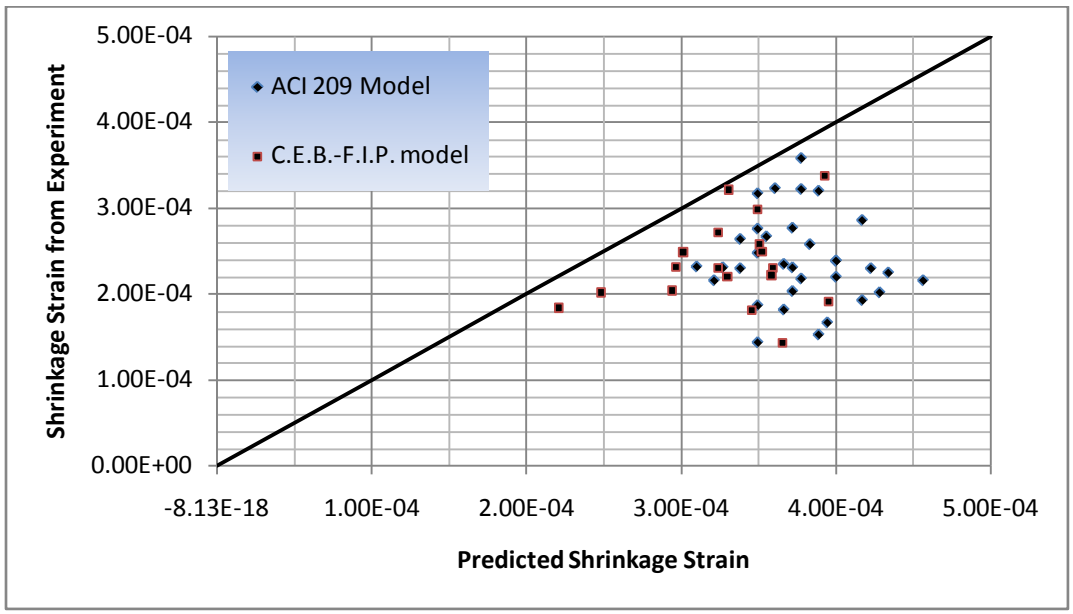

Figure 6-8. Comparison between the shrinkage strain at 91 days and the shrinkage strain calculated by ACI 209 model and C.E.B-F.I.P model

6.4 Prediction of Ultimate Shrinkage Strain

To predict the ultimate shrinkage strains of the concretes involved in this study, the following asymptotic equation was used to fit the experimental data:

$$(\varepsilon_{sh})_t = \left(\frac{t}{\gamma + t}\right)^{\alpha} \cdot \beta$$

where γ, α, and β are parameters obtained through regression analysis. $(\varepsilon_{sh})_t$ is the shrinkage strain in in./in. (mm/mm), and t is in days.

From the previous equation the function approaches a limiting value, β. Therefore, β is the ultimate shrinkage strain since it is assumed that concrete will approach this value.

The Least Square Method was used to perform the curve fitting regression analysis, and it's presented next.

6.4.1 Least Square Method of Curve-fitting

This method assumes that the best possible fit curve is one that has the least square error. This square error is calculated as the minimal summation of the deviations squared between the observed data and the regression model. This best-fit curve has the following form:

$$S = d_1^2 + d_2^2 + \ldots + d_n^2 = \sum_{i=1}^{n} d_i^2 = \sum_{i=1}^{n} [y_i - \hat{y}_i]^2 = a\ minimum$$

where d_i is the difference squared between the response value y_i and the estimated value $\hat{y}_i$, and S is the sum of squares error estimate.

6.4.2 Evaluation Methods on the Goodness of Fit

After the model was used to fit the data, an evaluation of the goodness of the fit was examined to determine whether the data is reasonable, as well as the model as the model coefficients. This helps determine variability of the data as well as how good the models can predict data.

DataFit 8.0.32 was used for the regression analysis, data, and graphical illustration of the results. The model is defined in the software, and the program returns various numerical measures such as goodness of fit statistics confidence, standard error, and regression correlation coefficient. The program returns the following information useful for the analysis and interpretation of the data:

- The sum of squares due to error (SSE)

  This statistic is used to measure the error as the total deviation of the response values from the model. It is also called 'the summed square of residuals,' and its formula is:

$$SSE = \sum_{i=1}^{n} w_i (y_i - \hat{y}_i)^2$$

  values closer to 0 correspond to smaller random error, and thus prediction model is good. From the above equation, it can be seen that the residual is calculated for each observation in the sample; it is squared, and then summed up to make up the SSE.

- R-square

  This statistic is used to measure scattering of the data. R^2 is the correlation between the observed data and the predicted data from the model. It is defined as the ratio of the sum of squares of the regression (SSR) and the total sum of squares (SST).

$$SSR = \sum_{i=1}^{n} w_i (\hat{y}_i - \bar{y})^2$$

  and SST, the sum of squares about the mean, can be calculated as

$$SST = \sum_{i=1}^{n} w_i (y_i - \bar{y})^2$$

where $SST = SSR + SSE$. R^2 is then defined as

$$R^2 = \frac{SSR}{SST} = 1 - \frac{SSE}{SST}$$

where R^2 ranges from 0 to 1. The closer R^2 gets to one, the less scattered the data, and thus the better the goodness of the fit.

- Root mean squared error (RMSE)

  The root mean squared error is a measure of variability in the response values about the regression model. The smaller the value of the root mean squared error, the smaller the standard error. The estimate of $\hat{\sigma}$ is

$$\hat{\sigma}^2 = \frac{\sum(Y - \hat{Y})^2}{n - (k+1)} = \frac{SSE}{df}$$

  the degrees of freedom df equals the sample size n minus the number of parameters in the model evaluated. RMSE is the square root of $\hat{\sigma}^2$ also known as the fit standard error. Values closer to 0 indicate a better goodness of fit.

- Confidence and Prediction Bounds

  Confidence intervals are used to indicate accuracy of the estimate by describing how close the estimate is likely to fall within a certain interval. The confidence coefficient is usually a number close to 1: the confidence coefficient used is .95 for our analysis, which is within two standard deviations (2σ) according to the Central Limit Theorem. The following figure depicts the sampling distribution of $\bar{Y}$ and possible confidence intervals for μ.

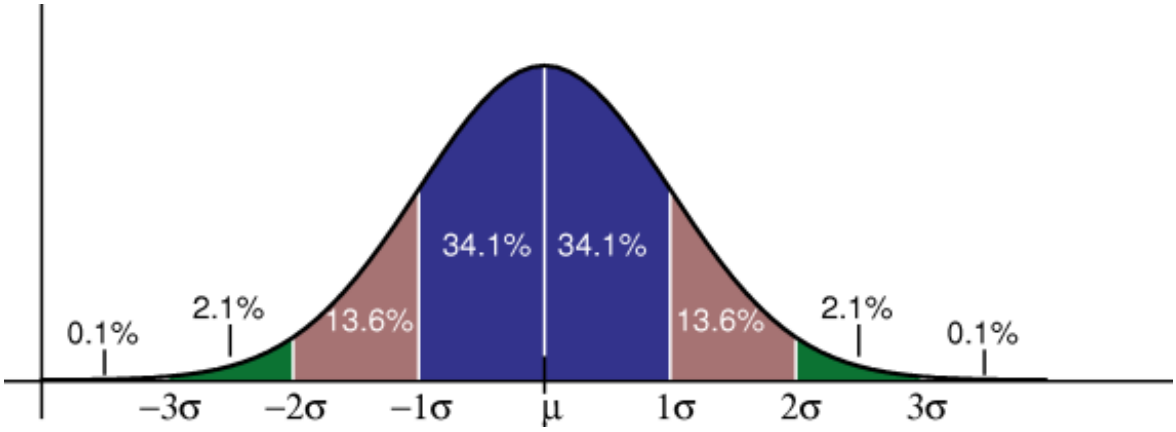

Figure 6-9. Confidence intervals based on 1, 2, and 3 standard deviations

6.4.3 Predicted Results

Table 6-8 shows the results of the regression analysis for all mixes of this study. The replicates of mixes Mix-8S and Mix-8GS were significantly different in shrinkage strains, thus they are presented separate instead of combined. The ultimate shrinkage is the limiting value β which is also presented in Table 6-8. Most mixes have a value close to 1 for α and the average of γ is 29.8. The average for α is 0.91. The maximum average ultimate shrinkage strain is in the order of 3.34×10^{-4} for normal-weight aggregate, and according to Dr. Liu's analysis 4.50×10^{-4} for light-weight aggregate. The results are graphed in Figure 6-9.

Figure 6-10. Prediction of ultimate shrinkage strains through regression analysis

Table 6-8. Results of regression analysis for prediction of shrinkage strain

Mix	α	SE	β	SE	γ	SE	R^2	SSE
1F	0.983	0.024	2.66E-04	2.70E-06	31.18	1.804	0.9997	1.20×10^{-6}
	1.122	0.049	2.27E-04	4.31E-06	31.10	3.117	0.9992	1.67×10^{-6}
2F	1.027	0.021	3.39E-04	1.51E-06	16.48	0.649	0.9998	1.27×10^{-6}
	1.137	0.042	3.21E-04	3.35E-06	19.13	1.515	0.9994	1.23×10^{-6}
3F	1.011	0.022	3.03E-04	1.69E-06	20.05	0.869	0.9998	1.19×10^{-6}
	0.920	0.031	2.85E-04	3.89E-06	31.74	2.545	0.9994	1.81×10^{-6}
4F	0.867	0.013	3.44E-04	2.74E-06	27.84	1.530	0.9999	1.10×10^{-7}
	0.855	0.032	3.24E-04	8.93E-06	32.44	3.910	0.9990	2.45×10^{-6}
5S	0.871	0.634	2.55E-04	2.99E-05	16.81	23.24	0.9652	1.64×10^{-5}
	0.812	0.026	2.29E-04	1.86E-05	20.88	1.427	0.9994	1.50×10^{-6}
6S	1.243	0.709	2.05E-04	1.13E-05	6.59	5.74	0.9890	7.93×10^{-6}
	1.282	0.484	1.99E-04	7.94E-06	7.53	4.48	0.9949	5.18×10^{-6}
7S	0.849	0.143	2.65E-04	9.83E-06	21.91	7.31	0.9964	5.03×10^{-6}
	0.732	0.315	2.61E-04	2.62E-05	24.27	22.64	0.9764	1.33×10^{-5}
8S(3m)	1.325	0.087	2.43E-04	1.82E-06	7.822	0.789	0.9989	2.42×10^{-6}
	1.232	0.089	2.20E-04	2.52E-06	11.61	1.406	0.9984	2.56×10^{-6}
8S(1y)	0.960	0.473	5.52E-04	9.28E-05	42.90	45.04	0.9842	2.06×10^{-5}
	0.981	0.234	4.58E-04	1.41E-05	26.27	10.30	0.9994	4.22×10^{-6}
9LF	0.836	0.030	3.95E-04	3.09E-06	20.53	1.220	0.9996	2.11×10^{-6}
	1.018	0.030	3.49E-04	4.89E-06	31.49	2.756	0.9992	2.51×10^{-6}
10LS	1.055	0.026	4.22E-04	3.30E-06	21.74	1.349	0.9983	4.42×10^{-6}
	0.851	0.066	3.96E-04	7.12E-06	21.04	2.796	0.9995	2.05×10^{-6}
1GF	0.857	0.920	2.23E-04	1.17E-04	38.74	108.23	0.8850	2.16×10^{-5}
	0.628	0.185	1.98E-04	2.69E-05	51.35	44.50	0.9919	6.11×10^{-6}
2GF	1.109	0.4871	3.18E-04	6.94E-05	27.16	27.44	0.9900	7.21×10^{-6}
	0.903	0.3142	3.08E-04	5.33E-05	36.26	31.81	0.9895	7.85×10^{-6}
3GF	0.981	0.266	2.49E-04	4.05E-05	34.64	24.09	0.9966	3.38×10^{-6}
	0.961	0.525	2.70E-04	9.88E-05	46.83	57.38	0.9600	1.13×10^{-5}
4GF	0.625	0.260	2.89E-04	3.44E-05	38.24	38.63	0.9624	1.53×10^{-5}
	0.509	0.544	3.38E-04	7.87E-05	36.81	95.71	0.8587	3.57×10^{-5}
5GS	0.320	0.060	2.35E-04	2.35E-05	90.95	75.46	0.9904	6.59×10^{-6}
	0.703	0.122	2.35E-04	1.12E-05	30.96	12.03	0.9969	4.10×10^{-6}
6GS	1.169	1.176	1.23E-04	3.20E-05	12.31	23.45	0.9696	5.50×10^{-6}
	1.348	2.504	1.50E-04	1.38E-05	3.46	8.52	0.9886	4.53×10^{-6}
7GS	0.496	0.245	2.48E-04	6.93E-05	56.34	99.71	0.9869	8.04×10^{-6}
	0.487	0.064	2.49E-04	2.88E-05	85.98	49.25	0.9964	3.64×10^{-6}
8GS(1y)	0.740	0.415	2.34E-04	1.66E-05	17.48	19.17	0.9801	1.10×10^{-6}
	0.868	0.500	2.10E-04	2.82E-05	33.61	41.36	0.9833	9.77×10^{-6}
8GS(3m)	0.632	0.197	7.54E-05	1.23E-05	30.99	28.94	0.9953	1.22×10^{-6}

6.5 Summary of Findings

This section presents the summary of findings of the results of this chapter.

(1) Mixes containing slag experience lower shrinkage strains at 91 days as compared to mixes containing fly ash.

(2) Mixes containing the highest water content experience the highest shrinkage.

(3) Mixtures containing Miami Oolite limestone aggregate shrink slightly higher than mixtures containing Georgia granite aggregate. This is consistent with most studies done on the effects of coarse aggregate on shrinkage strains of concrete. This is due to difference in the modulus of elasticity because it means that concrete with higher elastic modulus take relatively more stress to exhibit less strains.

(4) Regression analysis was carried to relate shrinkage strains at 91 days to compressive strength at 28 days. The results are presented next:

$$\varepsilon_{sh} = 4.139 \times 10^{-4} \cdot e^{-7.454 \times 10^{-5} f_c'}$$

where ε_{sh} is the shrinkage strain at 91 days, and f_c' is the compressive strength in psi.

(5) Regression analysis was carried to relate shrinkage strains at 91 days to the modulus of elasticity at 28 days. The results are presented next:

$$\varepsilon_{sh} = 5.616 \times 10^{-4} \cdot e^{-1.916 \times 10^{-7} E_c}$$

where ε_{sh} is the shrinkage strain at 91 days, and E_c is the elastic modulus in psi.

(6) The ultimate shrinkage strains for the mixes investigated in this study range from 2.02×10^{-4} to 3.34×10^{-4} for concretes containing Miami Oolite limestone as aggregate, 1.37×10^{-4} to 3.14×10^{-4} for concretes containing Georgia granite as aggregate, and 3.49×10^{-4} to 4.22×10^{-4} for the concretes with Stalite lightweight aggregate concrete.

CHAPTER 7
ANALYSIS OF CREEP TEST RESULTS

7.1 Introduction

The results of the creep tests of all mixes involved in this study are presented next. The creep strains as well as the creep coefficients are analyzed at 91 days. These results are evaluated and are related to strength and non-strength properties of concrete. The ultimate creep coefficient is calculated using regression analysis, and finally, the creep coefficient is computed from the data.

7.2 Result and Analysis of Creep Tests

Table B-1 presents the following information for all mixes involved in this study: the total strain, the shrinkage strain, the elastic strain, the creep strain, the creep coefficient, and the creep modulus. The creep strain is calculated by subtracting the shrinkage strain and the elastic strain from the total strain, the creep coefficient is calculated by dividing the creep strain by the elastic strain, and finally, the creep modulus is calculated by dividing the applied stress on the specimens in the creep frame by the total strain minus the shrinkage strain.

Figures7-1 and 7-2 show the creep strain at 91 days for all mixes in this study. Mixes with shorter curing times exhibit higher shrinkage strains at 91 days. These results are probably due to the higher degree of hydration, as the mixes that are cured for longer are also stronger and would resist creep relatively better. Curing conditions seem to have an effect on whether the mix contains slag or fly ash; mixes containing fly ash cured for 7 days have a higher creep strain at 91 days as compared to specimens cured for 14 days. For example, specimens cured for 7 days are 23% higher than specimens cured for 14 days for Mix-1F, 13% higher for Mix-2F, 12% higher for Mix-3F, and 9% higher for Mix-4F. Similar differences are found in mixes containing Georgia granite: specimens cured for 7 days are 21% higher than specimens cured for 14 days

7.2.1 Effect of Curing Conditions on Creep Behavior of Concrete

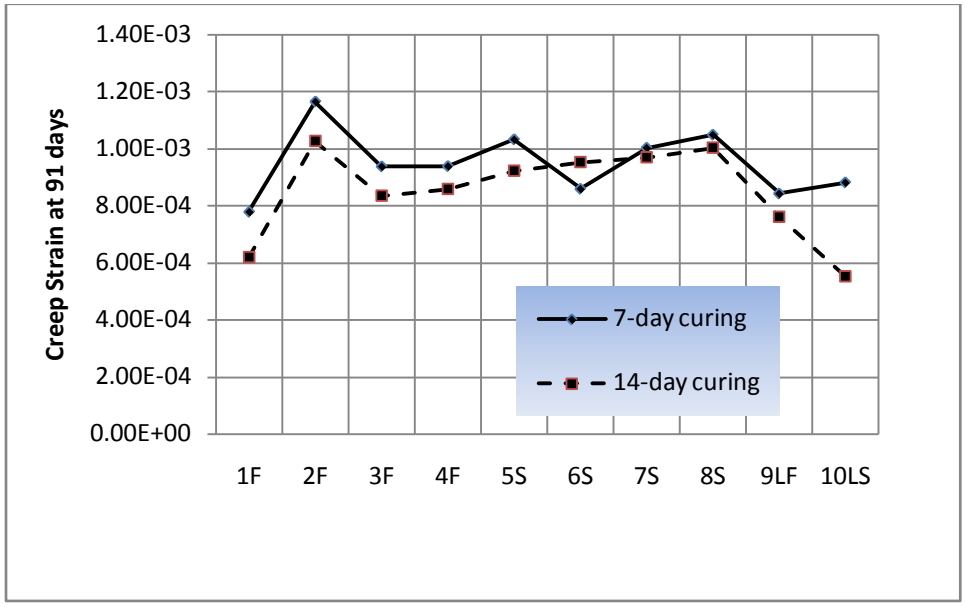

Figure 7-1. Effect of curing condition on creep of concrete of mixes containing Miami Oolite limestone and Lightweight aggregates.

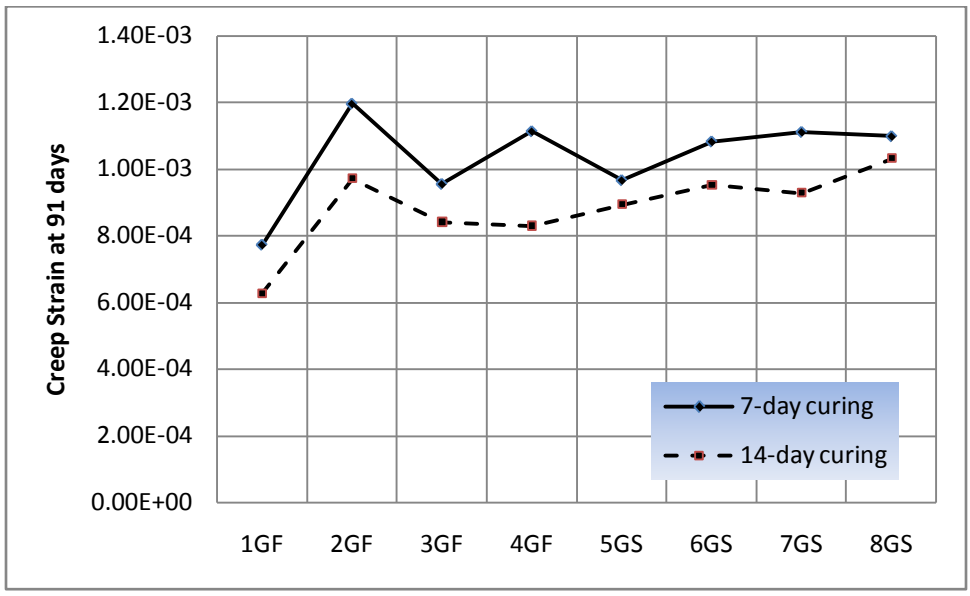

Figure 7-2. Effect of curing condition on creep of concrete of mixes containing Georgia granite.

for Mix-1GF, 21% higher for Mix-2GF, 13% higher for Mix-3GF, and 29% higher for Mix-4GF. Mixes containing slag exhibit less of a creep strain in comparison. For example, specimens cured for 7 days are 11% higher than specimens cured for 14 days for Mix-5S, 10%

higher for Mix-6S, 3% higher for Mix-7S, and 4% higher for Mix-8S. Similar differences are found in mixes containing Georgia granite: specimens cured for 7 days are 8% higher than specimens cured for 14 days for Mix-5GS, 13% higher for Mix-6GS, 13% higher for Mix-7GS, and 6% higher for

7.2.2 Effect of Aggregate Types on Creep Behavior of Concrete

The effects of aggregate type on creep behavior of concrete is analyzed and presented in Figure 7-3. From this figure it can be appreciated that 6 out the 8 mixes exhibit higher creep strains for those who contain Georgia granite. Since this is consistent with studies done on the effects of aggregate type on creep of concrete, it could be concluded that these 2 mixes, Mix-2 and Mix 5, might have a problem. Possible problem could come from errors in loading of the creep frames, inconsistency in the concrete mix procedure, problems with the cementitious materials themselves, etc.

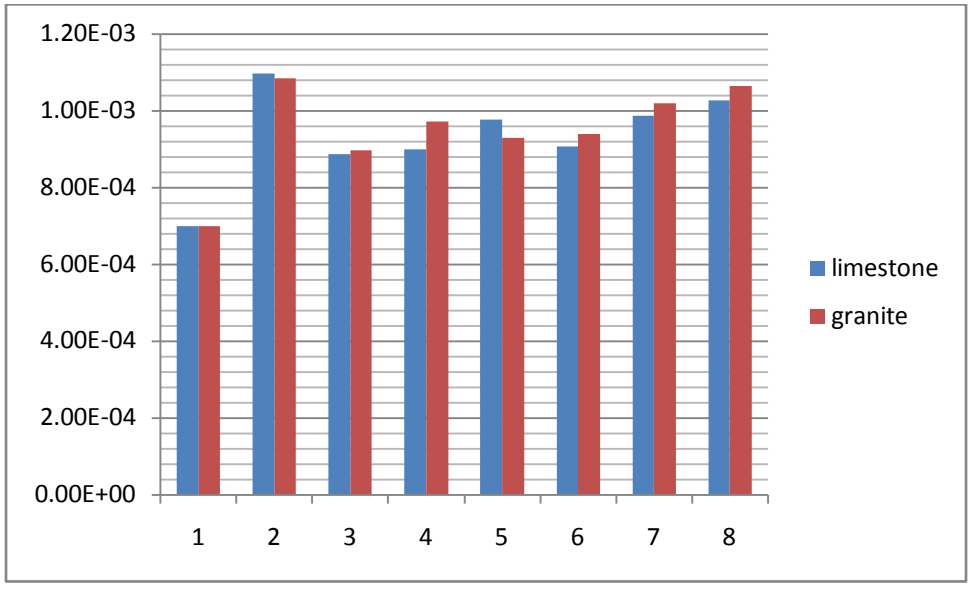

Figure 7-3. Effect of aggregate types on creep behavior of concrete

7.2.5 Effect of Water to Cementitious Materials Ratio

How much concrete creeps is related to the degree of hydration of the cement paste, and

movement of water. Figure 7-4 and Figure 7-5 show the relationships between creep strain at 91 days for each curing condition. The results show that for higher water to cementitious materials ratios, the creep strain is also higher. The results show also that the slope of the trend line is higher for the specimens that were cured for 7 days relative to the specimens cured for 14 days.

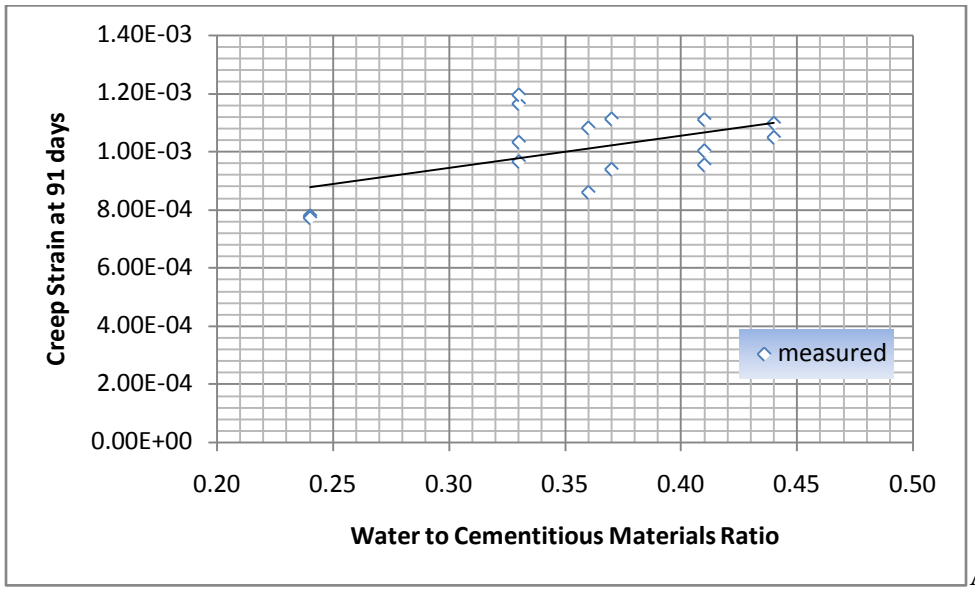

A

Figure 7-4. Effect of water to cementitious materials ratio on creep of concrete moist-cured for 7 days

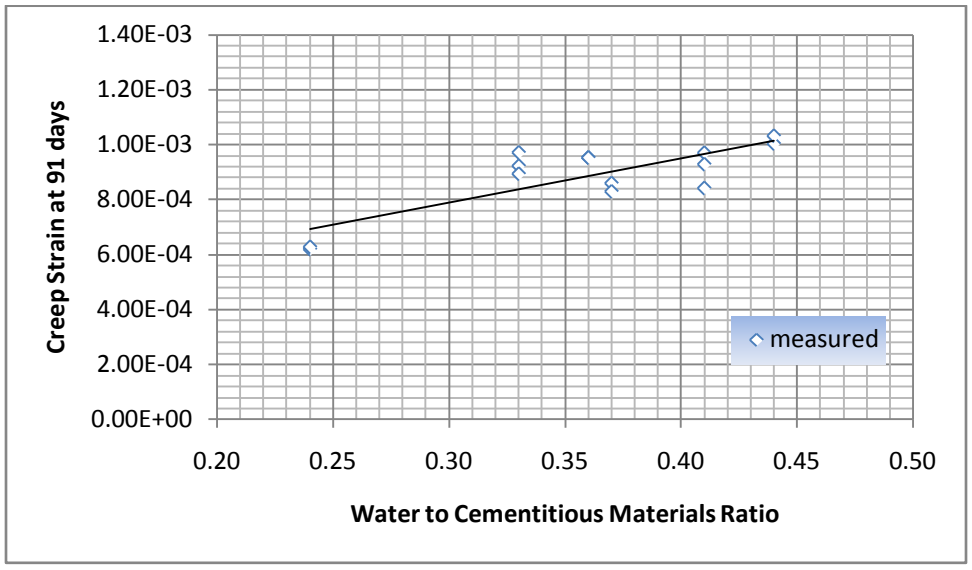

Figure 7-5. Effect of water to cementitious materials ratio on creep of concrete moist-cured for 14 days

7.2.6 Relationship between Compressive Strength and Creep Strain

It would be very useful to find a relationship between the compressive strength of concrete and its creep strain. The compressive strength test is relatively easier to perform and less time consuming than the creep strain. Regression analysis has been performed on the data and the findings are very exciting. From figures 7-7, 7-8, and 7-9, it can be seen that the compressive strength is linearly related to the creep strain of concrete. It also seems that this relationship is true regardless of type of aggregate or differences in proportions. Figure 7-7 presents the compressive strength and the creep strain for specimens cured for 7 days for both aggregate types. There seems to be an outlier in the data and it's from mix Mix-1GF. The creep strain seems to be relatively lower than the linear model and a look at the mix designs reveals that this mix is made up of only 5.7% water. The mix was extremely dry even after pushing both water-reducing admixtures content to the maximum limits. Figure 7-8 presents the compressive strength and the creep strain for specimens cured for 14 days for both aggregate types. The outlier is from the same Mix-1GF and the reason might be the same as previously explained. Figure 7-8 presents the compressive strength and the creep strain for all specimens under all curing conditions. From all these figures, it seems that the relationship is of linear nature, so the following simple linear function was used to develop the relationship:

$$\varepsilon_{c91} = \alpha \cdot f_c + \beta$$

where ε_{c91} is the creep strain at 91 days. Using these relationships, the creep strain could be approximated by just testing the concrete under compressive strength. The results of the regression analysis are presented on Table 7-1. The relationships indicate in general that as the compressive strength of concrete increases, the creep strain decreases.

Table 7-1. Regression analysis on relationship between compressive strength and creep strain

Curing condition	α	95% Confidence Interval	β	95% Confidence Interval	R^2	$S_{y.x}$
7-day moist curing	-5.05E-08	-7.98E-08 ~ -2.11E-08	1.36E-03	1.16E-03 ~ 1.56E-03	0.44	8.76E-05
14-day moist curing	-3.55E-08	-7.07E-08 ~ -2.45E-08	1.15E-03	9.09E-04 ~ 1.40E-03	0.21	9.43E-05
All curing conditions	-4.48E-08	-7.09E-08 ~ -1.86E-08	1.23E-03	1.78E-04 ~ 1.01E-03	0.24	1.14E-04

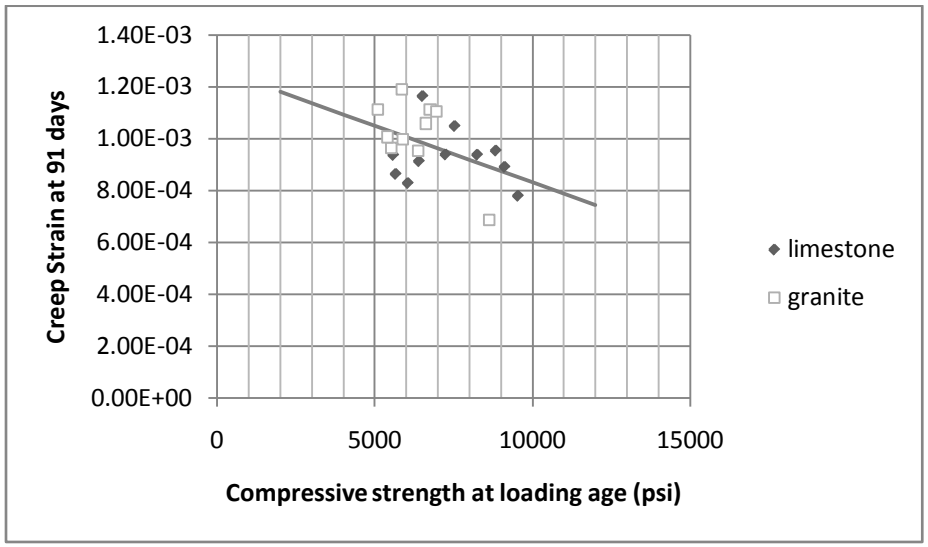

Figure 7-6. Relationship between compressive strength and creep strain of concrete moist-cured for 7 days

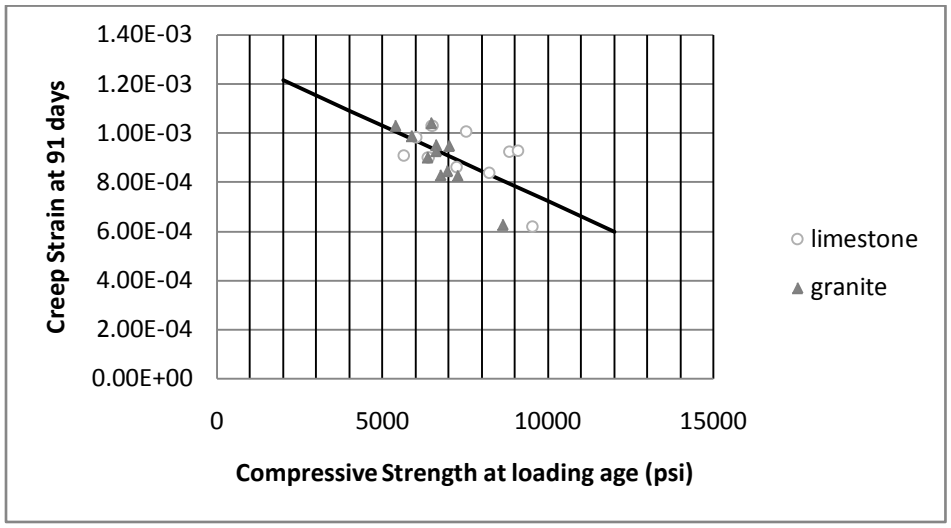

Figure 7-7. Relationship between compressive strength and creep strain of concrete moist-cured for 14 days

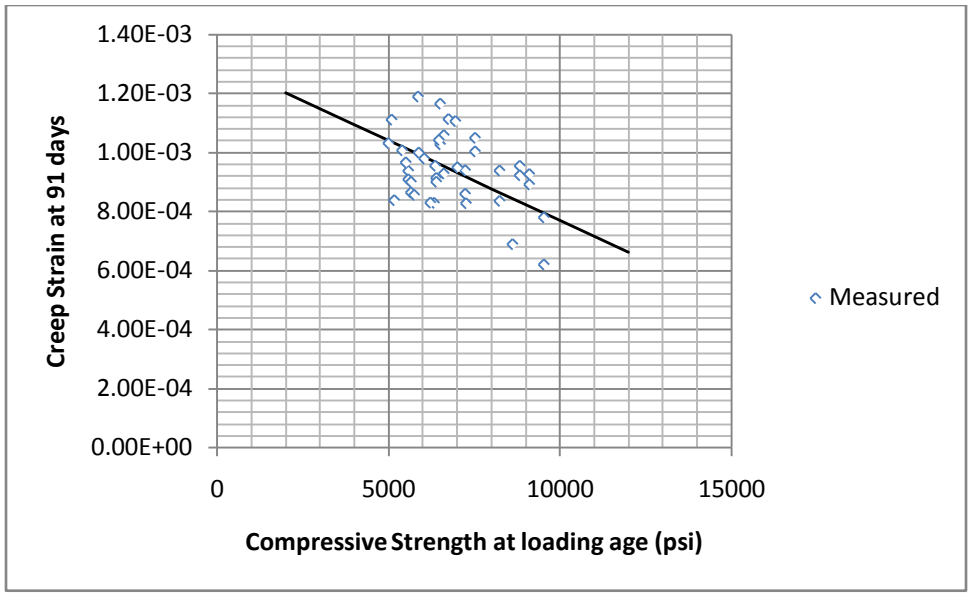

Figure 7-8. Relationship between compressive strength and creep strain of concrete under all curing conditions

Figure 7-9 shows another interesting relationship between the compressive strength of concrete and the instantaneous strain at the time of initial loading. The relationship shows that as the compressive strength increases, the instantaneous also increases

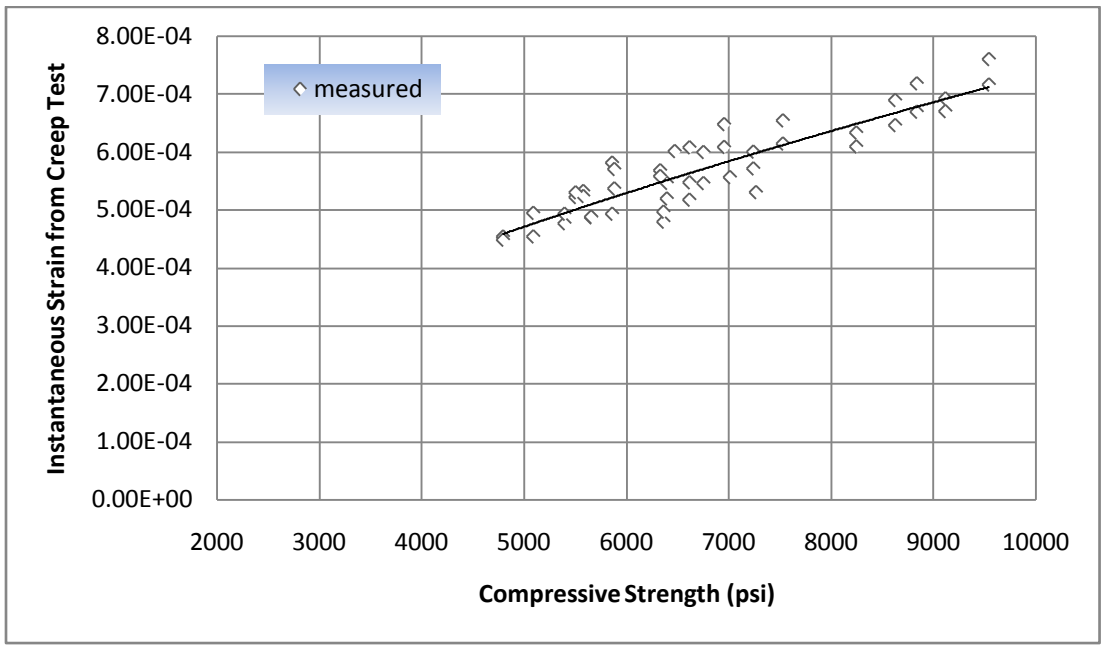

Figure 7-9. Relationship of compressive strength to instantaneous strain measured in creep test

7.3 Creep Coefficient

Creep coefficient is the ratio of creep strain to elastic strain and is an important parameter used on prestressed concrete design. This segment discusses the effects of curing conditions, water content, compressive strength, and elastic modulus of concrete on creep coefficient.

7.3.2 Effect of Curing Conditions on Creep Coefficient

Figure 7-10 presents the creep coefficient for all mixes for both curing conditions. In general, it seems that the difference in creep coefficient is larger in mixes containing fly ash as opposed to those containing slag. For example, the percent difference between creep coefficients for both curing conditions for Mix-1F is of 30%, 13% for Mix-2F, 12% for Mix-3F, and 4% for Mix 4F. The percent difference between creep coefficients for both curing conditions is 50%, 25%, and 20% for Mix-1GF, Mix-2GF, and Mix-4GF respectively. The percent difference seems to be smaller between creep coefficients for both curing conditions for Mix-5S of 12%, 16% for Mix-6S, 1% for Mix-7S, and 8% for Mix-8S. The percent difference between creep coefficients for both curing conditions is 16%, 28%, 28%, and 23% for Mix-5GS, Mix-6GS, Mix-7GS, and Mix-8GS respectively.

7.3.3 Effect of Water Content on Creep Coefficient

The factors that affect creep of concrete should affect the creep coefficient as well. Figure 7-11 shows the creep coefficient plotted against water content for all mixes. The results show that as water content increases, the creep coefficient also increases. There seems to be some scattering in the data, probably due to faulty use of the digital extensometer.

7.3.4 Effect of Compressive Strength at Loading Age on Creep Coefficient

Figure 7-2 shows the creep coefficient at 91 days plotted against the compressive strength at the time of loading for all curing conditions. From the graph, it can be seen that as the

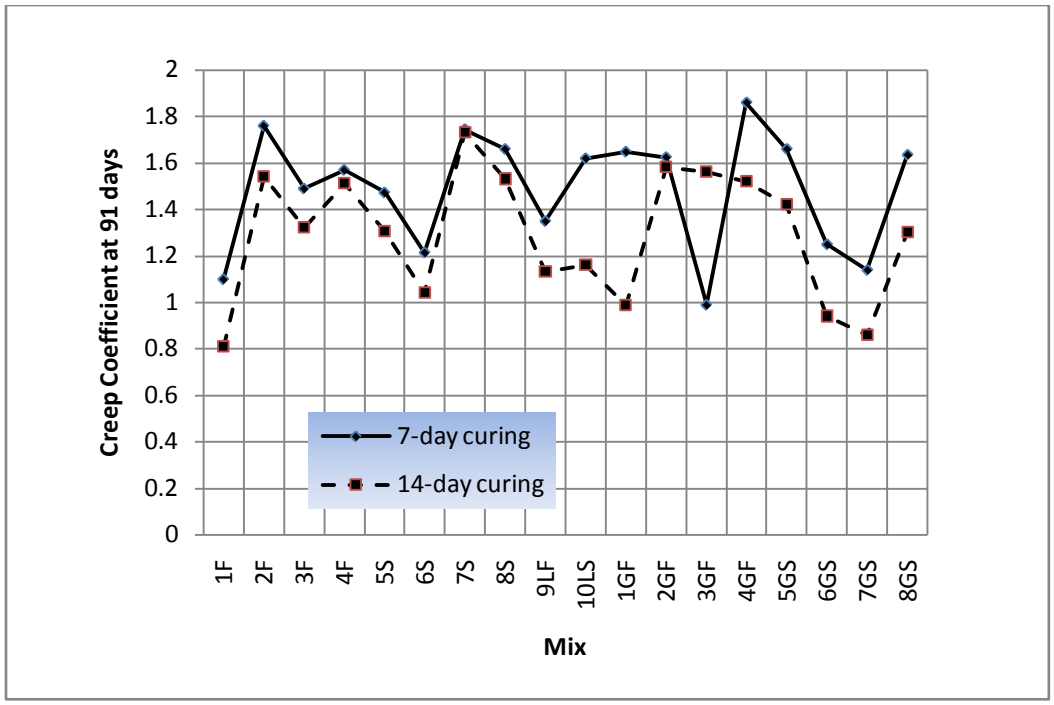

Figure 7-10. Effect of curing condition on creep coefficient of concrete

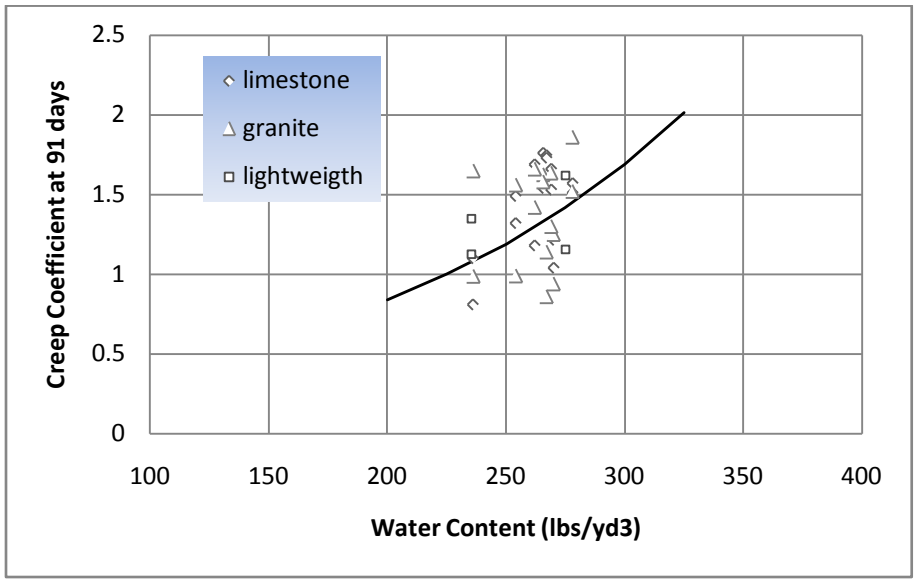

Figure 7-11. Effect of water content on creep coefficient at 91 days

compressive strength increases, the creep coefficient decreases which is expected because the elastic modulus should increase too providing more resistance to strain. Regression analysis was performed on the data was approximated using the simple linear function:

$$\varphi_c = \alpha \cdot f_c + \beta$$

where φ_c is the creep coefficient at 91 days. Table 7-3 shows the results of the regression analysis. Regression analysis was performed using the same simple linear model on the creep coefficient at 91 days for both curing conditions separately. These results are also presented in Table 7-2.

Table 7-2. Regression analysis on relationship of compressive strength to creep coefficient

Curing condition	α	95% Confidence Interval	β	95% Confidence Interval	R^2	$S_{y.x}$
7-day curing	-1.19E-04	-1.85E-04 ~ -5.28E-05	2.43	1.958 ~ 2.893	0.5148	0.1531

Table 7-2. Continued

14-day curing	-2.24E-04	-2.80E-04 ~ -1.68E-04	3.103	2.709 ~ 3.496	0.8414	0.1288
All curing conditions	-1.80E-04	-2.20E-04 ~ -1.41E-04	2.831	2.550 ~ 3.111	0.7411	0.1363

From the results presented on Table 7-2, it can be seen that the slope of the specimens cured for 7days is lower than the slope of the graph for the specimens cured for 14 days. This could be because longer curing times has a major influence on strength development and therefore creep coefficient.

7.3.5 Relationship between Elastic Modulus at Loading Age and Creep Coefficient

As presented in Chapter 5, a relationship can be established between the compressive strength of concrete and its modulus of elasticity. Because of that, we can also establish a relationship between the creep coefficient and the elastic modulus at the time of loading. The creep coefficient was plotted against the elastic modulus on Figure 7-13 and a simple linear model was used to approximate the results. The results are presented in Table 7-3 as well and they show that as the elastic modulus increases the creep coefficient decreases. These results are

expected since a higher elastic modulus means that the concrete will take more stress per unit strain. The linear function used in the regression analysis has the following form:

$$\varphi_c = \alpha \cdot E_c + \beta$$

where φ_c is the creep strain, and E_c is the modulus of elasticity at the time of loading.

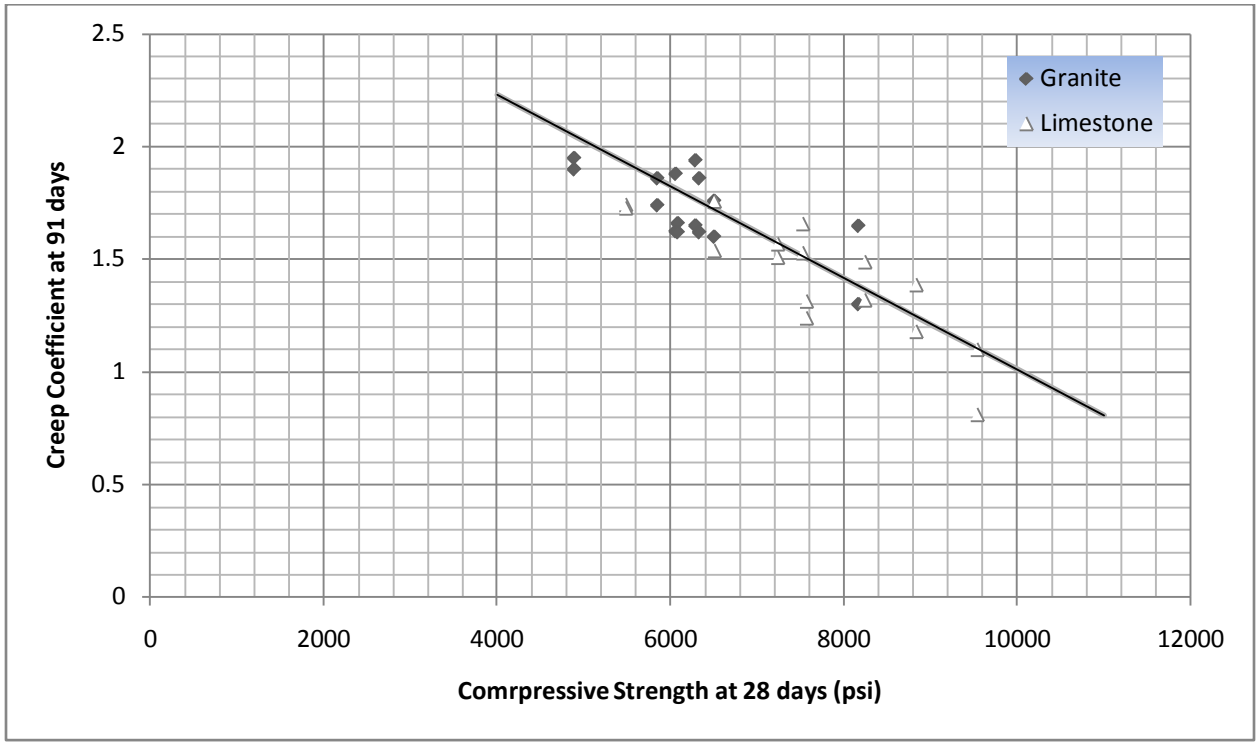

Figure 7-12. Relationship between compressive strength at loading age and corresponding creep coefficient at 91 days

From Table 7-3, it can be seen that α has a value of -3.43E-07 and has an intercept of β equal to 3.295.

Table 7-3. Regression analysis on relationship of elastic modulus to creep coefficient

α	95% confidence interval	β	95% confidence interval	R^2	SSE
-3.43E-07	-5.92E-07 ~ -9.37E-07	3.295	2.044 ~ 4.545	0.2084	0.2383

Not surprising, the relationship is also linear in nature: as this ratio increases, the creep strain decreases as well. The results of the regression analysis are presented in Table 7-4.

The linear model used in the regression analysis has the following form:

$$\varphi_c = \alpha \cdot \frac{f_c}{E_c} + \beta$$

where φ_c is the creep strain, α is the slope of the graph equal to -1057, and β is the intercept equal to 3.038.

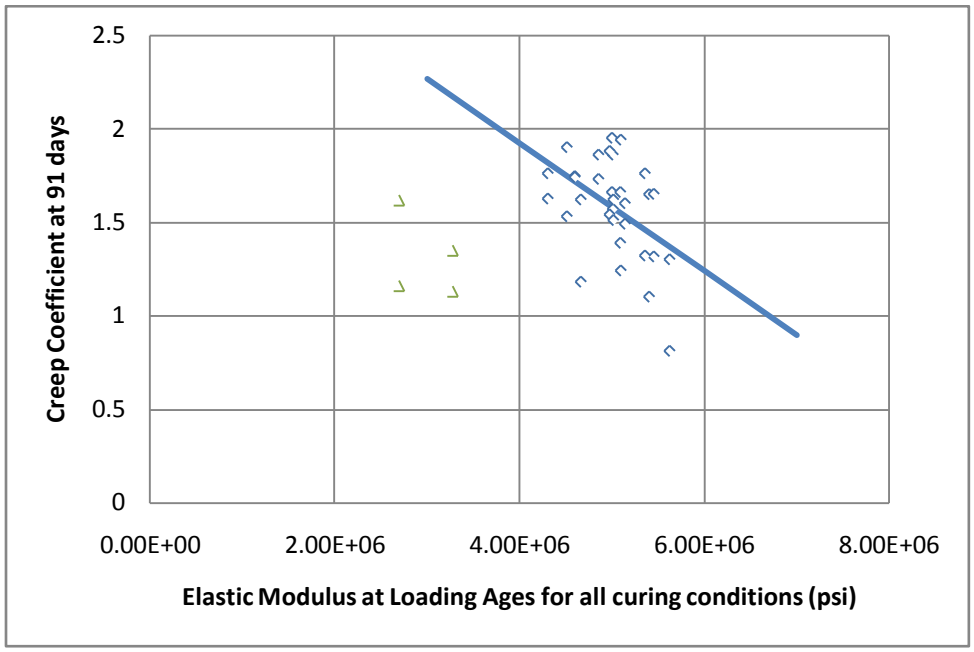

Figure 7-13. Effect of Elastic modulus at loading age on creep coefficient at 91 days

Table 7-4. Regression analysis on relation of creep coefficient to f_c/E_c

α	95% confidence interval	β	95% confidence interval	R^2	SSE
-1057	-1344 ~ -769	3.038	2.636 ~ 3.439	0.6406	0.1598

7.3.6 Effect of Coarse Aggregate Type on Creep Coefficient

Figures 7-15 and 7-16 show the creep coefficient at 91 days for all mixes for both curing conditions. It seems that overall, mixes containing Georgia granite aggregate have a higher creep coefficient as compared to those containing Miami Oolite limestone aggregate. According to Dr. Liu, this could be attributed to the lower elastic deformation in the concretes containing Georgia granite aggregate so then the ratio of creep strain to elastic strain is relatively higher.

7.4 Creep Modulus

Creep modulus is the ratio of total strain excluding the shrinkage strain to the elastic strain. It represents the stiffness of concrete, and results show that concretes with 14d curing times are stiffer, and therefore higher in creep modulus, than concretes with 7d curing times. Figure 7-17 shows a typical creep modulus curve behavior of concrete.

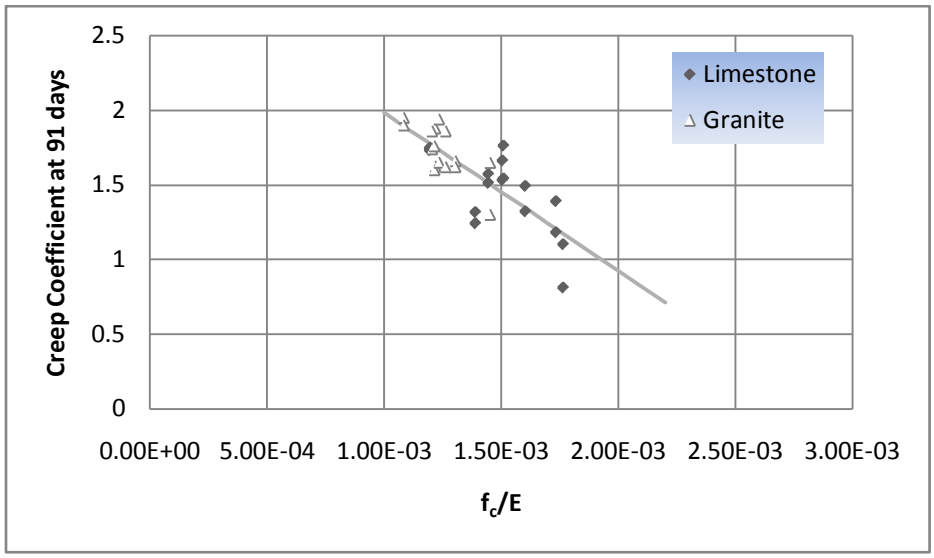

Figure 7-14. Relationship between creep coefficient at 91 days and f_c/E

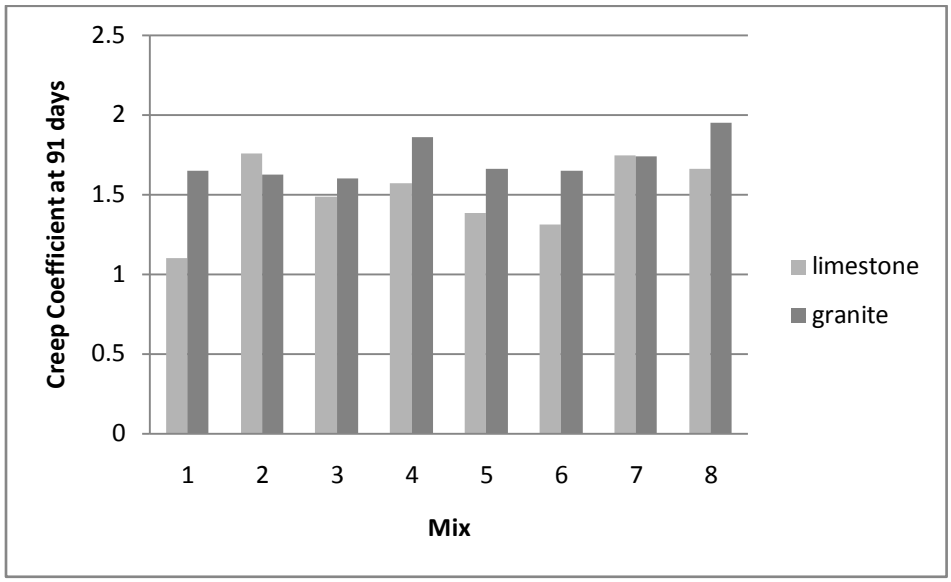

Figure 7-15. Effect of coarse aggregate type on creep coefficient at 91 days for 7d curing condition

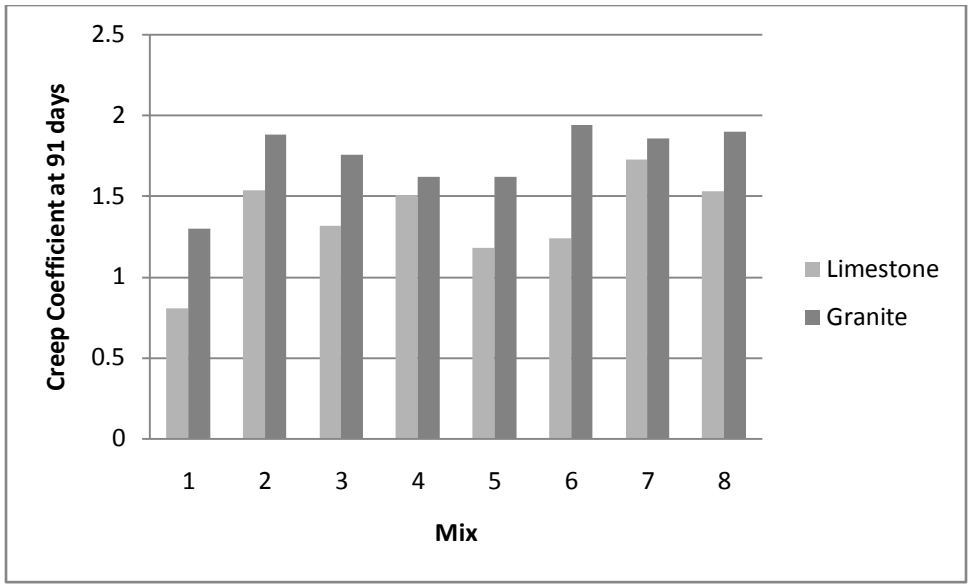

Figure 7-16. Effect of coarse aggregate type on creep coefficient at 91 days for 14d curing condition

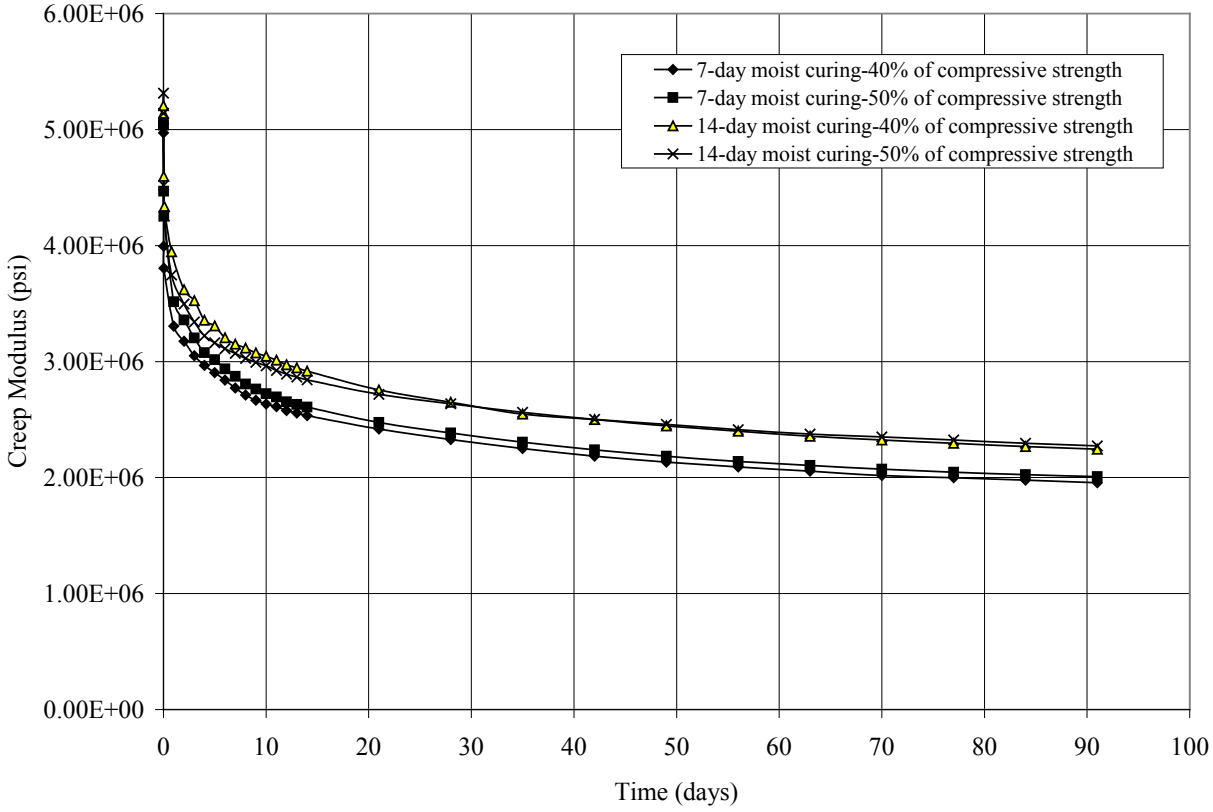

Figure 7-17. Typical decay curve of creep modulus with time

Regression analysis is performed on the elastic modulus of concrete at time of loading and the creep modulus at 91 days. The results of the regression analysis are presented in Table 7-5 and its graphical form in Figure 7-18. The model used in the regression analysis has the following form:

$$E = \alpha \cdot e^{\beta \cdot E_c}$$

where E is the elastic modulus of concrete at time of lading, E_c is the creep modulus at 91 days, and α and β are equal to 126468 and 5.55E-07 respectively.

Table 7-5. Regression analysis on relation of creep modulus and modulus of elasticity

Curing condition	α	95% confidence interval	β	95% confidence interval	R^2	SSE
7d curing	103812	2576 ~ 205048	5.93E-07	4.05E-07 ~ 7.82E-07	0.6888	290230
14d curing	144938	-19576 ~ 309452	5.40E-07	3.21E-07 ~ 7.22E-07	0.5693	361153
All curing conditions	126468	29286 ~ 223650	5.55E-07	4.06E-07 ~ 7.04E-07	0.6848	269929

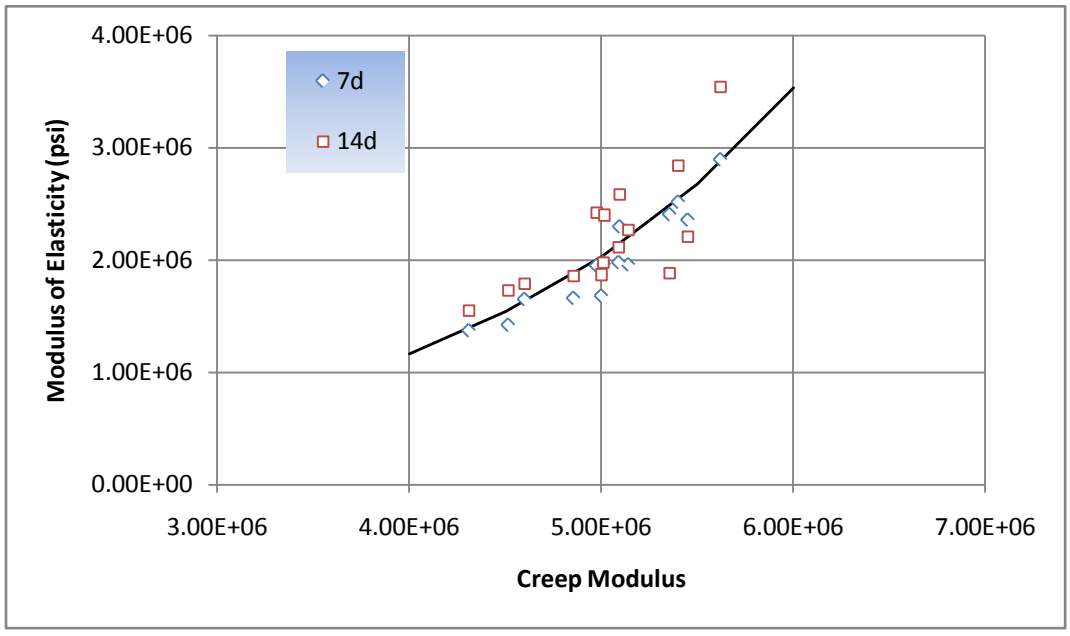

Figure 7-18. Relationship between creep modulus and modulus of elasticity

Another interesting relationship of linear nature was found relating the creep modulus to the water to cement ratio for the mixes evaluated in this study. The results in both tabular and graphical form are presented next. The results show that as the water to cement ratio increases, the creep modulus at 91 days decreases. The linear model used to approximate the data is presented next:

$$E_c = \alpha \cdot \frac{w}{c} + \beta$$

where E_c is the creep modulus at 91 days, α and β are parameters obtained through regression analysis.

Table 7-6. Regression analysis on relation of creep modulus and water cement ratio

Curing condition	α	95% confidence interval	β	95% confidence interval	R^2	SSE
7d curing	-4912634	-7399632 ~ 2425637	3848763	2926416 ~ 4771110	0.6069	263136
14d curing	-5114353	-7434229 ~ -2794476	4069080	3189690 ~ 4948470	0.6816	200326
All curing conditions	-4888843	-6522832 ~ 3254854	3909572	3297090 ~ 4522053	0.6030	237880

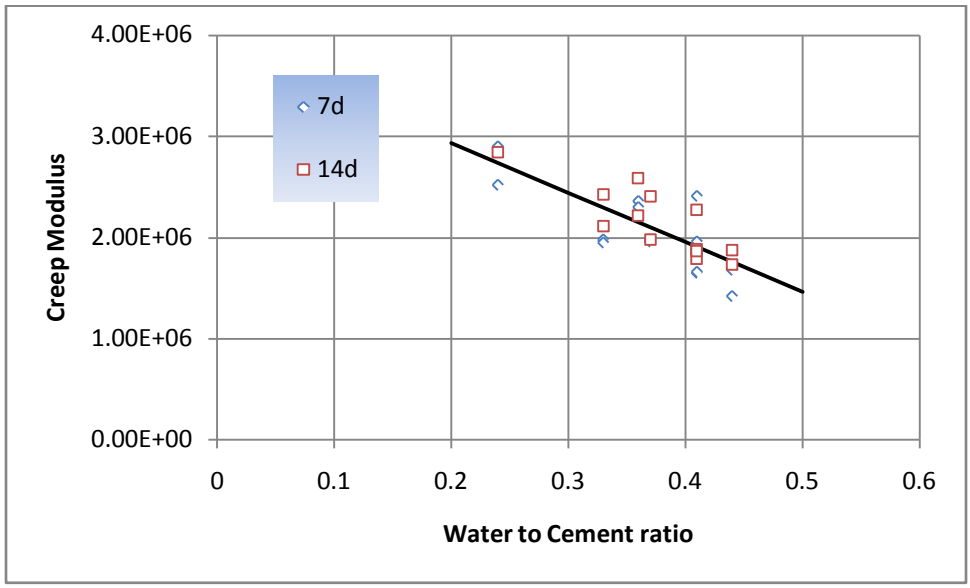

Figure 7-19. Relationship between water to cementitious ratio and creep modulus

7.5 Prediction of Ultimate Creep Strain

To predict the ultimate creep strain, the following asymptotic model was used to approximate the observed data:

$$\varepsilon_c = \alpha \cdot \left(\frac{t}{t+\gamma}\right)^{\beta}$$

where ε_c is the creep strain at 91 days, α is the ultimate creep strain obtained through regression analysis, t is the time in days, β is an unknown parameter obtained through regression analysis, and γ is a parameter related to relative humidity, and geometrical characteristics of the sample in question and has a value of 381.5. So, the equation becomes:

$$\varepsilon_c = \alpha \cdot \left(\frac{t}{t+381.5}\right)^{\beta}$$

Table 7-7 presents the values of the ultimate creep strain, α, and the calculated ultimate creep coefficient based on this ultimate creep strain.

Table 7-7. The predicted ultimate creep strain and creep coefficient

Predicted items	Ultimate creep strain				ultimate creep coefficient			
Curing conditions	curing condition 1		Curing condition 2		curing condition 1		Curing condition 2	
Loading conditions	40%	50%	40%	50%	40%	50%	40%	50%
Mix-1F	1.06E-03	1.30E-03	0.88E-03	1.03E-03	1.48	1.55	1.14	1.16
Mix-2F	1.93E-03	2.08E-03	1.66E-03	2.11E-03	2.91	2.59	2.37	2.44
Mix-3F	1.45E-03	1.86E-03	1.39E-03	1.56E-03	2.30	2.40	2.11	1.90
Mix-4F	1.37E-03	1.59E-03	1.24E-03	1.63E-03	2.28	2.14	2.14	2.32
Mix-5S	1.40E-03	1.84E-03	1.25E-03	1.64E-03	2.10	2.17	1.74	1.84
Mix-6S	1.68E-03	1.87E-03	1.55E-03	1.75E-03	2.51	2.23	2.23	2.05
Mix-7S	1.41E-03	1.69E-03	1.46E-03	1.60E-03	2.71	2.71	2.61	2.46
Mix-8S	1.58E-03	1.97E-03	1.45E-03	1.95E-03	2.57	2.72	2.21	2.34
Mix-9LF	1.11E-03	1.40E-03	0.99E-03	1.16E-03	1.78	1.83	1.46	1.49
Mix-10LS	0.94E-03	1.19E-03	0.76E-03	0.97E-03	1.61	1.45	1.32	1.26
Mix-1GF	1.70E-03	---	1.39E-03	---	2.47	---	2.09	---
Mix-2GF	1.71E-03	---	1.46E-03	2.10E-03	3.19	---	2.73	2.70
Mix-3GF	1.57E-03	---	1.78E-03	1.81E-03	3.28	---	3.04	2.72
Mix-4GF	1.95E-03	---	1.68E-03	---	3.25	---	3.08	---
Mix-5GS	1.44E-03	---	1.41E-03	1.77E-03	2.76	---	2.66	2.55
Mix-6GS	1.60E-03	---	1.56E-03	---	2.63	---	2.41	---
Mix-7GS	1.75E-03	---	1.68E-03	1.76E-03	3.05	---	2.88	2.69
Mix-8GS	2.18E-03	---	1.72E-03	---	3.75	---	3.49	---

Table 7-7 shows that most concretes have ultimate creep coefficients higher than 2.0, and the ultimate creep coefficients of concretes containing Georgia granite aggregate can go as high as 3.0 in magnitude.

7.6 Summary of Findings

Based on the analyzed data, the following conclusions can be made about the results of the creep tests:

(1) Curing conditions seem to have a bigger effect on creep strain at 91 days on concretes containing Georgia granite aggregate, as opposed to those containing Miami Oolite aggregate. This seems to be also the case for most mixes containing fly ash, as opposed to slag.

(2) The creep strain at 91 days seems to be inversely proportional to the compressive strength of concrete at the time of loading. As compressive strength increases, creep strain decreases. The simple linear function has the form of:

$$\varphi_c = \alpha \cdot f_c + \beta$$

with α equal to 1.80×10^{-4}, and β equal to 2.831

(3) Water to cementitious materials ratio seems to be proportional to creep strain at 91 days. The higher the water to cement ratio, the higher the creep strain. Water to cementitious materials ratio seems to be inversely proportional to creep modulus as well: the lower the w/c ratio, the higher the creep modulus at 91 days.

(4) The creep strain seems to be higher on mixes containing Georgia granite aggregate as compared to those containing Miami Oolite limestone aggregate. It also seems that the

containing Georgia granite aggregate exhibit much higher creep coefficient as compared to those containing Miami Oolite limestone aggregate.

(5) The modulus of elasticity seems to be inversely proportional to the creep strain at 91 days. As the elastic modulus increases, the creep strain decreases. The simple linear function has the form of:

$$\varphi_c = \alpha \cdot E_c + \beta$$

with α equal to 3.43×10^{-7}, and β equal to 3.295

(6) The ratio of compressive strength to modulus of elasticity seems to be inversely proportional to the creep strain at 91 days. As this ratio increases, the creep strain decreases. The simple linear function has the form of:

$$\varphi_c = \alpha \cdot \frac{f_c}{E_c} + \beta$$

with α equal to -1057, and β equal to 3.038

Among these equations, the R^2 has the largest magnitude on the equation relating creep strain to compressive strength, so this seems to give the best prediction.

(7) Mixes containing Miami Oolite limestone aggregate exhibit an ultimate creep coefficient of above 2.0, while mixes containing Georgia granite aggregate exhibit values in the low to 3.0.

APPENDIX A
MEASUREMENTS FROM STRENGTH TESTS

Table A-1. Results of compressive strength tests (psi)

No. of mix	Age of Testing (days)																	
	3			7			14			28			56			91		
	1	2	3	1	2	3	1	2	3	1	2	3	1	2	3	1	2	3
1F	8018	8091	8123	8556	8554	8607	8929	8869	9182	9319	9811	9479	10665	10799	10847	11123	11302	11376
2F	4110	4195	3927	4660	4680	4635	6053	6032	5999	6499	6268	6752	6661	6604	6648	7631	7582	7609
3F	5325	5424	5118	6448	6449	6512	7475	7649	7578	8229	8147	8349	8479	8400	8468	9415	9496	9366
4F	5669	5783	5684	7075	6762	6922	7224	7208	6910	7038	7509	7160	8668	8994	9325	9273	9072	9467
5S	5351	5772	5539	7059	7739	6908	7995	8208	8541	8684	8924	8888	9071	9255	9092	9348	9615	9406
6S	6300	6402	6423	7776	7316	8004	8211	8481	8169	8684	9127	9223	9604	9540	9593	9779	9734	9770
7S	4323	4482	4166	5311	5435	5375	5993	5902	5886	6346	6441	6389	6773	6812	6798	6990	6837	6923
8S	4415	5017	4954	5831	6202	6308	6879	6967	6971	7544	7282	7749	7856	8253	8249	8262	8148	8214
9LF	3019	3007	3092	3911	3939	3974	5039	5174	5194	5981	5999	5806	6655	6953	6462	7043	7092	6750
10LS	1486	1411	1504	2175	2310	2088	2749	2860	3201	3760	3811	3660	4496	4204	4236	4863	4725	4595
1GF	6341	6811	6505	7483	7854	7219	7119	7361	5579	7572	7776	8513	8797	8752	8541	-	-	-
2GF	3982	3867	3807	4922	5046	4888	5874	5812	5735	6440	6388	6579	6887	7001	6969	7387	6909	7308
3GF	2960	2865	3099	4810	4612	4655	5468	5778	5829	6816	7075	7134	7818	7801	7943	7862	7915	8105
4GF	4173	4154	4404	5321	3276	5832	5658	5424	5732	6117	6191	6348	7258	6967	7991	-	-	-
5GS	3746	3861	3847	5098	5211	5145	6196	6087	6127	7000	7409	7377	7895	7683	7769	8047	8090	7986
6GS	-	-	-	4998	4961	5177	5650	6432	6058	7051	6870	6931	6424	6984	6900	7301	7617	6840
7GS	2249	2205	2346	4433	4178	4298	5308	5182	5175	6601	6603	6632	7072	6629	7176	7226	7200	7273
8GS	-	-	-	3666	3433	3536	3807	3986	3905	4541	5023	4803	5568	5024	5320	5162	5316	5417

Table A-2. Results of splitting tensile strength tests (psi)

No. of	Age of Testing (days)																	
	3			7			14			28			56			91		
Mix	1	2	3	1	2	3	1	2	3	1	2	3	1	2	3	1	2	3
1F	621	573	582	657	613	614	673	768	706	823	794	770	833	826	844	863	834	851
2F	397	428	401	501	484	468	551	521	515	545	542	539	650	596	617	675	645	658
3F	503	527	510	550	502	568	579	541	567	644	620	608	678	673	671	740	722	731
4F	480	434	459	604	440	517	581	455	663	678	684	647	776	737	764	796	748	766
5S	492	429	405	567	557	599	724	507	677	757	615	697	716	704	713	748	772	695
6S	607	523	580	633	586	589	616	755	575	696	658	663	711	654	707	728	708	719
7S	430	415	434	467	476	475	553	509	493	567	604	473	489	657	625	572	602	616
8S	324	383	409	428	512	557	555	530	564	617	603	681	702	691	686	696	709	704
9LF	283	369	399	425	350	438	470	460	416	472	486	512	563	549	542	579	601	552
10LS	211	203	222	316	295	253	366	351	376	413	404	400	433	401	420	444	433	414
1GF	458	534	464	453	613	614	642	615	610	637	711	616	-	-	-	-	-	-
2GF	350	340	366	425	429	408	518	446	502	541	557	535	557	550	539	585	606	595
3GF	283	288	276	433	411	417	442	522	422	521	508	547	516	646	611	617	646	684
4GF	434	436	416	429	472	463	493	472	494	635	630	570	-	-	-	-	-	-
5GS	364	410	372	381	391	456	507	509	494	563	564	553	621	600	578	652	642	659
6GS	-	-	-	469	403	490	563	524	579	656	534	589	613	637	652	573	561	581
7GS	234	258	245	363	353	371	411	418	460	540	582	515	566	623	607	555	584	593
8GS	-	-	-	344	332	374	414	491	419	455	474	432	478	526	455	470	494	469

Table A-3. Results of elastic modulus tests ($\times 10^6$psi)

No. of	Age of Testing (days)											
	3		7		14		28		56		91	
Mix	1	2	1	2	1	2	1	2	1	2	1	2
1F	4.71	4.77	4.92	4.94	5.20	5.25	5.37	5.43	5.56	5.52	5.57	5.59
2F	3.47	3.38	3.72	3.82	4.11	4.04	4.28	4.34	4.46	4.40	4.77	4.50
3F	4.37	4.42	4.87	4.83	5.02	5.07	5.08	5.19	5.38	5.18	5.66	5.73
4F	4.50	4.47	4.63	4.59	4.85	4.90	4.98	5.03	5.16	5.14	5.33	5.25
5S	4.11	4.11	4.53	4.78	4.86	4.89	5.06	5.12	5.19	5.26	5.23	5.22
6S	4.42	4.11	4.97	4.86	5.08	5.28	5.23	5.67	5.48	5.75	5.54	5.78
7S	3.99	3.80	4.30	4.30	4.53	4.51	4.59	4.61	4.75	4.71	4.78	4.74
8S	3.87	4.04	4.43	4.35	4.90	4.78	5.02	4.98	5.14	5.12	5.16	5.15
9LF	2.71	2.81	2.94	2.90	3.16	3.10	3.29	3.25	3.34	3.36	3.69	3.31
10LS	1.77	1.73	2.01	1.74	2.40	2.32	2.73	2.65	3.07	2.94	2.98	3.09
1GF	5.10	4.98	5.53	5.30	5.43	5.80	5.48	5.53	5.83	5.65	-	-
2GF	3.61	3.99	4.10	4.33	4.59	4.63	4.85	5.07	5.17	5.06	5.25	5.12
3GF	4.08	4.21	4.28	4.95	5.56	5.48	5.62	5.59	5.83	6.03	5.95	5.97
4GF	4.63	4.35	3.05	5.15	4.78	4.93	5.10	5.10	5.58	5.85	-	-
5GS	3.24	3.06	3.66	3.97	4.54	4.76	5.42	4.92	5.48	5.26	5.47	5.64
6GS	-	-	4.15	4.55	4.95	5.10	5.38	5.45	5.60	5.65	5.70	5.75
7GS	2.63	2.74	3.28	3.48	4.05	4.14	5.17	5.33	5.64	5.56	5.77	5.68
8GS	-	-	3.30	3.80	4.40	4.30	4.95	4.80	5.05	4.95	4.85	4.90

APPENDIX B
MEASURED AND CALCULATED RESULTS FROM CREEP TESTS

Table B-1. Measured and calculated results from creep tests

No. of Mix	Curing condition	Load level	Strain	Age of testing (days) 3	7	14	28	56	91
1F	7-day moist cure	40%	Total	0.001160	0.001240	0.001330	0.001460	0.001600	0.001700
			Shrinkage	0.000021	0.000043	0.000076	0.000120	0.000160	0.000200
			Elastic	0.000716	0.000716	0.000716	0.000716	0.000716	0.000716
			Creep	0.000430	0.000480	0.000540	0.000620	0.000720	0.000780
			Creep coefficient	0.60	0.68	0.76	0.87	1.00	1.10
			Creep modulus	3.44E+06	3.16E+06	3.07E+06	2.88E+06	2.65E+06	2.52E+06
		50%	Total	0.001310	0.001420	0.001520	0.001660	0.001840	0.001970
			Shrinkage	0.000021	0.000043	0.000076	0.000120	0.000160	0.000200
			Elastic	0.000804	0.000804	0.000804	0.000804	0.000804	0.000804
			Creep	0.000450	0.000530	0.000610	0.000700	0.000840	0.000930
			Creep coefficient	0.54	0.64	0.72	0.84	1.00	1.13
			Creep modulus	3.32E+06	3.24E+06	3.02E+06	2.84E+06	2.65E+06	2.52E+06
	14-day moist cure	40%	Total	0.001070	0.001150	0.001230	0.001340	0.001450	0.001550
			Shrinkage	0.000014	0.000033	0.000063	0.000100	0.000140	0.000170
			Elastic	0.000760	0.000760	0.000760	0.000760	0.000760	0.000760
			Creep	0.000290	0.000350	0.000400	0.000470	0.000550	0.000620
			Creep coefficient	0.38	0.46	0.53	0.62	0.72	0.81
			Creep modulus	3.78E+06	3.58E+06	3.44E+06	3.26E+06	3.06E+06	2.84E+06
		50%	Total	0.001250	0.001340	0.001420	0.001530	0.001660	0.001760
			Shrinkage	0.000014	0.000033	0.000063	0.000100	0.000140	0.000170
			Creep	0.000350	0.000420	0.000480	0.000550	0.000640	0.000710
			Elastic	0.000880	0.000880	0.000880	0.000880	0.000880	0.000880
			Creep coefficient	0.40	0.48	0.54	0.62	0.73	0.81
			Creep modulus	3.71E+06	3.51E+06	3.35E+06	3.16E+06	2.98E+06	2.92E+06

Continued

2F	7-day moist cure	40%	Total	0.001141	0.001313	0.0015	0.001724	0.001961	0.002115
			Shrinkage	0.000051	0.000097	0.000154	0.000210	0.000261	0.000286
			Elastic	0.000663	0.000663	0.000663	0.000663	0.000663	0.000663
			Creep	0.000427	0.000553	0.000683	0.000851	0.001037	0.001166
			Creep coefficient	0.64	0.83	1.16	1.28	1.56	1.76
			Creep Modulus	2.21E+06	1.98E+06	1.80E+06	1.61E+06	1.46E+06	1.37E+06
		50%	Total	0.001471	0.001614	0.001811	0.002057	0.002306	0.002471
			Shrinkage	0.000051	0.000097	0.000154	0.000210	0.000261	0.000286
			Elastic	0.000803	0.000803	0.000803	0.000803	0.000803	0.000803
			Creep	0.000617	0.000714	0.000854	0.001044	0.001242	0.001382
			Creep coefficient	0.77	0.89	1.07	1.30	1.55	1.72
			Creep Modulus	2.10E+06	1.97E+06	1.80E+06	1.59E+06	1.42E+06	1.32E+06
	14-day moist cure	40%	Total	0.001114	0.001244	0.00139	0.001601	0.001834	0.001955
			Shrinkage	0.000031	0.000069	0.000112	0.000173	0.000233	0.000258
			Elastic	0.000669	0.000669	0.000669	0.000669	0.000669	0.000669
			Creep	0.000414	0.000506	0.000609	0.000759	0.000932	0.001028
			Creep coefficient	0.62	0.76	0.91	1.13	1.39	1.54
			Creep Modulus	2.45E+06	2.28E+06	2.09E+06	1.85E+06	1.66E+06	1.55E+06
		50%	Total	0.001385	0.001557	0.00176	0.001972	0.002232	0.002398
			Shrinkage	0.000031	0.000069	0.000112	0.000173	0.000233	0.000258
			Elastic	0.000842	0.000842	0.000842	0.000842	0.000842	0.000842
			Creep	0.000512	0.000646	0.000806	0.000957	0.001157	0.001298
			Creep coefficient	0.61	0.77	0.96	1.14	1.37	1.54
			Creep Modulus	2.45E+06	2.23E+06	2.02E+06	1.85E+06	1.66E+06	1.55E+06

Continued

3F	7-day moist cure	40%	Total	0.001032	0.001165	0.001318	0.001477	0.001669	0.001796
			Shrinkage	0.000040	0.000073	0.000124	0.000177	0.000221	0.000248
			Elastic	0.000609	0.000609	0.000609	0.000609	0.000609	0.000609
			Creep	0.000383	0.000483	0.000585	0.000691	0.000839	0.000939
			Creep coefficient	0.61	0.77	0.93	1.10	1.33	1.49
			Creep modulus	3.05E+06	2.77E+06	2.53E+06	2.33E+06	2.09E+06	1.96E+06
		50%	Total	0.001221	0.00139	0.001575	0.001764	0.00199	0.002132
			Shrinkage	0.000040	0.000073	0.000124	0.000177	0.000221	0.000248
			Elastic	0.000751	0.000751	0.000751	0.000751	0.000751	0.000751
			Creep	0.000430	0.000566	0.000700	0.000836	0.001018	0.001133
			Creep coefficient	0.57	0.75	0.93	1.11	1.36	1.51
			Creep modulus	3.20E+06	2.87E+06	2.61E+06	2.38E+06	2.14E+06	2.01E+06
	14-day moist cure	40%	Total	0.000957	0.001093	0.001217	0.001381	0.001557	0.001686
			Shrinkage	0.000021	0.000047	0.000087	0.000137	0.000182	0.000217
			Elastic	0.000633	0.000633	0.000633	0.000633	0.000633	0.000633
			Creep	0.000303	0.000413	0.000497	0.000611	0.000742	0.000836
			Creep coefficient	0.48	0.65	0.79	0.97	1.17	1.32
			Creep modulus	3.52E+06	3.15E+06	2.92E+06	2.76E+06	2.41E+06	2.27E+06
		50%	Total	0.001254	0.001389	0.001537	0.001700	0.001890	0.002023
			Shrinkage	0.000021	0.000047	0.000087	0.000137	0.000182	0.000217
			Elastic	0.000776	0.000776	0.000776	0.000776	0.000776	0.000776
			Creep	0.000457	0.000566	0.000674	0.000787	0.000932	0.001030
			Creep coefficient	0.59	0.73	0.87	1.01	1.20	1.33
			Creep modulus	3.34E+06	3.07E+06	2.84E+06	2.72E+06	2.41E+06	2.27E+06

Continued

4F	7-day moist cure	40%	Total	0.001060	0.001200	0.001340	0.001510	0.001680	0.001810
			Shrinkage	0.000037	0.000073	0.000120	0.000170	0.000230	0.000270
			Elastic	0.000600	0.000600	0.000600	0.000600	0.000600	0.000600
			Creep	0.000420	0.000530	0.000630	0.000740	0.000850	0.000940
			Creep coefficient	0.71	0.89	1.05	1.24	1.42	1.57
			Creep modulus	2.95E+06	2.68E+06	2.47E+06	2.28E+06	2.09E+06	1.98E+06
		50%	Total	0.001400	0.001523	0.001642	0.001804	0.001984	0.002120
			Shrinkage	0.000037	0.000073	0.000120	0.000170	0.000230	0.000270
			Elastic	0.000703	0.000703	0.000703	0.000703	0.000703	0.000703
			Creep	0.00066	0.000747	0.000819	0.000931	0.001051	0.001147
			Creep coefficient	0.94	1.06	1.17	1.32	1.50	1.63
			Creep modulus	2.79E+06	2.52E+06	2.32E+06	2.13E+06	1.96E+06	1.85E+06
	14-day moist cure	40%	Total	0.001078	0.001166	0.001259	0.001386	0.001543	0.001654
			Shrinkage	0.000021	0.000042	0.000080	0.000132	0.000186	0.000223
			Elastic	0.000571	0.000571	0.000571	0.000571	0.000571	0.000571
			Creep	0.000486	0.000553	0.000608	0.000683	0.000786	0.000860
			Creep coefficient	0.85	0.97	1.06	1.20	1.38	1.51
			Creep modulus	3.90E+06	2.68E+06	2.47E+06	2.31E+06	2.09E+06	1.98E+06
		50%	Total	0.001208	0.001361	0.001518	0.001699	0.001886	0.002020
			Shrinkage	0.000021	0.000042	0.000080	0.000132	0.000186	0.000223
			Elastic	0.000702	0.000702	0.000702	0.000702	0.000702	0.000702
			Creep	0.000485	0.000617	0.000736	0.000865	0.000998	0.001095
			Creep coefficient	0.69	0.88	1.05	1.23	1.42	1.56
			Creep modulus	3.90E+06	2.68E+06	2.47E+06	2.30E+06	2.09E+06	1.98E+06

Continued

5S	7-day moist cure	40%	Total	0.001168	0.001299	0.001423	0.001587	0.001744	0.00184
			Shrinkage	0.000044	0.000088	0.000130	0.000170	0.000201	0.000216
			Elastic	0.000669	0.000669	0.000669	0.000669	0.000669	0.000669
			Creep	0.000455	0.000542	0.000624	0.000748	0.000874	0.000955
			Creep coefficient	0.409	0.580	0.683	1.101	1.320	1.476
			Creep modulus	2.99E+06	2.69E+06	2.49E+06	2.28E+06	2.09E+06	1.98E+06
		50%	Total	0.001455	0.00162	0.001783	0.001977	0.002175	0.002299
			Shrinkage	0.000044	0.000088	0.000130	0.000170	0.000201	0.000216
			Elastic	0.000846	0.000846	0.000846	0.000846	0.000846	0.000846
			Creep	0.000565	0.000686	0.000807	0.000961	0.001128	0.001237
			Creep coefficient	0.67	0.81	0.95	1.14	1.33	1.46
			Creep modulus	2.99E+06	2.69E+06	2.49E+06	2.28E+06	2.09E+06	1.98E+06
	14-day moist cure	40%	Total	0.001222	0.001323	0.001439	0.001594	0.001747	0.001834
			Shrinkage	0.000043	0.000074	0.000110	0.000149	0.000178	0.000193
			Elastic	0.000718	0.000718	0.000718	0.000718	0.000718	0.000718
			Creep	0.000461	0.000531	0.000611	0.000727	0.000851	0.000923
			Creep coefficient	0.64	0.74	0.85	1.01	1.19	1.29
			Creep modulus	3.00E+06	2.79E+06	2.60E+06	2.38E+06	2.19E+06	2.11E+06
		50%	Total	0.001464	0.001596	0.001747	0.001937	0.002118	0.002212
			Shrinkage	0.000043	0.000074	0.000110	0.000149	0.000178	0.000193
			Elastic	0.000889	0.000889	0.000889	0.000889	0.000889	0.000889
			Creep	0.000532	0.000633	0.000748	0.000899	0.001051	0.001130
			Creep coefficient	0.62	0.74	0.87	1.04	1.22	1.31
			Creep modulus	2.99E+06	2.79E+06	2.60E+06	2.38E+06	2.19E+06	2.11E+06

Continued

6S	7-day moist cure	40%	Total	0.000975	0.001105	0.001255	0.001405	0.001600	0.001758
			Shrinkage	0.000042	0.000082	0.000123	0.000157	0.000183	0.000196
			Elastic	0.000670	0.000670	0.000670	0.000670	0.000670	0.000670
			Creep	0.000263	0.000353	0.000462	0.000588	0.000747	0.000892
			Creep coefficient	0.39	0.54	0.70	0.90	1.15	1.34
			Creep modulus	3.58E+06	3.22E+06	2.91E+06	2.65E+06	2.38E+06	2.36E+06
		50%	Total	0.001194	0.001391	0.001550	0.001707	0.001901	0.002048
			Shrinkage	0.000042	0.000082	0.000123	0.000157	0.000183	0.000196
			Elastic	0.000837	0.000837	0.000837	0.000837	0.000837	0.000837
			Creep	0.000325	0.000472	0.000570	0.000713	0.000891	0.001015
			Creep coefficient	0.41	0.54	0.69	0.87	1.08	1.25
			Creep modulus	3.54E+06	3.15E+06	2.89E+06	2.62E+06	2.31E+06	2.30E+06
	14-day moist cure	40%	Total	0.001037	0.001164	0.001291	0.001448	0.001648	0.001796
			Shrinkage	0.000038	0.000076	0.000114	0.000141	0.000163	0.000177
			Elastic	0.000692	0.000692	0.000692	0.000692	0.000692	0.000692
			Creep	0.000307	0.000396	0.000485	0.000615	0.000793	0.000927
			Creep coefficient	0.43	0.57	0.71	0.89	1.11	1.27
			Creep modulus	3.70E+06	3.40E+06	3.15E+06	2.87E+06	2.56E+06	2.21E+06
		50%	Total	0.001263	0.001467	0.001567	0.001727	0.001941	0.002104
			Shrinkage	0.000038	0.000076	0.000114	0.000141	0.000163	0.000177
			Elastic	0.000854	0.000854	0.000854	0.000854	0.000854	0.000854
			Creep	0.000371	0.000537	0.000599	0.000732	0.000924	0.001073
			Creep coefficient	0.44	0.57	0.70	0.87	1.06	1.21
			Creep modulus	3.69E+06	3.35E+06	3.12E+06	2.85E+06	2.51E+06	2.10E+06

Continued

7S	7-day moist cure	40%	Total	0.000907	0.001094	0.001264	0.001399	0.001561	0.001656
			Shrinkage	0.000039	0.000080	0.000126	0.000170	0.000202	0.000223
			Elastic	0.000519	0.000519	0.000519	0.000519	0.000519	0.000519
			Creep	0.000349	0.000495	0.000619	0.00071	0.00084	0.000914
			Creep coefficient	0.67	0.95	1.19	1.37	1.62	1.76
			Creep modulus	2.66E+06	2.33E+06	2.11E+06	1.92E+06	1.74E+06	1.65E+06
		50%	Total	0.001101	0.001285	0.001486	0.001664	0.001836	0.001941
			Shrinkage	0.000039	0.000080	0.000126	0.000170	0.000202	0.000223
			Elastic	0.000616	0.000616	0.000616	0.000616	0.000616	0.000616
			Creep	0.000446	0.000589	0.000744	0.000878	0.001018	0.001102
			Creep coefficient	0.72	0.96	1.21	1.43	1.65	1.79
			Creep modulus	2.78E+06	2.45E+06	2.17E+06	1.98E+06	1.81E+06	1.72E+06
	14-day moist cure	40%	Total	0.000948	0.001081	0.001209	0.001384	0.001556	0.001651
			Shrinkage	0.000038	0.000073	0.000111	0.000148	0.000183	0.000204
			Elastic	0.000546	0.000546	0.000546	0.000546	0.000546	0.000546
			Creep	0.000364	0.000462	0.000552	0.00069	0.000827	0.000901
			Creep coefficient	0.67	0.85	1.01	1.26	1.51	1.65
			Creep modulus	2.84E+06	2.57E+06	2.36E+06	2.09E+06	1.89E+06	1.79E+06
		50%	Total	0.001160	0.001308	0.001466	0.001646	0.001821	0.001921
			Shrinkage	0.000038	0.000073	0.000111	0.000148	0.000183	0.000204
			Elastic	0.000643	0.000643	0.000643	0.000643	0.000643	0.000643
			Creep	0.000479	0.000592	0.000712	0.000855	0.000995	0.001074
			Creep coefficient	0.74	0.92	1.11	1.33	1.55	1.67
			Creep modulus	2.78E+06	2.52E+06	2.30E+06	2.08E+06	1.90E+06	1.82E+06

Continued

8S	7-day moist cure	40%	Total	0.001131	0.001263	0.001409	0.000157	0.001762	0.001914
			Shrinkage	0.000073	0.000123	0.000161	0.000194	0.000228	0.000250
			Elastic	0.000614	0.000614	0.000614	0.000614	0.000614	0.000614
			Creep	0.000443	0.000526	0.000633	0.000761	0.000920	0.001050
			Creep coefficient	0.72	0.86	1.03	1.24	1.50	1.71
			Creep modulus	2.71E+06	2.53E+06	2.34E+06	2.04E+06	1.82E+06	1.68E+06
		50%	Total	0.001296	0.001438	0.001606	0.001821	0.002048	0.002227
			Shrinkage	0.000073	0.000123	0.000161	0.000194	0.000228	0.000250
			Elastic	0.000722	0.000722	0.000722	0.000722	0.000722	0.000722
			Creep	0.000500	0.000592	0.000722	0.000904	0.001098	0.001254
			Creep coefficient	0.69	0.82	1.00	1.25	1.52	1.74
			Creep modulus	2.56E+06	2.38E+06	2.17E+06	1.97E+04	1.77E+06	1.63E+06
	14-day moist cure	40%	Total	0.001140	0.001262	0.001394	0.001549	0.001733	0.001889
			Shrinkage	0.000050	0.000098	0.000136	0.000169	0.000202	0.000230
			Elastic	0.000654	0.000654	0.000654	0.000654	0.000654	0.000654
			Creep	0.000436	0.000510	0.000604	0.000726	0.000877	0.001004
			Creep coefficient	0.67	0.78	0.92	1.11	1.34	1.53
			Creep modulus	2.92E+06	2.68E+06	2.51E+06	2.26E+06	2.02E+06	1.87E+06
		50%	Total	0.001374	0.001524	0.001677	0.001881	0.002118	0.002294
			Shrinkage	0.000050	0.000098	0.000136	0.000169	0.000202	0.000230
			Elastic	0.000831	0.000831	0.000831	0.000831	0.000831	0.000831
			Creep	0.000493	0.000596	0.000710	0.000881	0.001084	0.001233
			Creep coefficient	0.59	0.72	0.85	1.06	1.30	1.48
			Creep modulus	2.71E+06	2.53E+06	2.34E+06	2.14E+06	1.93E+06	1.78E+06

Continued

9LF	7-day moist cure	40%	Total	0.001118	0.001231	0.001380	0.001528	0.001684	0.001792
			Shrinkage	0.000049	0.000096	0.000162	0.000226	0.000288	0.000322
			Elastic	0.000626	0.000626	0.000626	0.000626	0.000626	0.000626
			Creep	0.000443	0.000510	0.000592	0.000677	0.000771	0.000844
			Creep coefficient	0.71	0.82	0.95	1.08	1.23	1.35
			Creep modulus	1.99E+06	1.85E+06	1.74E+06	1.62E+06	1.51E+06	1.43E+06
		50%	Total	0.001337	0.001487	0.001642	0.001811	0.001987	0.002112
			Shrinkage	0.000049	0.000096	0.000162	0.000226	0.000288	0.000322
			Elastic	0.000767	0.000767	0.000767	0.000767	0.000767	0.000767
			Creep	0.000521	0.000624	0.000713	0.000819	0.000932	0.001023
			Creep coefficient	0.68	0.81	0.93	1.07	1.22	1.33
			Creep modulus	1.92E+06	1.81E+06	1.69E+06	1.58E+06	1.47E+06	1.40E+06
	14-day moist cure	40%	Total	0.001169	0.001272	0.001392	0.001507	0.001633	0.001714
			Shrinkage	0.000046	0.000081	0.000137	0.000189	0.000239	0.000276
			Elastic	0.000677	0.000677	0.000677	0.000677	0.000677	0.000677
			Creep	0.000447	0.000514	0.000579	0.000641	0.000718	0.000762
			Creep coefficient	0.66	0.76	0.86	0.95	1.06	1.13
			Creep modulus	2.29E+06	2.12E+06	2.00E+06	1.91E+06	1.79E+06	1.72E+06
		50%	Total	0.001297	0.001433	0.001564	0.001691	0.001836	0.001940
			Shrinkage	0.000046	0.000081	0.000137	0.000189	0.000239	0.000276
			Elastic	0.000777	0.000777	0.000777	0.000777	0.000777	0.000777
			Creep	0.000474	0.000576	0.000651	0.000726	0.000820	0.000888
			Creep coefficient	0.61	0.74	0.84	0.93	1.06	1.14
			Creep modulus	2.21E+06	2.08E+06	1.98E+06	1.88E+06	1.79E+06	1.72E+06

Continued

			Total	0.001206	0.001314	0.001433	0.001559	0.001694	0.001789
			Shrinkage	0.000070	0.000130	0.000198	0.000260	0.000319	0.000360
			Elastic	0.000546	0.000546	0.000546	0.000546	0.000546	0.000546
		40%	Creep	0.000590	0.000639	0.000690	0.000753	0.000830	0.000883
			Creep coefficient	1.08	1.17	1.26	1.38	1.52	1.62
	7-day moist cure		Creep modulus	1.16E+06	1.10E+06	1.04E+06	0.97E+06	0.92E+06	0.88E+06
			Total	0.001517	0.001648	0.001780	0.001939	0.002098	0.002224
			Shrinkage	0.000070	0.000130	0.000198	0.000260	0.000319	0.000360
			Elastic	0.000721	0.000721	0.000721	0.000721	0.000721	0.000721
		50%	Creep	0.000726	0.000797	0.000861	0.000958	0.001058	0.001143
			Creep coefficient	1.01	1.10	1.19	1.33	1.47	1.59
			Creep modulus	1.03E+06	0.99E+06	0.95E+06	0.90E+06	0.85E+06	0.82E+06
10LS			Total	0.000874	0.000898	0.000941	0.000997	0.001062	0.001116
			Shrinkage	0.000038	0.000090	0.000152	0.000209	0.000279	0.000320
			Elastic	0.000781	0.000898	0.001083	0.001123	0.001274	0.001377
		40%	Creep	0.000276	0.000337	0.000380	0.000486	0.000501	0.000554
			Creep coefficient	0.62	0.74	0.82	0.93	1.05	1.16
	14-day moist cure		Creep modulus	1.67E+06	1.58E+06	1.51E+06	1.42E+06	1.33E+06	1.26E+06
			Total	0.001169	0.001286	0.001406	0.001539	0.001694	0.001809
			Shrinkage	0.000038	0.000090	0.000152	0.000209	0.000279	0.000320
			Elastic	0.000713	0.000713	0.000713	0.000713	0.000713	0.000713
		50%	Creep	0.000418	0.000482	0.000540	0.000617	0.000702	0.000776
			Creep coefficient	0.59	0.68	0.76	0.87	0.99	1.09
			Creep modulus	1.67E+06	1.58E+06	1.51E+06	1.42E+06	1.33E+06	1.26E+06

Continued

1GF	40%	7-d	Total	8.66E-04	9.73E-04	1.07E-03	1.17E-03	1.28E-03	1.35E-03
			Shrinkage	2.34E-05	4.46E-05	7.16E-05	1.06E-04	1.42E-04	1.65E-04
			Elastic	6.89E-04	6.89E-04	6.89E-04	6.89E-04	6.89E-04	6.89E-04
			Creep	1.53E-04	2.39E-04	3.08E-04	3.76E-04	4.46E-04	4.98E-04
			Creep coefficient	0.22	0.35	0.45	0.55	0.65	0.72
			Creep modulus	4.09E+06	3.72E+06	3.46E+06	3.24E+06	3.04E+06	2.90E+06
		14-d	Total	7.47E-04	8.31E-04	9.06E-04	9.86E-04	1.07E-03	1.13E-03
			Shrinkage	2.16E-05	4.24E-05	6.83E-05	1.00E-04	1.32E-04	1.51E-04
			Elastic	6.66E-04	6.66E-04	6.66E-04	6.66E-04	6.66E-04	6.66E-04
			Creep	5.94E-05	1.23E-04	1.72E-04	2.20E-04	2.71E-04	3.09E-04
			Creep coefficient	0.09	0.18	0.26	0.33	0.41	0.46
			Creep modulus	4.75E+06	4.37E+06	4.12E+06	3.89E+06	3.68E+06	3.54E+06
2GF	40%	7-d	Total	9.28E-04	1.03E-03	1.12E-03	1.22E-03	1.32E-03	1.39E-03
			Shrinkage	3.28E-05	6.91E-05	1.13E-04	1.63E-04	2.08E-04	2.32E-04
			Elastic	5.36E-04	5.36E-04	5.36E-04	5.36E-04	5.36E-04	5.36E-04
			Creep	3.58E-04	4.25E-04	4.73E-04	5.20E-04	5.76E-04	6.21E-04
			Creep coefficient	0.67	0.79	0.88	0.97	1.07	1.16
			Creep modulus	2.53E+06	2.35E+06	2.24E+06	2.14E+06	2.03E+06	1.95E+06
		14-d	Total	7.51E-04	8.42E-04	9.24E-04	1.01E-03	1.10E-03	1.17E-03
			Shrinkage	3.28E-05	6.91E-05	1.13E-04	1.63E-04	2.08E-04	2.32E-04
			Elastic	5.35E-04	5.35E-04	5.35E-04	5.35E-04	5.35E-04	5.35E-04
			Creep	1.83E-04	2.38E-04	2.76E-04	3.13E-04	3.59E-04	3.98E-04
			Creep coefficient	0.34	0.45	0.52	0.58	0.67	0.74
			Creep modulus	3.15E+06	2.93E+06	2.79E+06	2.67E+06	2.53E+06	2.42E+06

Continued

3GF	40%	7-d	Total	6.06E-04	7.15E-04	8.16E-04	9.28E-04	1.05E-03	1.14E-03
			Shrinkage	2.08E-05	4.33E-05	7.34E-05	1.13E-04	1.55E-04	1.81E-04
			Elastic	4.79E-04	4.79E-04	4.79E-04	4.79E-04	4.79E-04	4.79E-04
			Creep	1.07E-04	1.92E-04	2.63E-04	3.36E-04	4.15E-04	4.76E-04
			Creep coefficient	0.22	0.40	0.55	0.70	0.87	0.99
			Creep modulus	3.93E+06	3.43E+06	3.10E+06	2.82E+06	2.57E+06	2.41E+06
		14-d	Total	8.76E-04	9.90E-04	1.09E-03	1.20E-03	1.32E-03	1.40E-03
			Shrinkage	2.03E-05	4.04E-05	6.76E-05	1.05E-04	1.48E-04	1.77E-04
			Elastic	5.86E-04	5.86E-04	5.86E-04	5.86E-04	5.86E-04	5.86E-04
			Creep	2.70E-04	3.64E-04	4.39E-04	5.12E-04	5.84E-04	6.36E-04
			Creep coefficient	0.46	0.62	0.75	0.87	1.00	1.09
			Creep modulus	2.69E+06	2.42E+06	2.24E+06	2.09E+06	1.96E+06	1.88E+06
4GF	40%	7-d	Total	1.11E-03	1.22E-03	1.32E-03	1.43E-03	1.54E-03	1.61E-03
			Shrinkage	5.62E-05	9.01E-05	1.27E-04	1.69E-04	2.09E-04	2.32E-04
			Elastic	5.99E-04	5.99E-04	5.99E-04	5.99E-04	5.99E-04	5.99E-04
			Creep	4.55E-04	5.34E-04	5.97E-04	6.60E-04	7.28E-04	7.79E-04
			Creep coefficient	0.76	0.89	1.00	1.10	1.21	1.30
			Creep modulus	2.56E+06	2.38E+06	2.26E+06	2.14E+06	2.03E+06	1.96E+06
		14-d	Total	9.99E-04	1.09E-03	1.18E-03	1.26E-03	1.35E-03	1.41E-03
			Shrinkage	9.07E-05	1.33E-04	1.75E-04	2.20E-04	2.61E-04	2.84E-04
			Elastic	5.46E-04	5.46E-04	5.46E-04	5.46E-04	5.46E-04	5.46E-04
			Creep	3.63E-04	4.15E-04	4.54E-04	4.95E-04	5.41E-04	5.79E-04
			Creep coefficient	0.67	0.76	0.83	0.91	0.99	1.06
			Creep modulus	2.97E+06	2.81E+06	2.70E+06	2.59E+06	2.48E+06	2.40E+06

Continued

5GS	40%	7-d	Total	7.51E-04	8.40E-04	9.20E-04	1.01E-03	1.09E-03	1.16E-03
			Shrinkage	7.81E-05	1.01E-04	1.23E-04	1.48E-04	1.73E-04	1.88E-04
			Elastic	5.21E-04	5.21E-04	5.21E-04	5.21E-04	5.21E-04	5.21E-04
			Creep	1.51E-04	2.18E-04	2.75E-04	3.36E-04	3.99E-04	4.45E-04
			Creep coefficient	0.29	0.42	0.53	0.64	0.77	0.85
			Creep modulus	3.27E+06	2.98E+06	2.76E+06	2.57E+06	2.39E+06	2.28E+06
		14-d	Total	7.54E-04	8.40E-04	9.16E-04	9.98E-04	1.08E-03	1.14E-03
			Shrinkage	4.27E-05	7.16E-05	1.03E-04	1.39E-04	1.72E-04	1.91E-04
			Elastic	5.30E-04	5.30E-04	5.30E-04	5.30E-04	5.30E-04	5.30E-04
			Creep	1.82E-04	2.39E-04	2.83E-04	3.29E-04	3.79E-04	4.19E-04
			Creep coefficient	0.34	0.45	0.53	0.62	0.72	0.79
			Creep modulus	3.09E+06	2.86E+06	2.71E+06	2.56E+06	2.42E+06	2.32E+06
6GS	40%	7-d	Total	8.68E-04	9.65E-04	1.05E-03	1.14E-03	1.23E-03	1.30E-03
			Shrinkage	2.05E-05	3.70E-05	5.69E-05	8.10E-05	1.05E-04	1.20E-04
			Elastic	6.08E-04	6.08E-04	6.08E-04	6.08E-04	6.08E-04	6.08E-04
			Creep	2.39E-04	3.19E-04	3.85E-04	4.52E-04	5.21E-04	5.72E-04
			Creep coefficient	0.39	0.53	0.63	0.74	0.86	0.94
			Creep modulus	3.20E+06	2.92E+06	2.73E+06	2.56E+06	2.40E+06	2.30E+06
		14-d	Total	7.61E-04	8.61E-04	9.51E-04	1.05E-03	1.15E-03	1.22E-03
			Shrinkage	6.95E-05	8.69E-05	1.04E-04	1.25E-04	1.51E-04	1.71E-04
			Elastic	6.48E-04	6.48E-04	6.48E-04	6.48E-04	6.48E-04	6.48E-04
			Creep	4.36E-05	1.26E-04	1.99E-04	2.76E-04	3.53E-04	4.04E-04
			Creep coefficient	0.07	0.20	0.31	0.43	0.54	0.62
			Creep modulus	3.92E+06	3.50E+06	3.20E+06	2.94E+06	2.71E+06	2.58E+06

Continued

7GS	40%	7-d	Total	1.01E-03	1.10E-03	1.19E-03	1.27E-03	1.36E-03	1.42E-03
			Shrinkage	5.63E-05	8.30E-05	1.11E-04	1.43E-04	1.75E-04	1.95E-04
			Elastic	5.73E-04	5.73E-04	5.73E-04	5.73E-04	5.73E-04	5.73E-04
			Creep	3.77E-04	4.46E-04	5.01E-04	5.56E-04	6.13E-04	6.55E-04
			Creep coefficient	0.66	0.78	0.87	0.97	1.07	1.14
			Creep modulus	2.14E+06	2.00E+06	1.90E+06	1.80E+06	1.72E+06	1.66E+06
		14-d	Total	7.43E-04	8.56E-04	9.58E-04	1.07E-03	1.19E-03	1.27E-03
			Shrinkage	4.78E-05	7.07E-05	9.56E-05	1.26E-04	1.58E-04	1.80E-04
			Elastic	5.84E-04	5.84E-04	5.84E-04	5.84E-04	5.84E-04	5.84E-04
			Creep	1.11E-04	2.01E-04	2.79E-04	3.61E-04	4.47E-04	5.10E-04
			Creep coefficient	0.19	0.34	0.48	0.62	0.76	0.87
			Creep modulus	2.93E+06	2.59E+06	2.36E+06	2.15E+06	1.97E+06	1.86E+06
8GS	40%	7-d	Total	8.20E-04	1.06E-03	1.31E-03	1.60E-03	1.94E-03	2.20E-03
			Shrinkage	5.33E-05	8.82E-05	1.24E-04	1.59E-04	1.88E-04	2.03E-04
			Elastic	9.76E-04	9.76E-04	9.76E-04	9.76E-04	9.76E-04	9.76E-04
			Creep	-2.09E-04	-3.66E-06	2.05E-04	4.62E-04	7.72E-04	1.02E-03
			Creep coefficient	-0.21	0.00	0.21	0.47	0.79	1.04
			Creep modulus	2.81E+06	2.22E+06	1.83E+06	1.50E+06	1.23E+06	1.08E+06
		14-d	Total	1.05E-03	1.24E-03	1.42E-03	1.62E-03	1.83E-03	1.98E-03
			Shrinkage	2.39E-05	4.57E-05	7.26E-05	1.06E-04	1.40E-04	1.60E-04
			Elastic	7.93E-04	7.93E-04	7.93E-04	7.93E-04	7.93E-04	7.93E-04
			Creep	2.35E-04	4.03E-04	5.54E-04	7.18E-04	8.98E-04	1.03E-03
			Creep coefficient	0.30	0.51	0.70	0.91	1.13	1.30
			Creep modulus	2.10E+06	1.80E+06	1.60E+06	1.43E+06	1.28E+06	1.18E+06

LIST OF REFERENCES

A. Momayez a, M. E. (2004). Cylindrical specimen for measuring shrinkage in repaired concrete members. *Construction and Building Materials* , 10.

ACI. (1996). *ACI Manual of Concrete Practice.* American Concrete Institute.

ACI. (2005). Report on Factors Affecting Shrinkage and Creep of Hardened Concrete. *ACI 209.1R-05* , 12.

Acker, P., & Ulm, F.-J. (2001). Creep and shrinkage of concrete: physical origins and practical measurements. *Nuclear Engineering and Design* , 16.

Aitcin, P. C., & Mehta, P. K. (1990). Effect of Coarse-Aggregate Characteristics on Mechanical Properties of High-Strength Concrete. *ACI Materials Journal* , 5.

Al-Oraimi, S. K., Taha, R., & Hassan, H. F. (2004). The effect of the mineralogy of coarse aggregate on the mechanical properties of high-strength concrete. *Construction and Building Materials* , 5.

ASTM. (1997). *ASTM - Section 4* . American Society for Testing Materials.

Aydin, A. C., Arslan, A., & Gul, R. (2007). Mesoscale simulation of cement based materials time-dependent behavior. *Computational Materials Science* , 7.

Bazant, Z. P. (2001). Prediction of concrete creep and shrinkage: past, present and future. *Nuclear Engineering and Design* , 12.

Chindaprasirt, P., Jaturapitakkul, C., & Sinsiri, T. (2005). Effect of fly ash fineness on compressive strength and pore size of blended cement paste. *Cement & Concrete Composites* , 4.

Han, M. C., Han, C. G., & Lee, G. C. (2006). Mixture and Material Factors Affecting the Strength and Shrinkage of High Performance Concrete. *Journal of Asian Architecture and Building Engineering* , 7.

Iravani, S. (1996). Mechanical Properties of High-Performance Concrete. *ACI Materials Journal*, 11.

James G. MacGregor, J. K. (2005). *Reinforced Concrete - Mechanics and Design.* Pearson Education, Inc. .

Jianyong, L., & Yan, Y. (2001). A study on creep and drying shrinkage of high performance concrete. *Cement and Concrete Research* , 4.

Kiyoshi, E., & Kohji, T. (2004). Prediction equation of drying shrinkage of concrete based on composite model. *Cement and Concrete Research* , 11.

Lo, T. Y., Tang, W. C., & Cui, H. Z. (2007). The effects of aggregate properties on lightweight concrete. *Building and Environment* , 5.

Mazloom, M. (2008). Estimating long-term creep and shrinkage of high-strength concrete. *Cement & Concrete Composites* , 11.

Mehta, P. K., & Paulo, J. M. (2006). *Concrete - Microstructure, Properties, and Materials.* McGraw-Hill.

Mohamad, M. B. (2005). *The use of Limestone Aggregate in Concrete.* Universiti Teknologi Malaysia.

Mokarem, D. W. (2002). *Dvelopment of Concrete Shrinkage Performance Specifications.* Blacksburg: Virginia Polytechnic Institute and State University.

National Cooperative Highway Research Program. (2003). Aggregate Tests for Portland Cement Concrete Pavements: Review and Recommendations. *Research Results Digest* , 28.

Neville, A. M. (1970). *Creep of concrete: plain, reinforced, and prestressed.*

Neville, A. M. (1996). *Properties of concrete* . John Wiley & Sons .

Olek, J., Lu, A., Feng, X., & Magee, B. (2002). *Performance-Related Specifications of Concrete Bridge Superstructures.* West Lafayette: Civil Engineering Joint Transportation Research Program.

Oluokun, F. A. (1991). Prediction of Tensile Strength from its Compressive Strength: Evaluation of Existing Relations for Normal Weight Concrete. *ACI Materials Journal* , 8.

Paul Klieger, J. F. (2006). *Significance of Tests and Properties of Concrete and Concrete-Making Materials.* ASTM.

Pickett, G. (1954). Effect of Aggregate on Shrinkage of Concrete and a Hypothesis Concerning Shrinkage. *Journal of the American Concrete Institute* , 10.

Popovics, S. (1921). *Strength and related properties of concrete - a quantitative approach* . Wiley; Har/Dis edition.

Richard L. McReynolds, P. (2005). *Construction of Crack-Free Concrete Bridge Decks.* KSDOT.

RILEM, C. f. (1990). *Properties of fresh concrete* .

Rouse, J. M., & Billington, S. L. (2007). Creep and Shrinkage of High-Performance Fiber-Reinforced Cementitious Composites. *ACI Materials Journal* , 8.

Sear, L. K., Dews, J., Kite, B., & Harris, F. C. (1996). Abrams law, air and high water-to-cement ratios. *Construction and Building Materials* , 6.

Sideris, K. K., Manita, P., & Sideris, K. (2004). Estimation of ultimate modulus of elasticity and Poisson ratio of normal concrete. *Cement & Concrete Composites* , 9.

Vandewalle, L. (2000). Concrete creep and shrinkage at cyclic ambient conditions. *Cement & Concrete Composites* , 8.

Wittmann, F. (1982). *Fundamental Research on Creep and Shrinkage of Concrete.* Martinus Nijhoff Publishers.

Wu, K.-R., Chen, B., Yao, W., & Zhang, D. (2001). Effect of coarse aggregate type on mechanical properties of high-performance concrete. *Cement and Concrete Research* , 5.

Ziehl, P. H., Cloyd, J. E., & Kreger, M. E. (2004). Investigation of Minimum Longitudinal Reinforcement Requirements for Concrete Columns Using Present-Day Construction Materials. *ACI Structural Journal* , 11.

BIOGRAPHICAL SKETCH

Boris Haranki is a civil engineer born in 1979. He earned his bachelor's degree at the University of Florida in 2007. He earned his Master of Engineering degree at the University of Florida in 2009.